

# **A New Strain Sensor Based on Pure CNT Films**

A Thesis Submitted to the College of Graduate Studies and Research in Partial

Fulfillment of the Requirements for the Degree of Master of Science in the

Department of Mechanical Engineering

University of Saskatchewan

Saskatoon

By

Yu (Paul) Miao

## ABSTRACT

The use of carbon nanotubes (CNTs) as a material for construction of sensors is a promising effort. This is due to some unique characteristics of CNTs. In recent years, strain sensors built from CNT composite films have been developed. This thesis study first proposed that the piezoresistive sensitivity of CNT composite films can be limited due to the presence of one of the constituent elements in the CNT composite films, that is, surfactant. CNT films free of surfactants were thus hypothesized to have a great promise to improve piezoresistive sensitivity. The motivation of this thesis study was to explore this promise.

This thesis presents an experimental study on Single-Wall CNT (SWNT) films free of surfactants. Such SWNT films are called pure SWNT films. The study has concluded: (1) the gauge factor of one layer SWNT film is much higher than that of CNT composite film; (2) the fabrication of multilayered pure CNT films is highly possible; (3) the gauge factor of multilayered pure SWNT films (10 layers and 0.8mg/ml concentration) can reach as high as 2.59 with non-linearity of 0.89% and repeatability of 0.1%, which outperforms the strain sensor built from CNT composite films; (4) the role of surfactants is indeed restrictive to piezoresistive

response, and (5) the junction theory is likely applicable to pure SWNT film sensors.

The main contributions of this thesis study are: (1) the finding of a new type of strain sensors built from pure CNT films and (2) the development of a fabrication process for multilayered pure SWNT films.

## **ACKNOWLEDGEMENTS**

I would like to express my appreciation to my supervisor, Professor W.J. (Chris) Zhang for his guidance, support, and suggestion. I also would like to extend my gratitude to my co-supervisor Professor Li Chen for his provision of electrical devices used in this study.

I appreciate the support I received from the Saskatchewan Structural Sciences Centre (SSSC), especially Dr. R. Sammynaiken and Dr. J. Maley, for providing me with the fabrication facility and the research device. I also appreciate the help of Mr. Hans-Jürgen Steinmetz, from the material test laboratory and the staff of engineering workshops at the University of Saskatchewan for providing me with the testing laboratory and testing materials. I am grateful to the SBS Buhentechnik Co.Ltd for financial support for my master study at the University of Saskatchewan.

Dedicated to my family

# TABLE OF CONTENTS

<b>ABSTRACT</b> .....	<b>i</b>
<b>ACKNOWLEDGEMENTS</b> .....	<b>iii</b>
<b>LIST OF TABLES</b> .....	<b>ix</b>
<b>LIST OF FIGURES</b> .....	<b>x</b>
<b>1. Introduction</b> .....	<b>1</b>
<b>1.1 Motivation</b> .....	<b>1</b>
<b>1.2 Objectives</b> .....	<b>2</b>
<b>1.3 Method of Research</b> .....	<b>3</b>
<b>1.4 Organization of the Thesis</b> .....	<b>4</b>
<b>2. Background and Literature Review</b> .....	<b>7</b>
<b>2.1 Introduction</b> .....	<b>7</b>
<b>2.2 Strain sensors</b> .....	<b>7</b>
<b>2.3 Carbon Nanotubes</b> .....	<b>11</b>
<b>2.3.1 Electrical properties</b> .....	<b>13</b>
<b>2.3.2 Mechanical properties</b> .....	<b>14</b>
<b>2.3.3 Thermal properties</b> .....	<b>14</b>
<b>2.4 Application of CNTs in sensors</b> .....	<b>15</b>

<b>2.5 Piezoresistive properties of CNTs.....</b>	<b>16</b>
<b>2.5.1 Band gap based piezoresistive properties of CNTs.....</b>	<b>17</b>
<b>2.5.2 The junction based piezoresistive properties of CNTs .....</b>	<b>21</b>
<b>2.6 Method for the pure CNT film fabrication.....</b>	<b>24</b>
<b>2.7 Van der Waals interaction in CNT networks.....</b>	<b>25</b>
<b>2.8 Conclusion .....</b>	<b>28</b>
<b>3. Piezoresistive Response of Pure SWNT films.....</b>	<b>30</b>
<b>3.1 Introduction.....</b>	<b>30</b>
<b>3.2 Materials and methods .....</b>	<b>31</b>
<b>3.3 Results and discussion .....</b>	<b>36</b>
<b>3.4 Conclusion .....</b>	<b>40</b>
<b>4. Fabrication of Pure SWNT films.....</b>	<b>41</b>
<b>4.1 Introduction.....</b>	<b>41</b>
<b>4.2 Materials for fabrication of the pure SWNT film.....</b>	<b>41</b>
<b>4.3 Fabrication of the one layer pure SWNT film.....</b>	<b>42</b>
<b>4.4 Fabrication of the multilayered pure SWNT film .....</b>	<b>46</b>
<b>4.5 Uniformity of multilayered pure SWNT networks.....</b>	<b>47</b>
<b>4.6 Conclusion .....</b>	<b>54</b>
<b>5. Optimizing Piezoresistive Sensitivity of the SWNT film.....</b>	<b>55</b>
<b>5.1 Introduction.....</b>	<b>55</b>
<b>5.2 Control experiment I .....</b>	<b>55</b>
<b>5.3 Control experiment II.....</b>	<b>56</b>

5.4 Control experiment III .....	57
5.5 Results and Discussion.....	59
5.5 Conclusion .....	69
<b>6. Roles of Surfactants in CNT Networks for Strain Detection.....</b>	<b>71</b>
6.1 Introduction.....	71
6.2 The SWNT/PSS and SWNT/SDS composite networks .....	72
6.3 Results and discussion .....	73
6.4 Conclusion .....	78
<b>7. Repeatability of Piezoresistive Response of Pure SWNT Films .....</b>	<b>80</b>
7.1 Introduction.....	80
7.2 Low cycle compression experiment.....	80
7.3 Low cycle tensile experiment .....	82
7.4 Discussion.....	83
7.5 Conclusion .....	85
<b>8. Electrical System for the Pure SWNT Film Sensor.....</b>	<b>87</b>
8.1 Introduction.....	87
8.2 Amplification circuit.....	87
8.3 Data acquisition (DAQ) system.....	92
8.4 Summary.....	96
<b>9. Conclusion and Recommendation.....</b>	<b>97</b>
9.1 Overview of the thesis.....	97
9.2 Conclusion .....	98



<b>9.2.1 Comparison with CNT composite films .....</b>	<b>99</b>
<b>9.2.2 Comparison with traditional metal foil gauges .....</b>	<b>101</b>
<b>9.3 Contribution .....</b>	<b>103</b>
<b>9.4 Future work .....</b>	<b>104</b>
<b>References .....</b>	<b>107</b>
<b>Appendix I .....</b>	<b>116</b>
<b>Appendix II .....</b>	<b>116</b>

## LIST OF TABLES

Table 4-1: The value of amplitude at $1590\text{ cm}^{-1}$ shift in the pure CNT film (10 layers of CNT network at $0.8\text{mg/ml}$ ).....	53
Table 4-2: The value of amplitude at $1590\text{ cm}^{-1}$ shift in the pure CNT film (20 layers of CNT network at $0.8\text{mg/ml}$ ).....	53
Table 5-1: Gauge factors at different numbers of layers of SWNT networks with different concentration of SWNT solution.....	61
Table 5-2: Linearity at different numbers of layers of SWNT networks with different concentration of SWNT solution .....	64
Table 5-3: Gauge Factor and linearity of SWNT films ( $0.8\text{mg/ml}$ SWNT) at different sonication hours .....	67

## LIST OF FIGURES

Figure 2-1: A model of strain sensors from the target to the monitoring station .....	8
Figure 2-2: Definition of strain and piezoresistive response in the material .....	9
Figure 2-3: A model of a typical metallic strain gauge .....	10
Figure 2-4: Three silicon gauges (in red circle) mounted on the surface for strain detection (Ahmed <i>et al.</i> 2008) .....	11
Figure 2-5: Schematic structure of a single wall carbon nanotube (SWNT) ( <a href="http://jnm.snmjournals.org/cgi/content/full/48/7/1039/FIG1">Http://jnm.snmjournals.org/cgi/content/full/48/7/1039/FIG1</a> ) .....	12
Figure 2-6: Schematic structure of a multiwall carbon nanotube (MWNT) ( <a href="http://chattahbox.com/images/2009/06/carbon_nanotubes.jpg">http://chattahbox.com/images/2009/06/carbon_nanotubes.jpg</a> ) .....	12
Figure 2-7: Rolling angle of graphite sheet to form a carbon nanotube .....	13
Figure 2-8: Schematic model of an AFM needle pushing down a SWNT to detect voltage changes on gold pads (Tomblor <i>et al.</i> 2000) .....	17
Figure 2-9: Simulation of parameters for three different kinds of CNTs (Yang <i>et al.</i> 2007) .....	18
Figure 2-10: Strain versus Gauge factor (Yang <i>et al.</i> 2007) .....	19
Figure 2-11: SEM micrographs of CNTs grown perpendicularly on the substrate (Yong <i>et al.</i> 2003) .....	20

Figure 2-12: A product of “Buckypaper” fabricated by the method proposed by Dharap <i>et al.</i> (2004) .....	23
Figure 2-13: Illustration of the layer-by-layer process to manufacture SWNT-PVA/PSS films (Lynch <i>et al.</i> 2008) .....	24
Figure 2-14: Schematic model of two SWNTs with different radii $R_1$ and $R_2$ at a van der Waals gap $g$ (Sun <i>et al.</i> 2005) .....	27
Figure 2-15: Schematic diagram of separation of single tube from a hexagonal array of SWNTs (Cao <i>et al.</i> 2007) .....	28
Figure 3-1: Transparent pure SWNT film purchased from Unidym Inc.....	31
Figure 3-2: An experiment sample: A pure SWNT film glued onto the aluminum 6061-T6 tensile test sample .....	32
Figure 3-3: Loading the aluminum 6061-T6 in the tester Instron 5500R, the multimeter used to record the changes in resistance of the pure CNT film .....	33
Figure 3-4: Linear relation between resistance and strain in a one layer pure SWNT film which is attached on a 6061-T6 sample under the low tensile stress .....	34
Figure 3-5: Loading a pure SWNT film under the tester Instron 1122, the changes in resistance of pure CNT films measured by a multimeter .....	35
Figure 3-6: Linear relation between resistance and strain in the pure SWNT film with one layer SWNT networks under in-plane stretching .....	35
Figure 3-7: Schematic model of the pure SWNT film: the semi-conductive SWNTs	

randomly distributed on the PET polymer substrate.....	37
Figure 3-8: The pure SWNT film under the SEM spectroscopy (Provided by Unidym, Inc.) .....	37
Figure 3-9: A conductive path established through semi-conductive SWNTs and junctions between SWNTs in CNT networks .....	38
Figure 3-10: Schematic model of piezoresistive response in the pure SWNT film: the conductive paths change as CNT networks experience the elongation ...	39
Figure 4-1: Sonicator BRANSON SONIFIER 150 sonicate the CNT solution at 40W.....	43
Figure 4-2: Centrifuge SWNT-SDS solution at 14000 rpm for 30 minutes in the Centrifuge EPPENDORF.....	44
Figure 4-3: PET substrate heated through an aluminum plate by a red infrared bulb during the spray coating process.....	45
Figure 4-4: Rinsing off SDS in distilled water after the spray coating one layer of CNT networks on the PET substrate.....	46
Figure 4-5: Fabrication multilayered pure CNT film by repeating four steps.....	47
Figure 4-6: Identify the coating area which contains CNT networks by a multimeter .....	48
Figure 4-7: The spectral acquisition setups, including the information about Laser device, Grating name and detector name .....	49
Figure 4-8: The spectral acquisition setups, including the information about the laser power, exposure time and accumulations .....	49

Figure 4-9: Spectrum results of the PET substrate under the Raman Microscope Renishaw 2000.....	50
Figure 4-10: Spectrum of SWNT deposited on PET substrate (in red) and Spectrum of the PET substrate (in black), the difference between the two spectrums marked in red circles presenting the existence of SWNTs .....	51
Figure 4-11: Amplitudes of Count Peaks in different scanning spots at $1589\text{cm}^{-1}$ shift, the variance of amplitude representing the difference of density of SWNTs at each scanning spot.....	52
Figure 5-1: A linear relation of resistance versus elongation in a SWNT film with 10 layers of SWNT networks at CNT concentration $1\text{ mg/ml}$ .....	57
Figure 5-2: Calculated linear function and linear regression of the SWNT film with 10 layers of SWNT networks at CNT concentration $1\text{mg/ml}$ .....	58
Figure 5-3: Gauges factor versus numbers of layers of SWNT networks at different concentration of SWNT solution .....	60
Figure 5-4: Linear relation between resistance and elongation in the pure SWNT film with 10 layers of SWNT networks at the CNT concentration $0.5\text{ mg/ml}$	62
Figure 5-5: Linear relation between resistance and elongation in the pure SWNT film with 10 layers of SWNT networks at the CNT concentration $1\text{mg/ml}$ ....	63
Figure 5-6: Piezoresistive linearity versus numbers of layers of SWNT networks at different concentration of SWNT solution.....	64
Figure 5-7: Resistance of the pure SWNT film at different sonication time (three samples measured at each sonication time) .....	66

Figure 5-8: Gauge factor versus different sonication time in the pure SWNT film with 10 layers of SWNT networks at the CNT concentration  $0.8\text{mg/ml}$  .67

Figure 5-9: Linearity versus different sonication hours in the pure SWNT film with 10 layers of SWNT networks at the CNT concentration  $0.8\text{mg/ml}$  .....68

Figure 5-10: Relation between load and elongation in the PET substrate and the PET substrate with different layers of SWNT networks.....69

Figure 6-1: Linear relation between resistance and elongation in the film with 40 layers of the SWNT/PSS networks.....74

Figure 6-2: Gauge factor in the SWNT/SDS film and the pure SWNT film at different layers of SWNT networks.....75

Figure 6-3: Schematic representation of SDS adsorb onto the nanotube surface. Tube stabilization depends on the surfactant molecules that lie on the tube surface parallel to the cylindrical axis (Islam *et al.* 2003).....76

Figure 6-4: Relation between elongation and resistance of the film with 5 layers of SWNT/SDS composite networks.....77

Figure 6-5: Linearity of piezoresistive response in the SWNT/SDS film and the pure SWNT film at different layers of SWNT networks .....77

Figure 7-1: A pure CNT film affixed on a PVC block and connected to an amplification circuit for the compression test, (the PVC block loaded in the tester Instron 5500 with crosshead speed  $0.5\text{min/mm}$ ).....81

Figure 7-2: Three cycle compression load applied on the PVC block to generate 5000

microstrain on the pure CNT film.....	82
Figure 7-3: Three cycle tensile load applied on the pure SWNT film to generate 3500 microstrain on the film.....	83
Figure 7-4: Piezoresistive response of the 10 layered pure CNT film with the concentration of $0.8\text{mg/ml}$ under the three cycle compression load.....	84
Figure 7-5: Piezoresistive response of the 10 layered pure CNT film with the concentration of $0.8\text{mg/ml}$ under the three cycle tensile load.....	85
Figure 8-1: Amplification circuit: Precision 6.28-20 mA Loop Transmitter with Noninteractive Trim, (National Instrument (NI) Inc).....	88
Figure 8-2: Wheatstone bridge, including two balance resistors ( $R_2$ and $R_3$ ), one compensate resistor ( $R_4$ ) and one pure CNT film ( $R_1$ ) .....	89
Figure 8-3: Relation between input ( $V_0$ ) and output ( $R_s I_{\text{out}}$ ) in the linear amplification circuit (red line: the theoretical results calculated by Equation (8-1) to (8-3); blue line: the experimental results from the adjustment).....	92
Figure 8-4: Electrical system of the pure CNT film sensor, containing the amplification circuit, a D/A transducer and the monitoring computer ....	93
Figure 8-5: The function panel programmed in the LABVIEW 2009, (The DAQ assistant: the signal collection in the card NI-PCI-M10164-4, the experimental results saved and shown in the “Write to measurement file” and in the “Waveform Chart”, respectively) .....	94
Figure 8-6: Tensile load applied on the pure CNT film to test the electrical system...	95
Figure 8-7: Piezoresistive response in the pure CNT film processed in the Labview	



2009 by the electrical system.....96

Figure 9-1: Gauge factor of CNT composite films and the pure CNT. The pure CNT film with 10 layers of CNT networks at the CNT concentration of  $0.8\text{mg/ml}$ .....101

Figure 9-2: Gauge factor of different metal foil gauges and the pure SWNT film. The pure SWNT film with 10 layers of CNT networks at the CNT concentration of  $0.8\text{mg/ml}$  ..... 103

# Chapter 1

## Introduction

### 1.1 Motivation

Carbon nanotube (CNT) composite films have been found to exhibit piezoresistive response under in-plane or in-film workload. Piezoresistive response in a material refers to the resistance change along the direction of strain due to the piezoelectric effect. Piezoresistive response, qualified for strain sensor, is found in many different CNT composite films. The study performed by Dharap *et al.* (2004) has shown the piezoresistive response of CNT composite films and explained its relevance with the structure of CNT networks. However, the CNT composite films usually show low gauge factor (or piezoresistive sensitivity in the case here) and inferior mechanical properties. Gauge factor in piezoresistive response refers to the ratio of the change in electrical resistance to the mechanical strain.

The essential steps of the CNT composite film fabrication reported in the literature are first to develop a CNT solution and then to coat the solution on a substrate with different coating techniques. In this fabrication procedure, surfactants have to be used

in order to suspend and disperse the CNTs in an aqueous solution. Lynch *et al.* (2008) proposed that the surfactants left in these CNT composite films are the main factor affecting their sensitivity and their piezoresistive response. Therefore, any fabrication that can get rid of the surfactant will be promising to improve the quality of piezoresistive response in CNT networks.

The fabrication technique for transparent or pure CNT films was developed by Kaempgen *et al.* (2006) in the application of CNT films in touch panel. CNT networks in these films are randomly deposited on the substrate without surfactants left. This thesis research hypothesized that such networks (i.e., pure CNT films) should exhibit a better piezoresistive sensitivity compared with the CNT composite films or networks. For simplicity, the CNT films free of surfactants are called pure CNT films throughout this thesis. Furthermore, this thesis throughout will use word 'film' and word 'network' interchangeably. Motivation for testing this hypothesis led to several objectives of this thesis study.

## **1.2 Objectives**

*Objective 1: Verify the hypothesis that the pure CNT film free of surfactants exhibits a better piezoresistive sensitivity compared with the CNT composite film.* It is noted that a commercially available one layer pure CNT film which is free of surfactants will be used in the experiments.

*Objective 2: Develop a fabrication process to build multilayered pure CNT films.* This is for the purpose to study multilayered pure CNT films more systematically, as at the time of this study, multilayered pure CNT films were not available.

*Objective 3: Optimize the piezoresistive response in the multilayered pure CNT film.*

This includes two attributes: piezoresistive sensitivity and linearity.

*Objective 4: Investigate the influence of surfactants on piezoresistive response in the multilayered pure CNT film.* This will focus on multilayered pure CNT films with different surfactants and is expected to advance our understanding of surfactants.

*Objective 5: Study the repeatability of piezoresistive response of the strain sensor built using the pure CNT film.* Repeatability is another important property of the sensor, which needs to be known. In the repeatability study, a dynamic loading scheme will be applied; while in the study of Objective 1, Objective 3, and Objective 4, a static loading scheme is applied.

### **1.3 Method of Research**

The general method taken for this thesis research is experiment-oriented with exploration of governing mechanisms. The experimental facilities include (1) the tester Instron 5500R (for low strain) and 1122 (for high strain) for testing

piezoresistive response, (2) electrical instruments such as amplification circuit, A/D transducer and data acquisition card for getting electrical signals, and (3) the Raman device Renishaw 2000 for examining some properties of the strain sensor built upon the CNT film. Furthermore, the experimental results were compared with well-established strain sensors in order to understand the promise of the new type of strain sensor developed in this thesis research.

#### **1.4 Organization of the Thesis**

The thesis consists of nine chapters including Chapter 1, which are designed to present the study for the five objectives, respectively.

Chapter 2 will give background of the knowledge necessary to conduct this research and discuss the literature to further confirm the originality of the proposed hypothesis along with the proposed research objectives

Chapter 3 will present the experimental study of piezoresistive response in the pure CNT film to test the hypothesis presented in Objective 1. The governing mechanism for piezoresistive response in the pure CNT film will also be discussed.

Chapter 4 will present a new fabrication process for multilayered pure CNT films to achieve Objective 2. There is also a discussion of the use of Raman spectroscopy to

examine the uniformity of multilayered CNT films.

Chapter 5 will then present the experimental study of optimization of the new fabrication process described in Chapter 4 to improve piezoresistive response in the multilayered pure CNT film. The work presented in this chapter will achieve Objective 3.

Chapter 6 will present the study of how surfactants affect piezoresistive response in multilayered CNT networks to furnish more knowledge regarding the role of surfactants in CNT composite films in general. The work presented in Chapter 6 achieves Objective 4.

Chapter 7 will present an experiment to study the repeatability of piezoresistive response in pure CNT films in low cycle straining. The pure CNT films used here are fabricated by the proposed method presented in Chapter 4. The work presented in Chapter 7 achieves Objective 5.

Chapter 8 will present the design of a general electrical system of the test bed for all the pure CNT film sensors studied and presented in the preceding chapters. This system includes an electrical circuit and a data acquisition system.

Chapter 9 concludes this thesis by summarizing the research conducted along with

salient findings, discussing contributions of the research, and proposing the future work.

## **Chapter 2**

### **Background and Literature Review**

#### **2.1 Introduction**

In this chapter, some important background and state of knowledge regarding CNT-based strain sensors will be discussed. In particular, section 2.2 presents the basic concepts of strain sensors. Section 2.3 introduces carbon nanotubes and discusses their properties. Section 2.4 presents the application of CNTs in sensors. In section 2.5, the current research on piezoresistive response in CNTs is summarized, which will also include the fabrication techniques for the CNT strain sensors. Section 2.6 introduces the fabrication process for pure CNT films. Section 2.7 discusses physics in CNT networks. Section 2.8 gives a concluding remark regarding the state of knowledge in the field of CNT-based strain sensors to highlight the importance of the proposed hypothesis along with the research objectives presented in Chapter 1.

#### **2.2 Strain sensors**

Strain sensors are one of the most common devices used in a structural health



monitoring system (SHM). Figure 2-1 shows a model of the application of strain sensors in the SHM, where when the structure experiences deformation, the deformation will be detected by strain sensors and the sensed signal will be transmitted to a monitoring station.

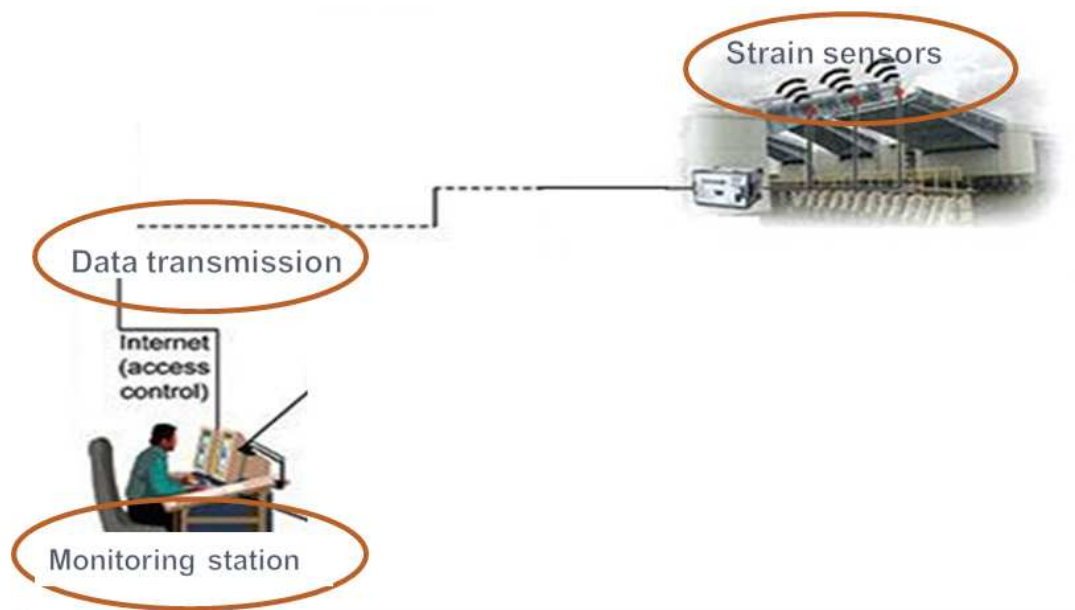


Figure 2-1: A model of strain sensors from the target to the monitoring station

There are several methods to measure deformation (i.e., to build the strain sensor).

The most common method is based on a material property called piezoresistivity.

Piezoresistive response happens in materials, as shown in Figure 2-2.

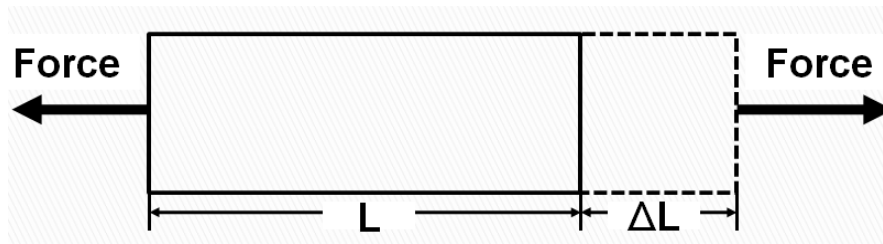


Figure 2-2: Definition of strain and piezoresistive response in the material

As a pair of loads is applied on materials, the elongation leads to the change of electrical resistance in the materials, and more importantly, this change in resistance is linearly proportional to the amount of strain in the materials. In strain sensors, piezoresistive sensitivity can be represented by gauge factor (GF), calculated by Equation (2-1).

$$GF = \frac{\Delta R/R}{\Delta L/L} = \frac{\Delta R/R}{\epsilon} \quad (2-1)$$

where  $\epsilon$  is strain,  $R$  is the resistance of materials,  $\Delta R$  is the changes in resistance.

Piezoresistive response can happen in many metallic materials such as platinum, tungsten, and nickel. The strain sensors made from these metals are called the metallic strain gauges. The metallic strain gauges are the most widely used strain sensors in the current market.

The metallic strain gage consists of fine wires or in a grid pattern, as shown in Figure 2-3. The grid pattern maximizes the amount of metallic wires to strain in the parallel direction. The cross-sectional area of the grid is minimized to reduce the effect of shear strain and Poisson strain. The strain gauge is attached directly to the structure.

Therefore, as strain happens in a structure it is transferred directly to the strain gauge, which responds to a linear change in electrical resistance. The gauge factor of metallic strain gauges commercially available is about 2.



Figure 2-3: A model of a typical metallic strain gauge

Piezoresistive response has also been found in other kinds of materials, such as silicon and carbon nanotube (CNT). Experiments have shown that the gauge factor of silicon is around 130, which is quite higher than the existing metallic strain gauge. The silicon strain sensor is commonly used in micro-scale detection due to its small size. Figure 2-4 shows three silicon strain sensors mounted on the surface, of which the area is smaller than 1 *mm*. The application of CNTs in strain sensors will be further discussed in the next section.

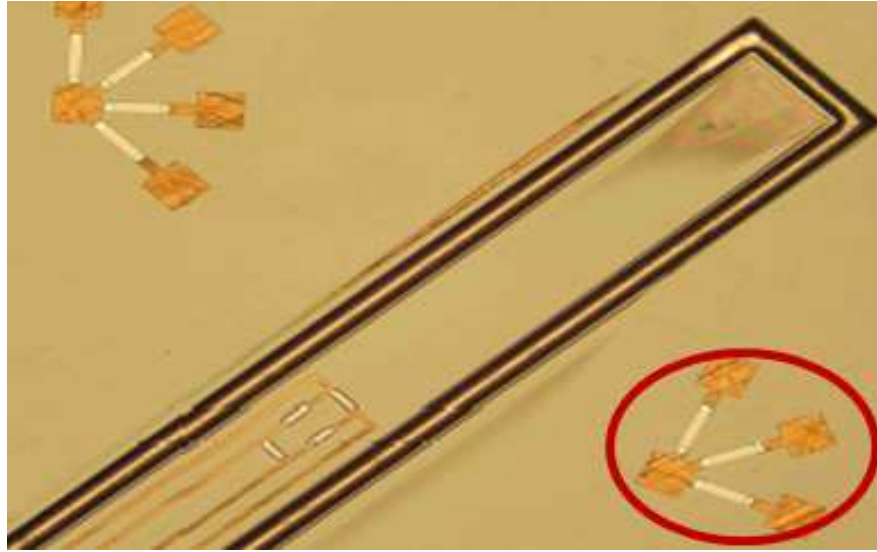


Figure 2-4: Three silicon gauges (in red circle) mounted on the surface for strain detection (Ahmed *et al.* 2008)

### 2.3 Carbon Nanotubes

Carbon Nanotubes (CNTs), first reported by Iijima *et al.* (1991), are hexagonal networks of carbon atoms of approximately 1 *nm* in diameter and 1 to 100  $\mu\text{m}$  in length. Dresselhaus *et al.* (1996) suggested that CNTs can essentially be thought of as a layer of graphite rolled-up into a cylinder. Depending on the arrangement of their graphene cylinders, there are two types of nanotubes: single-walled nanotubes (SWNTs) and multi-walled nanotubes (MWNTs). SWNTs have only one layer of graphene cylinders, as shown in Figure 2-5; while MWNTs have many layers (approximately 50), as shown in Figure 2-6.

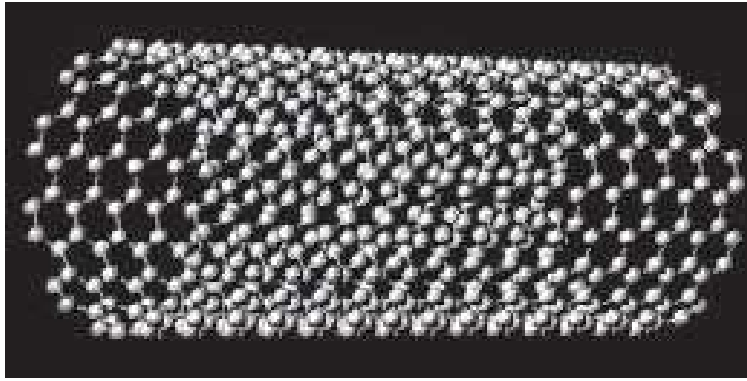


Figure 2-5: Schematic structure of a single wall carbon nanotube (SWNT)  
([Http://jnm.snmjournals.org/cgi/content/full/48/7/1039/FIG1](http://jnm.snmjournals.org/cgi/content/full/48/7/1039/FIG1))



Figure 2-6: Schematic structure of a multiwall carbon nanotube (MWNT)  
([http://chattahbox.com/images/2009/06/carbon\\_nanotubes.jpg](http://chattahbox.com/images/2009/06/carbon_nanotubes.jpg))

Since the discovery of CNTs more than a decade ago, they have attracted great

attention from researchers due to their unique properties which are especially good to sensor development. In this section, the properties of CNTs, including electrical, mechanical and thermal properties, will be discussed.

### 2.3.1 Electrical properties

Electrically, CNTs can be either metallic or semi-conducting, depending upon the tube diameter and the chirality (the sheet direction in which the graphite sheet is rolled to form a nanotube cylinder). The mode that the graphene sheet is wrapped can be represented by a pair of indices  $(n, m)$  called the chiral vector shown in Figure 2-7.

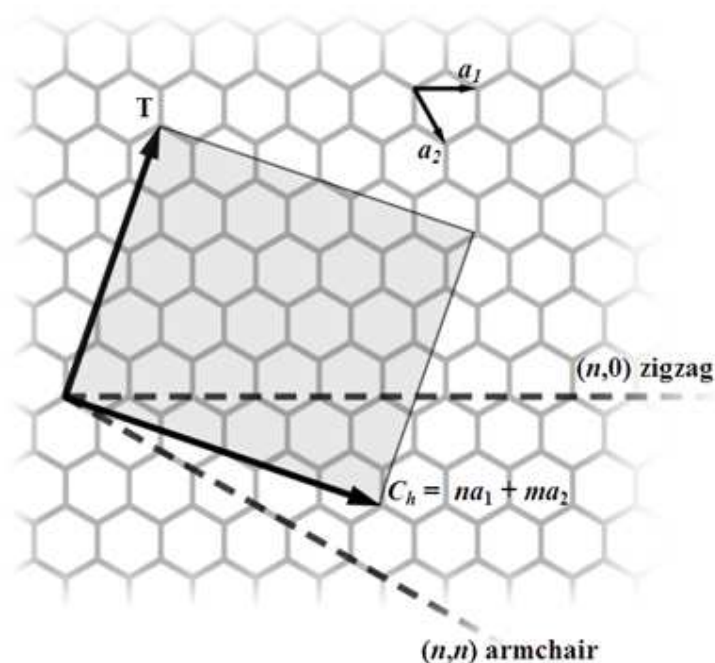


Figure 2-7: Rolling angle of graphite sheet to form a carbon nanotube

(<http://en.wikipedia.org/wiki/File:CNTnames.png>)

The integer's  $n$  and  $m$  denote the number of unit vectors along two directions in the honeycomb crystal lattice of graphene. If  $m = 0$ , the nanotubes are called "zigzag". If  $n = m$ , the nanotubes are called "armchair"; otherwise, they are called "chiral". For a given  $(n, m)$  nanotube, if  $n = m$ , the nanotube is metallic; if  $n - m$  is a multiple of 3, the nanotube is semi-conducting with a very small band gap; otherwise the nanotube is a moderate semiconductor.

### **2.3.2 Mechanical properties**

Mechanically, CNTs are currently one of the strongest known materials because the carbon-carbon bond observed in graphite is one of the strongest in nature. Treacy *et al.* (1996) have estimated the Young's modulus of a single MWNT by measuring the amplitude of their intrinsic thermal vibrations in the transmission electron microscope (TEM). The average value of Young's modulus was found to be 1800 *GPa*. Wagner *et al.* (1998) reported the Young's modulus of SWNT as 2800–3600 *GPa*.

### **2.3.3 Thermal properties**

Thermally, Hone *et al.* (2000) suggested that the specific heat and thermal conductivity of CNTs are dominated by photons and the electronic contribution is negligible due to the low density of free charge carriers. Mizel *et al.* (1999) measured

the specific heat of MWNT and SWNT in the temperature ranging from 1 K  $<T<200K$  and revealed that there is a linear dependence of the specific heat of MWNT on the temperature and SWNT has a steep temperature dependence at low temperatures. Kim *et al.* (2001) observed that the thermal conductivity for a single MWNT is greater than  $333W/mK$ .

## **2.4 Application of CNTs in sensors**

Due to the superior properties of CNTs, such as their small size, exceptional mechanical properties, convertible electrical properties and excellent thermal conductivity, CNTs have been used as the sensing material in many different types of sensors. For instance; Liu *et al.* (2002) created a piezoresistive pressure sensor made by CNTs. In their studies, SWNTs were grown on suspended square polysilicon membranes. When air pressure was applied to a membrane, a change in resistance in the SWNTs was observed.

Dharap *et al.* (2004) adopted the “buckypaper” fabrication to produce CNT composite films, CNT/DMF, which will be further discussed later in this thesis. They developed a CNT film sensor for strain sensing on a macro scale. Their experimental results revealed a nearly linear relationship between the measured change in resistance and the strains in CNT films when they were in tensile and compressive strain.



Kane *et al.* (2000) discovered CNT temperature dependent resistivity both in theory and experimentally. They found that there is a linear relationship between resistivity of CNT and temperature.

CNT sensors can also be used as chemical sensors. A study by Kong *et al.* (2000) revealed that the electrical resistance of semiconducting SWNTs dramatically changes when exposed to gaseous molecules such as nitrogen dioxide ( $NO_2$ ), ammonia ( $NH_3$ ), and oxygen ( $O_2$ ). At the 3rd International Workshop on Structural Health Monitoring, O'Keeffe *et al.* (2002) proposed a chemical sensor based on CNTs to detect the chemical absorption of gas molecules.

In addition, other types of CNT based sensors have been proposed, such as Wong *et al.* (2003) who manipulated bulk MWNTs which served as temperature sensor. Someya *et al.* (2003) reported alcohol vapor sensors based on SWNT field effect transistors (FETs). Gorski *et al.* (2005) used NTs in a polymeric matrix to develop an electrochemical sensing platform.

## **2.5 Piezoresistive properties of CNTs**

Piezoresistive properties of CNTs in application of strain sensors can come from two different characterized responses. Piezoresistive responses are contributed from the energy gap of an individual CNT, known as “band gap based piezoresistive properties

of CNTs” (Tomblor *et al.* 2000). The other kind of piezoresistive responses is contributed from the changes in junctions between CNTs, known as “junctions based piezoresistive properties of CNTs” (Dharap *et al.* 2004).

## 2.5.1 Band gap based piezoresistive properties of CNTs

### 2.5.1.1 Theory of piezoresistive response based on the band gap of CNTs

Tomblor *et al.* (2000) proposed that the conductance of a single carbon tube can decrease when strained by an atomic force microscope (AFM) tip, as shown in Figure 2-8; a local distortion of the band gap where the tube is pushed by AFM tip causes the drop in conductance.

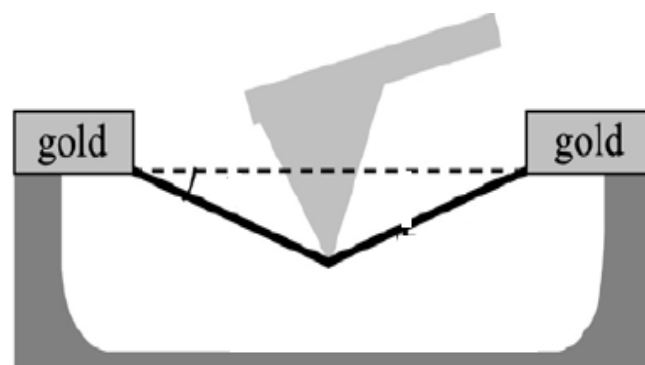


Figure 2-8: Schematic model of an AFM needle pushing down a SWNT to detect voltage changes on gold pads (Tomblor *et al.* 2000)

Inspired by this result, Minot *et al.* (2003) presented measurements to demonstrate the effects of strain on the band structure of the tube and further predicted the value for the rate of change of band gap with respect to strain. Based on their experiments, the relation between band gap and applied strain is presented by Yang *et al.* (2007), shown in Equation (2-2) and (2-3), respectively.

$$R_{tot}(\varepsilon) = R_s + \frac{1}{|t|^2} \frac{h}{8e^2} \left[ 1 + \exp\left(\frac{E_g}{kT}\right) \right] \quad (2-2)$$

$$E_g = E_g^0 + \frac{dE_g}{d\varepsilon} \varepsilon \quad (2-3)$$

$$R_{tot}(0) = R_s + \frac{1}{|t|^2} \frac{h}{8e^2} \left[ 1 + \exp\left(\frac{E_g^0}{kT}\right) \right] \quad (2-4)$$

where  $\varepsilon$  is applied strain,  $t$  is 0.5,  $h$  is Plank's constant,  $k$  is  $1.38 \times 10^{-23} \text{ J/K}$ ,  $e$  is  $1.6 \times 10^{-19} \text{ C}$ ,  $T$  is lab temperature (300K) and  $R_s$  is negligible. In addition, they also calculated the gage factor and other important parameters, shown in Figure 2-9.

$$GF = \frac{\Delta R/R}{\varepsilon} = \frac{[R_{tot} - R_{tot}(0)]/R_{tot}(0)}{\varepsilon} \quad (2-5)$$

where  $R_{tot}$  is the current resistance of CNTs,  $R_{tot}(0)$  is the original resistance of CNTs.

	Metallic-CNT	Semiconductor-CNT	SGS-CNT
$E_g$ (meV)	0	160	40.5
$dE_g/d\varepsilon$ (meV/%)	35	-53	180

Figure 2-9: Simulation of parameters for three different kinds of CNTs (Yang *et al.* 2007)

Both the experiment and calculations based on Equation (2-5) show that the gauge factor of CNTs can reach 200 and gauge factors of different kinds of CNTs are shown in Figure 2-10.

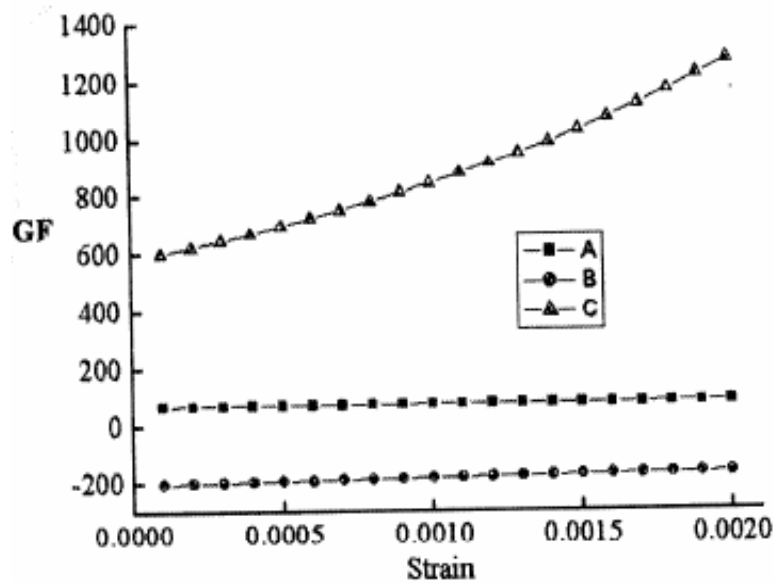


Figure 2-10: Strain versus Gauge factor (Yang *et al.* 2007)

A Metallic-CNT    B Semiconductor-CNT    C SGS-CNT

### 2.5.1.2 Fabrication of CNT strain sensors based on the band gap theory

The CNT strain sensor based on the band gap theory was fabricated by Yong *et al.* (2003). The fabrication process was such that CNTs were synthesized by hot filament chemical vapor deposition with mixed catalysts *Ni* and *Fe*. Figure 2-11 shows that the CNTs have been perpendicularly grown on the *Ni/Fe/Si* substrate under scanning

electron microscopy (SEM).

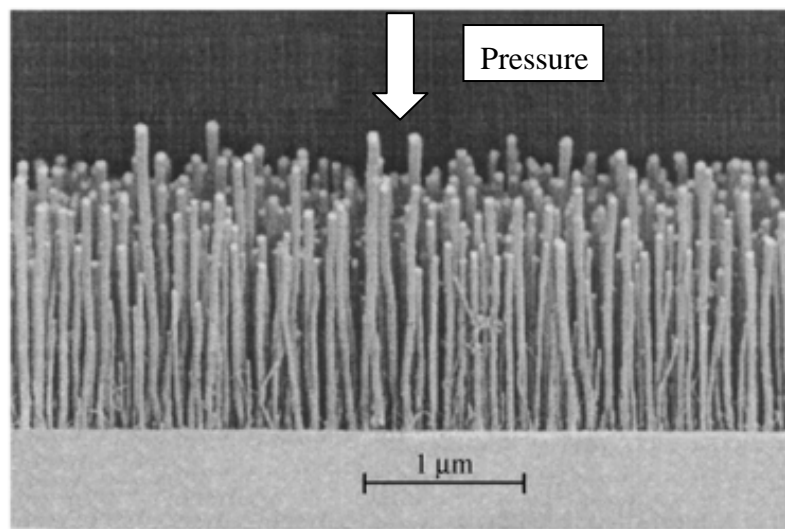


Figure 2-11: SEM micrographs of CNTs grown perpendicularly on the substrate (Yong *et al.* 2003)

The well fabricated sample was studied under a three-point test device and yield gauge factor 60. However, the resistance of this sample will have dramatic changes at different temperatures (Yong *et al.*, 2003). It is noted that the strain here is the tube itself or the pressure is loaded along the tube, as shown in Figure 2-11.

Lie *et al.* (2008) used sodium dodecyl benzene sulfonate (SDBS) to disperse SWNTs in the solution and deposit the SWNT-SDBS solution on the polymer substrate. This SWNT thin film is further loaded under pressure and achieved the gauge factor of 10-20. Lie *et al.* (2008) explained this phenomenon based on the band gap theory that the deformation of SWNT caused by pressure results in changes in conductivity of SWNTs. Following Lie's work, Lee *et al.* (2010) improved the SWNT film

fabrication for a better output of the piezoresistive response of the SWNT film under the pressure along with the tube.

## **2.5.2 The junction based piezoresistive properties of CNTs**

### **2.5.2.1 Theory of piezoresistive response based on junctions between CNTs**

The strain sensors, based on the junction based piezoresistive properties of CNTs, were first found by Dharap *et al.* (2004). They used single wall carbon nanotubes and N-Dimethylformamide (DMF) to form CNT composite films called “buckypaper” and discovered linear changes in voltage as the film was strained in low tension–compression cycles. In the buckypaper specimen, CNTs were randomly distributed on the film, joined with DMF. They suggested that because of the insulator property of DMF polymers, the changes in resistance of the film were due to CNTs. However, the low stress applied on the CNT/DMF composite film cannot cause any deformation of CNT itself. The resistance changes must be caused by other properties of CNTs rather than the deformation of band gap in CNTs.

Hecht *et al.* (2007) studied the conductive percolation regime in the CNT network. They suggested that the conductivity of CNT networks should be represented as a power law with an exponent between 0 (when the junction resistance is negligible) and 2.48 (when the junction resistance dominates the network resistance). According

to this analysis, the junctions between CNTs form conductive paths that allow electrons to pass through the CNT films. Based on their studies, these conductive paths are changed in the CNT/DMF film during the tensile and compressive cycle of strain. The changes in the paths are detected with the resistance changes in the CNT/DMF composite film.

### **2.5.2.2 Fabrication of the CNT strain sensor based on the junction theory**

Several fabrication techniques have been developed for CNT composite films used for “in-plane” strain sensors. The essential steps of these techniques for CNT composite films are to develop a CNT solution and then to apply different coating techniques to coat the solution to the substrate. So far, two common fabrication methods of CNT composite films are known as the buckypaper method and Layer-by-layer method.

Buckypaper method:

Dharap *et al.* (2004) proposed a fabrication process called “buckypaper method” to make CNT composite films. In their process, CNT/DMF solution was poured onto a filter paper and dried in a vacuum oven to slowly evaporate the solvent and then the freestanding buckypaper film was peeled off, as shown in Figure 2-12. This film is composed of highly entangled SWNT bundles which are held together by VDW interaction.



Figure 2-12: A product of “Buckypaper” fabricated by the method proposed by Dharap et al. (2004)

(<http://www.autodescuento.com/blog/wp-content/uploads/2008/10/buckypaper-foil.jpg>)

Following the Dharap’s work, many researchers used different materials to improve the piezoresistive response of CNT strain sensors based on the “buckypaper” fabrication. Kang *et al.* (2006) used polymethyl methacrylate (PMMA) to replace DMF and form a new CNT composite film known as the SWNT/PMMA film. The new film was proven to have a superior interfacial adhesion, and its piezoresistive response changes can be applied up to 2000 microstrain and even more.

Layer-by-layer method:

The Layer-By-Layer (LBL) procedure was first demonstrated by Paloniemi *et al.* (2005) in CNT film fabrication. The LBL method relies on the sequential deposition of alternating charged polycations and polyanions to form homogeneous thin films upon a substrate. This process can be repeated to fabricate multilayered CNT



composite films.

Further work by Lynch *et al.* (2007) has shown that the Layer-by-Layer (LBL) method to combine poly sodium 4-styrene sulfonate (PSS) and polyvinyl acetates (PVA) to form a new CNT composite film (PSS/PVA) for strain detection, as shown in Figure 2-13.

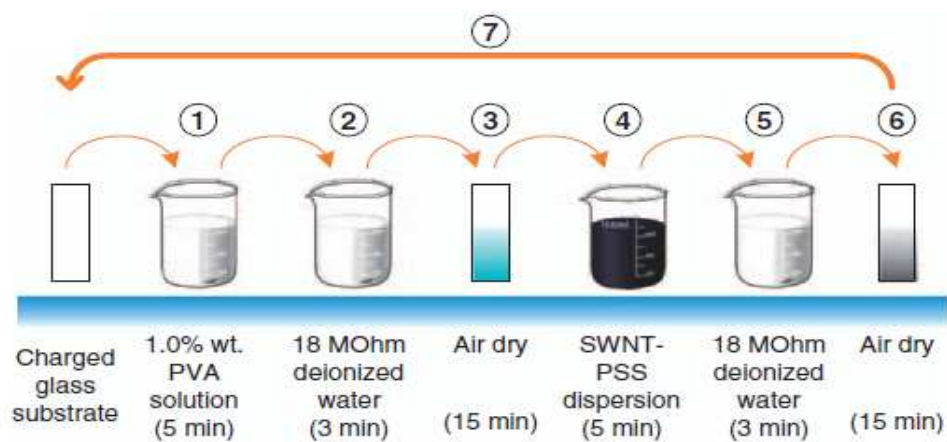


Figure 2-13: Illustration of the layer-by-layer process to manufacture SWNT-PVA/PSS films (Lynch *et al.* 2008)

More importantly, the LBL fabrication allows changing the fabrication parameters to tailor and control the aforementioned strain sensor properties. With such an idea, Lynch *et al.* (2007) developed optimal fabrication parameters for the SWNT-PVA/PSS film and yielded the best gauge factor of 1.5 with 100 layers of SWNT-PVA/PSS.

## 2.6 Method for the pure CNT film fabrication

The pure CNT film consists of pure CNT networks deposited on the substrate. Unlike CNT composite films, there is no polymer composite in CNT networks in a pure CNT film.

Kaempgen *et al.* (2005) first presented a method to fabricate pure CNT films to build a transistor. In their processes, SWNTs were dispersed first in 1%*wt* aqueous sodium dodecyl sulfate (SDS) to form a CNT/SDS solution. The CNT/SDS solution then was deposited on the substrate by an airbrush gun. After air drying, the CNT/SDS film was dipped into distilled water to rinse off the SDS. The pure SWNT film as deposited on the substrate is hereafter called the pure CNT film in this thesis.

Dan *et al.* (2009) created a method to fabricate pure CNT films for touch screens. The fabrication of the CNT solution is the same as the method proposed by Kaempgen *et al.* (2006). In the coating process, however, they chose a rod coating instead of air spraying to deposit the CNT solution on the substrate. They developed a fabrication process which is at the industrial-scale production of pure CNT films for commercial use in the touch screen or transparent transistor.

## **2.7 Van der Waals interaction in CNT networks**

In the CNT networks, the CNTs are connected to each other based on the physical connection called “van der Waals” interaction. Van der Waals (VDW) interaction,

named after the Dutch scientist Van der Waals, is an attractive or a repulsive force between molecules (or between parts of the same molecule) other than those of covalent bonds or to the electrostatic interaction of ions with one another or with neutral molecules.

Ruoff *et al.* (1994) suggested that the VDW interaction plays an important role in the junction theory for piezoresistive response of CNT films. In the CNT composite film, the VDW interaction happens between individual CNTs and forms the connection between CNTs and the composite polymers. The studies by Moore *et al.* (2003) have shown that the composite polymer with higher molecular weight provides a strong VDW interaction to CNTs. In the pure CNT film, however, the VDW interactions between CNTs are the only interaction in the CNT networks.

So far, the VDW interaction in the pure CNT networks have been studied by many researchers; however, most of these studies focus on well arranged CNT networks due to the complexity in the randomly distributed CNT networks. For example, the VDW interactions between two parallel CNTs were studied by Sun *et al.* (2005). In their work, they built a model to study the VDW potential per length of SWNTs, as shown in Figure 2-14.

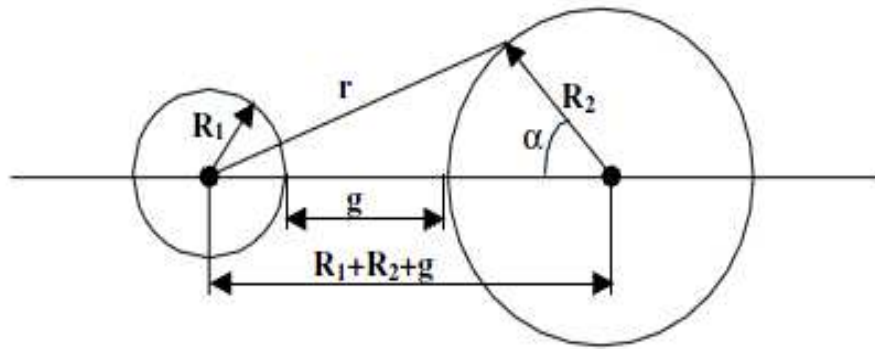


Figure 2-14: Schematic model of two SWNTs with different radii  $R_1$  and  $R_2$  at a van der Waals gap  $g$  (Sun *et al.* 2005)

Cao *et al.* (2007) further formulated a model for cohesive energy per carbon atom between parallel CNTs, and the model is represented by

$$\phi_{TT}^{\text{Carbon}} = -6.313 \times D^{-0.4645} \text{ (meV/C)}, \quad (2-6)$$

where  $D$  (nm) is the diameter of CNT. For regular SWNTs, the diameter is around 1.5nm. In this case, 5MeV energy per carbon atom is needed to separate a pair of SWNTs. More importantly, they described the total VDW between SWNTs in a CNT bundle which is shown in Figure 2-15.

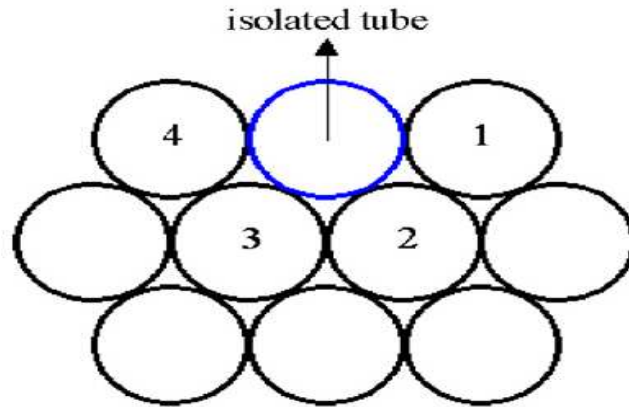


Figure 2-15: Schematic diagram of separation of single tube from a hexagonal array of SWNTs (Cao *et al.* 2007)

In Figure 2-15, a cohesive energy of  $20\text{MeV/C}$  ( $5\text{MeV} \times 4$ ) is needed to separate a single tube of  $1.5\text{nm}$  from the stable hexagonal array.

## 2.8 Conclusion

The strain sensors discussed in this chapter are based on the material property called piezoresistivity. In the current literature, CNT composite films have been found to have this property and are widely recognized to make them as strain sensors. There are two mechanisms which explain the piezoresistivity in CNT composite films: band gap theory and junction theory for short.

The CNT film without surfactants is available for the application of touch screens, and it is called pure CNT film. The pure CNT film for strain sensors under an in-plane

load has yet to be explored. The fabrication technique for one layer pure CNT film is available in the current literature. However, the fabrication technique for multilayered pure CNT films is not available in the current literature.

Therefore, the hypothesis as described in Chapter 1 is reasonable and novel, which also provides a justification for objective 1 as described in Chapter 1. Objective 2 is original and potentially significant to the CNT-based strain sensor technology.

Objectives 3-5 are necessary to provide a comprehensive knowledge base for the strain sensor built upon the pure CNT film, and they may also provide further knowledge about the mechanisms for piezoresistive response in both pure CNT films and CNT composite films.

## **Chapter 3**

### **Piezoresistive Response of Pure SWNT films**

#### **3.1 Introduction**

In CNT composite films, piezoresistive response happens in the CNT composite networks based on the change of junctions between CNTs. However, piezoresistive sensitivity of such CNT composite films is not as sensitive as would be expected.

Surfactants are known as the main factor contributing to this low sensitivity in piezoresistive response Lynch *et al.* (2008). In particular, Lynch *et al.* (2008) argued that surfactants are the reason for a low gauge factor with the CNT composite film which includes PSS (1,000,000  $M_w$ ) composite with CNTs.

In the pure SWNT film, the SWNTs are deposited on the substrate forming pure SWNT networks. Piezoresistive response in the pure SWNT networks may also be based on the junction between CNTs. Without surfactants in the CNT networks, piezoresistive sensitivity of such pure SWNT films may be quite different from that in the composite films. This is a hypothesis, as described in Chapter 1. In the following, an experiment on testing this hypothesis, especially to measure the piezoresistivity or

gauge factor for one layer pure SWNT film, is described. The experimental study on the role of surfactants will be presented later in Chapter 6.

### 3.2 Materials and methods

The pure CNT films we chose in the experiment were purchased from Unidym, Inc. The pure CNT films are made from the fabrication process developed by Dan *et al.* (2009). The sample film has one layer of SWNT networks with polyethylene terephthalate (PET) as the substrate, as shown in Figure 3-1. The thickness of one layer pure SWNT networks is  $50nm$ . Two experiments were carried out to study the piezoresistive response of the one layer pure CNT film.



Figure 3-1: Transparent pure SWNT film purchased from Unidym Inc



## Experiment I:

The thin films were cut into rectangles ( $2\text{cm} \times 10\text{cm}$ ) and affixed to aluminum 6061-T6 tensile test samples using a glue (Prism 401 Loctite) and primer (770 Loctite).

Electrical contact was established by drying the silver paste (MG chemical) over the twisted-strand wire to form two probes on the SWNT film, as shown in Figure 3-2.

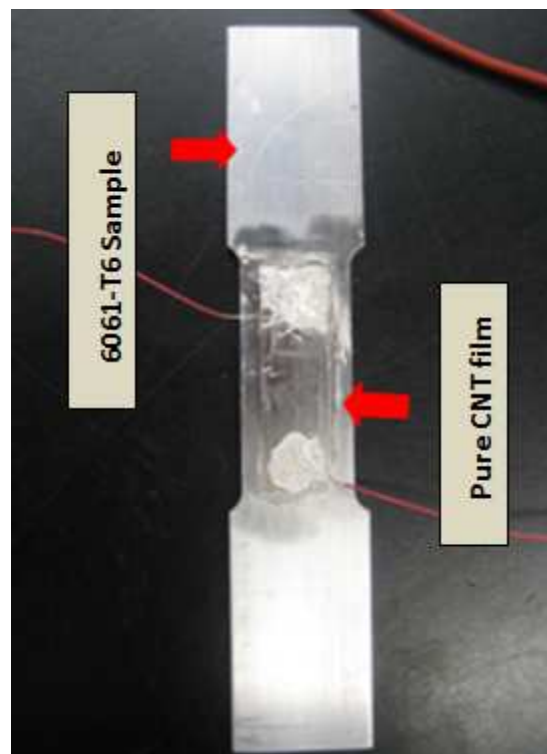


Figure 3-2: An experiment sample: A pure SWNT film glued onto the aluminum 6061-T6 tensile test sample

After 12 hours' drying, the tensile test samples were loaded in the Instron tensile test device 5500R with crosshead speed  $0.5\text{mm}/\text{min}$  as shown in Figure 3-3. Under

laboratory conditions ( $20\text{ }^{\circ}\text{C}$  and 20% humidity), a resistance change under an applied

strain was measured by a multimeter. The applied strain was also recorded to provide a comparison of the pure SWNT film with the resistivity data, as shown in Figure 3-4.

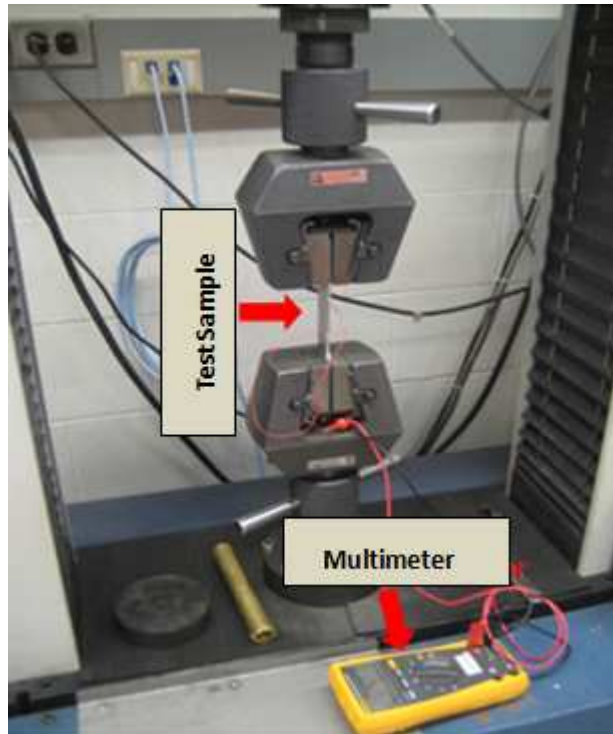


Figure 3-3: Loading the aluminum 6061-T6 in the tester Instron 5500R, the multimeter used to record the changes in resistance of the pure CNT film

In Figure 3-4, the nonlinear section from 0 microstrain to 1500 microstrain is due to a failure of the glue to affix the SWNT film on the aluminum 6061-T6 tensile test sample.

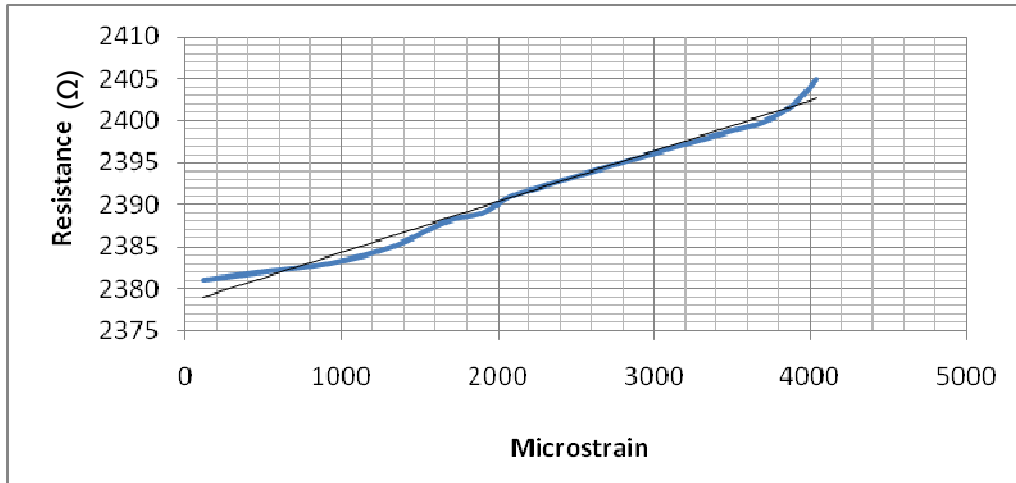


Figure 3-4: Linear relation between resistance and strain in a one layer pure SWNT film which is attached on a 6061-T6 sample under the low tensile stress

#### Experiment II:

In order to remove this dislocation effect from glue, another test was conducted by loading the SWNT film itself in the tester Instron 1122. The SWNT film first was cut into rectangles ( $25\text{mm} \times 160\text{mm}$ ); electrical connection remained the same as the first test. After 24 hours' drying, the SWNT films were loaded in the Instron 1122 with crosshead speed  $2\text{mm}/\text{min}$ , as shown in Figure 3-5. The result is shown in Figure 3-6 where the resistance has an excellent linear relation with the strain. The gauge factor of the test is calculated as 2.4.

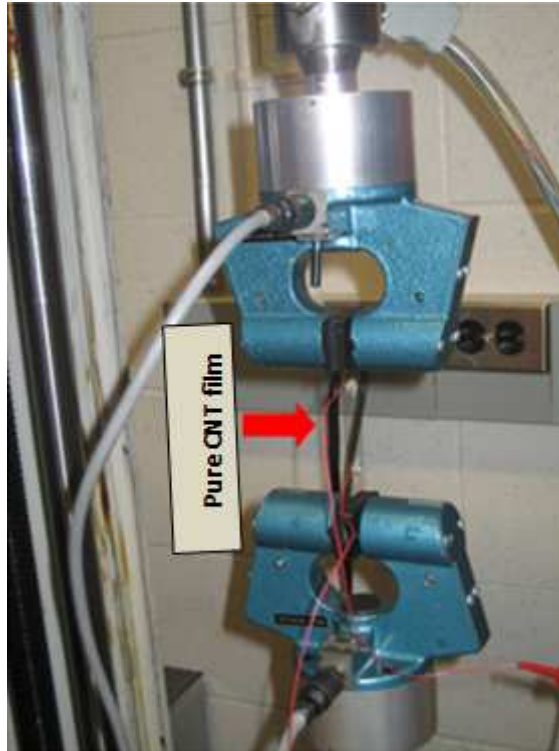


Figure 3-5: Loading a pure SWNT film under the tester Instron 1122, the changes in resistance of pure CNT films measured by a multimeter

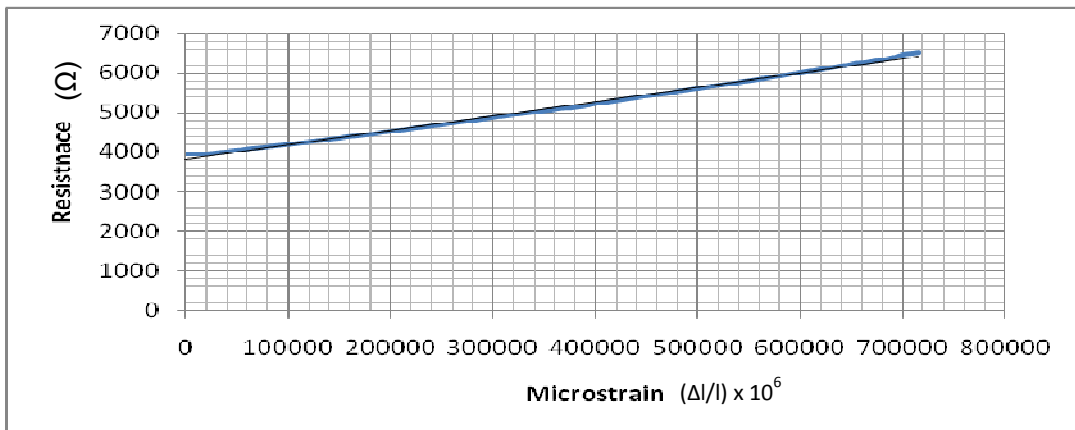


Figure 3-6: Linear relation between resistance and strain in the pure SWNT film with one layer SWNT networks under in-plane stretching

### 3.3 Results and discussion

In the test of piezoresistive response in the pure SWNT film, the changes in resistance due to the changes in the strain can be detected. More importantly, the relation of resistance and strain can be represented by a linear line shown in Figure 3-6. The slope of this line represents the gauge factor of the pure SWNT film, which is 2.4 in this case.

The structure of the pure SWNT film can be represented by the model shown in Figure 3-7. In this model, SWNTs are randomly distributed on the PET polymer substrate. The bonding between the PET polymer substrate and SWNT networks is VDW interaction. Figure 3-8 shows the structure of these CNT networks on the PET substrate under the SEM spectroscopy. In the SWNT networks, no chemical bonding happens among SWNTs; thus SWNTs are connected to each other through junctions which are formed by the van der Waals interaction. Because the SWNTs we used are semi-conductive SWNTs; the conductive paths are thus established through SWNTs and junctions, as shown in Figure 3-9.

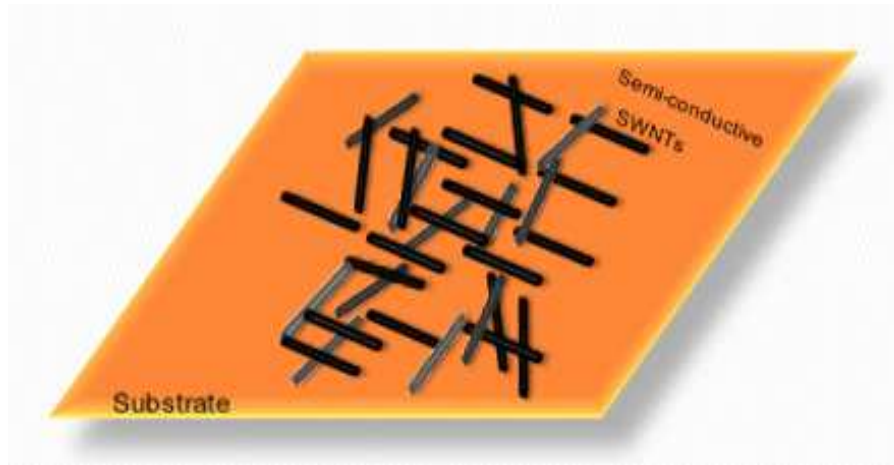


Figure 3-7: Schematic model of the pure SWNT film: the semi-conductive SWNTs randomly distributed on the PET polymer substrate

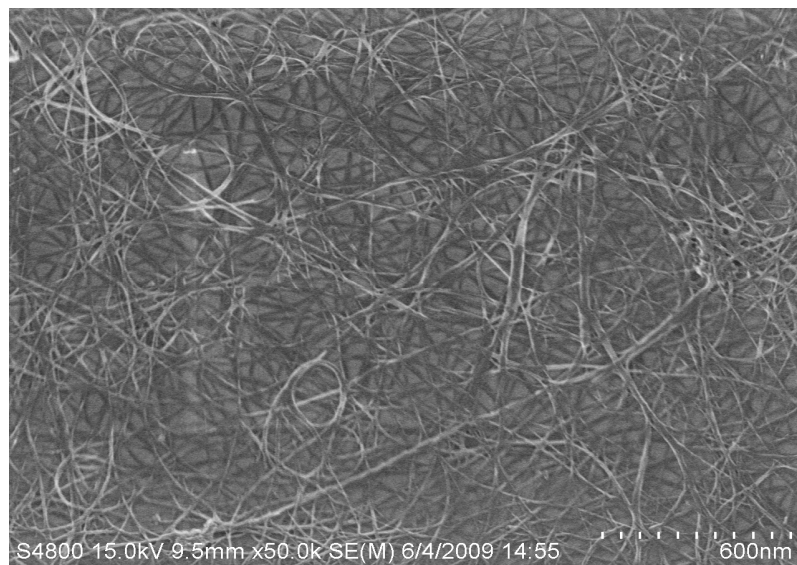


Figure 3-8: The pure SWNT film under the SEM spectroscopy (Provided by Unidym, Inc.)

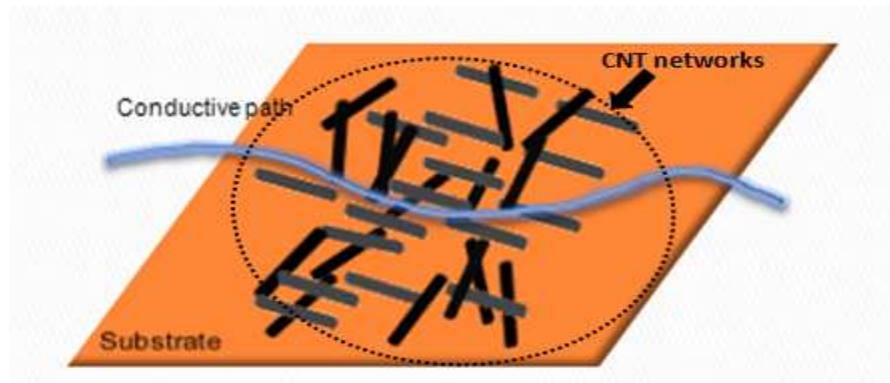


Figure 3-9: A conductive path established through semi-conductive SWNTs and junctions between SWNTs in CNT networks

The experiment conducted by Tan *et al.* (2007) showed that the polymer matrixes can provide a stronger VDW interaction with SWNTs, which is much stronger than the VDW interaction, existed between SWNTs in the CNT networks. As a result, when the polymer substrate experiences the strains, the original VDW bonding between SWNTs is broken first in the SWNT networks. The new SWNT networks are formed where the new conductive paths are established. The change between the old and new conductive paths can be represented by a schematic model, as shown in Figure 3-10, and these changes can be detected by the change of resistance in pure SWNT networks.

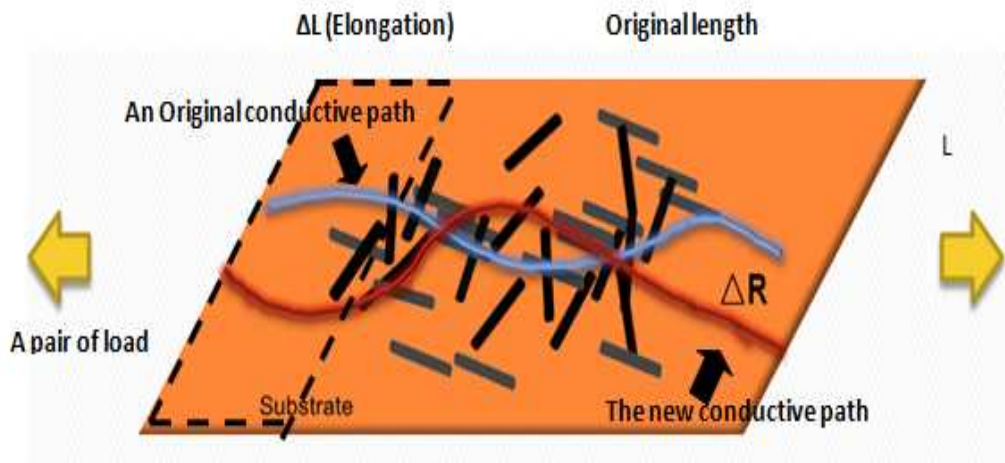


Figure 3-10: Schematic model of piezoresistive response in the pure SWNT film: the conductive paths change as CNT networks experience the elongation

Based on the above discussion, piezoresistive sensitivity and linearity can be affected by the number of junctions, distribution of CNT networks and other important factors. The influence caused by these factors will be further discussed later in Chapter 5.

It is interesting to note that the piezoresistive sensitivity of that one layer pure SWNT film is higher than that of the CNT composite film, such as SWNT-PVA/PSS film (1.5) fabricated by Lynch *et al.* (2008) and CNT/PMMA film (1.76) fabricated by Kang *et al.* (2006).

It is thus highly speculative that such improvement may likely be because the absence of surfactants in the CNT networks. This speculation will be further discussed in Chapter 6.



### **3.4 Conclusion**

The experiment of piezoresistive response in pure CNT films has shown a linear relation between resistance and strain in the pure SWNT film. The piezoresistive response in the pure SWNT networks is mostly based on the changes of junctions between SWNTs during in-plane stretching. The piezoresistive sensitivity of the pure SWNT film is about GF 2.4, which is higher than that in the CNT composite film. Such improvement is likely due to the absence of surfactants in the CNT networks.

## **Chapter 4**

### **Fabrication of Pure SWNT films**

#### **4.1 Introduction**

The fabrication of pure SWNT films includes four steps which were proposed by Kaempgen *et al.* (2005). However, detailed information of the fabrication process is not reported in the literature. In this thesis, the fabrication technique for both one layer and multilayered pure SWNT films was studied. The substrate considered is PET. In addition, the uniformity of multilayered pure SWNT networks is investigated with Raman spectroscopy.

#### **4.2 Materials for fabrication of the pure SWNT film**

The materials for fabrication of the pure SWNT film are discussed as follows:

HiPCo SWNTs:

The HiPCo SWNTs were purchased from Unidym, Inc. in The United States. The diameter of the HiPCo SWNTs is around  $1.5\text{nm}$ . The SWNT powders contain

13% iron ash content. The HiPCo SWNTs are made from a high pressure carbon monoxide process, which was developed at Rice University. During the process, catalyst particles enter the HiPCo reactor at room with  $1000^{\circ}C$  to facilitate the growth of SWNTs on the metal substrates

PET films:

The polyethylene terephthalate (PET) film, called Melinex 451, was purchased from DuPont, Inc. in the United States. The film is  $0.7mm$  in thickness and transparent. The PET film is a polyester film made from polyethylene terephthalate. PET films usually have superior mechanical properties and thermal stability compared with other polymer films. Thus, the PET film was used as the substrate for fabrication of pure SWNT networks.

Sodium dodecyl sulfate (SDS):

SDS powders which were obtained from Sigma Aldrich, Inc in Canada. SDS are the common surfactants used in many cleaning and hygiene products. The molecule structure of SDS has long alkyl chains that can facilitate dispersion of CNTs during sonication.

### **4.3 Fabrication of the one layer pure SWNT film**

Step 1: Sonication

SDS was used as the surfactant to disperse and stabilize HiPCo SWNTs in solution by a probe sonicator 340 shown in Figure 4-1. The concentration of SDS was 1%wt, which allows that SWNTs are adequately dispersed in the SDS solution. The concentration of SWNT and the sonication time can be varied to meet different requirements. Before sonication, the CNTs in aqueous surfactants stick to each other and appear as bundles. Jeong *et al.* (2002) suggested that sonication of CNTs in an appropriate solvent can cut the nanotubes and break CNT bundles. The dispersion was sonicated for various lengths of times, from 1 hour to 21 hours.

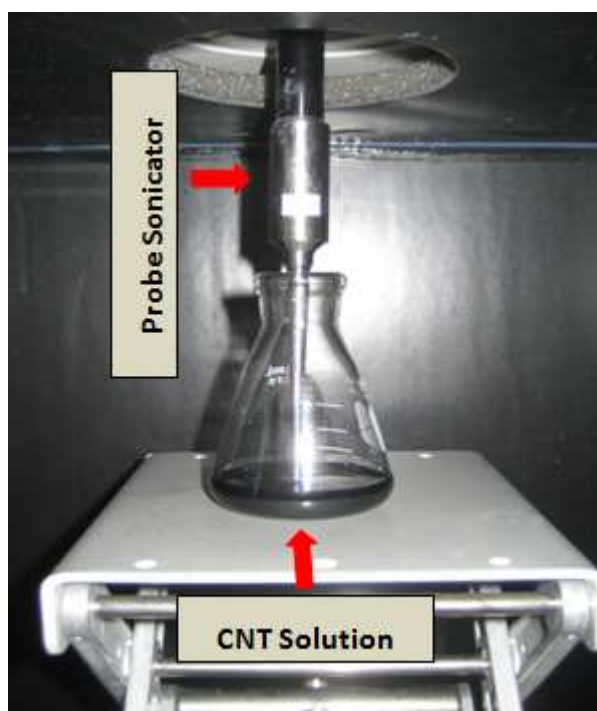


Figure 4-1: Sonicator (BRANSON SONIFIER 150) sonicate the CNT solution at 40W

## Step 2: Centrifuge

After various lengths of time of the sonication, the SWNT-SDS solution was removed from the dispersion and centrifuges for 30mins at 14 000 *rpm* in the centrifuge EPPENDORF, as shown in Figure 4-2. The centrifuge has two purposes. First, the centrifuging improves the uniformity of the CNT solution. Second, Artukovic *et al.* (2005) suggested that after centrifugation, the suspension can be decanted so that only the supernatant of the centrifuged material is included in the final suspension.

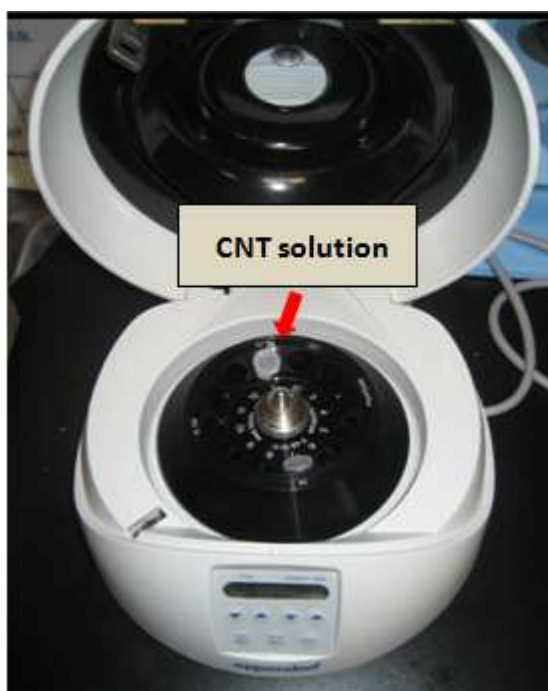


Figure 4-2: Centrifuge SWNT-SDS solution at 14000 rpm for 30 minutes in the Centrifuge (EPPENDORF)

## Step 3: Spray Coating

The SWNT-SDS solution was carefully decanted into the spray gun and ready for the

coating process. Before coating, the PET substrate was heated through an aluminum plate to 70 °C by a 150W infrared light bulb shown in Figure 4-3. High temperature will prevent water from accumulating on the PET substrate when the SWNT-SDS solution is sprayed on it.

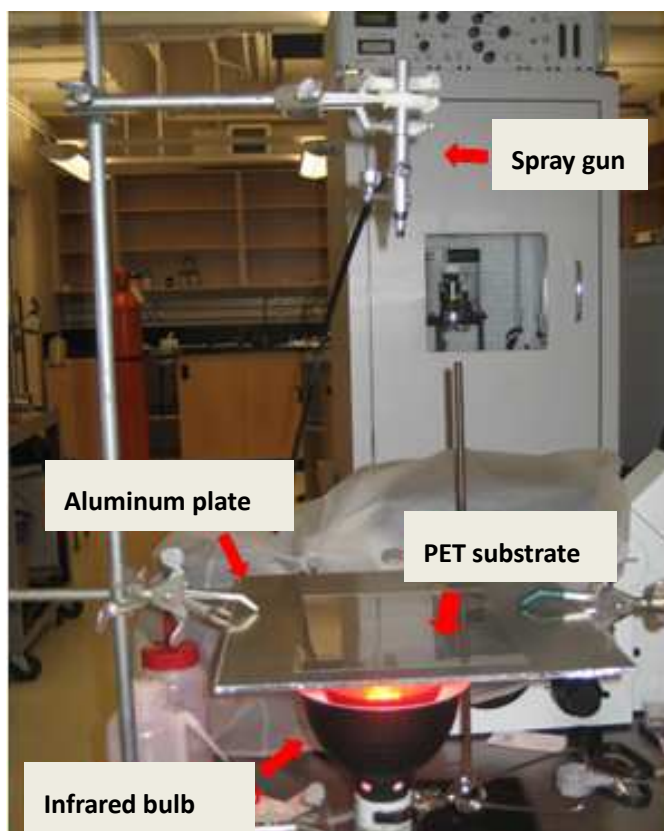


Figure 4-3: PET substrate heated through an aluminum plate by a red infrared bulb during the spray coating process

#### Step 4: Rinsing off the SDS

After a layer of SWNT networks was coated on the substrate, SDS was rinsed off by dipping the films in distilled water. On the final product of pure SWNT films, the SWNTs are randomly distributed over the PET substrate without SDS in CNT

networks.

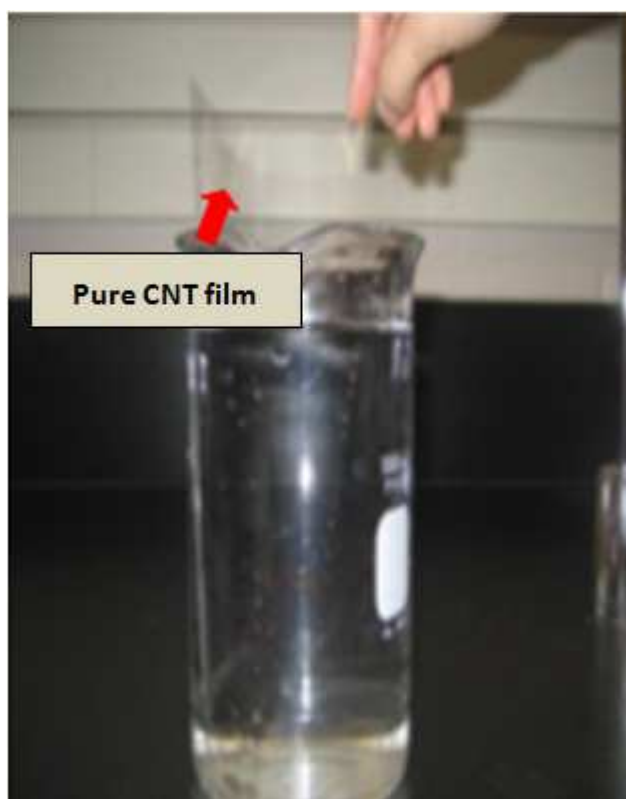


Figure 4-4: Rinsing off SDS in distilled water after the spray coating one layer of CNT networks on the PET substrate

#### 4.4 Fabrication of the multilayered pure SWNT film

After the preceding four steps, one layer of the pure SWNT networks has been deposited on the PET substrate. The process can be repeated to fabricate multilayered pure SWNT networks, as shown in Figure 4-5. The fabrication method for the multilayered pure SWNT film was inspired by the LBL fabrication technique proposed by Lynch *et al.* (2007). In their research, they repeated the dip coating

process to build multilayered CNT composite film for strain detection.

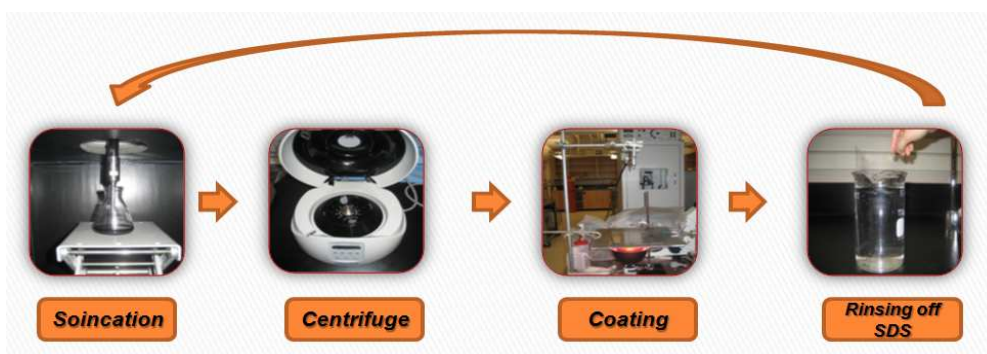


Figure 4-5: Fabrication multilayered pure CNT film by repeating four steps

#### 4.5 Uniformity of multilayered pure SWNT networks

In the fabrication of multilayered SWNT networks, uniform multilayered SWNT networks were deposited on the PET substrate by the spray coating. The uniformity of the multilayered SWNT networks is important to the quality of the films. The Raman spectroscopy was employed to measure the uniformity of CNT networks. Hagrasy *et al.* (2006) proposed this method for the determination of coating uniformity with assistance of Raman spectroscopy. In their work, they compared data obtained from 2 sources: Raman's results and samples in real. The results showed that the two data sets were in agreement. The measurement of uniformity of the SWNT networks includes five steps.

Step1: Identifying the coating area



The area with SWNT networks which shows resistance can be measured by a multimeter with two conductive probes shown in Figure 4-6.



Figure 4-6: Identify the coating area which contains CNT networks by a multimeter

#### Step 2: Scanning the PET substrate

The PET substrate was scanned under the Raman Microscope Renishaw 2000. The scanning of the PET substrate is to identify the elements in PET materials, which provide a comparison with the scanning of the pure CNT film. The spectral acquisition setups in the Raman scanning are shown in Figure 4-7 and Figure 4-8.

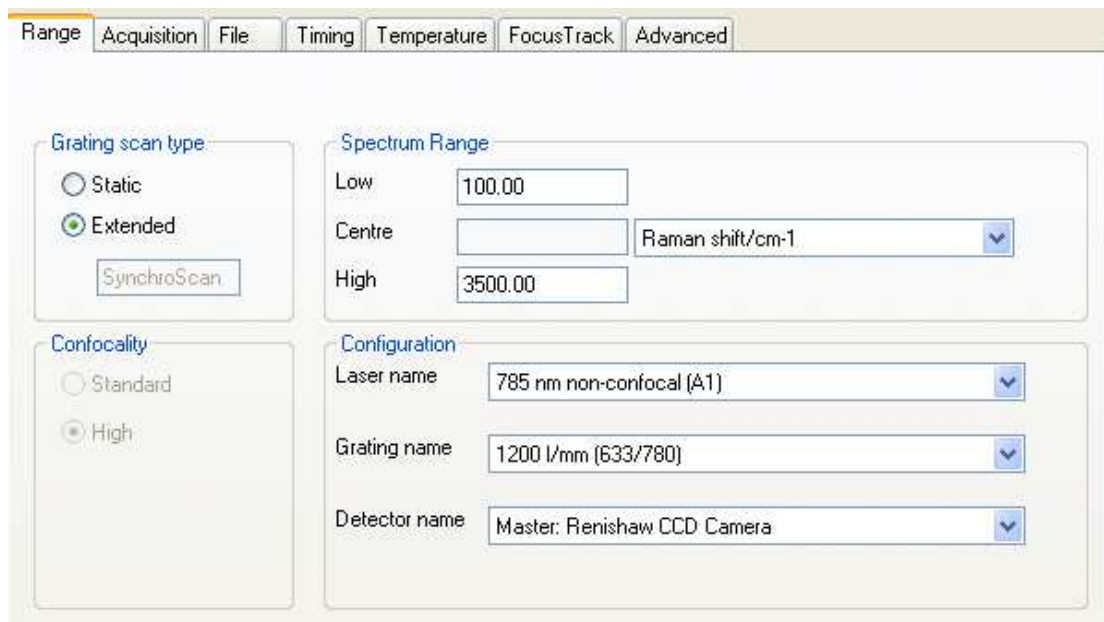


Figure 4-7: The spectral acquisition setups, including the information about Laser device, Grating name and detector name

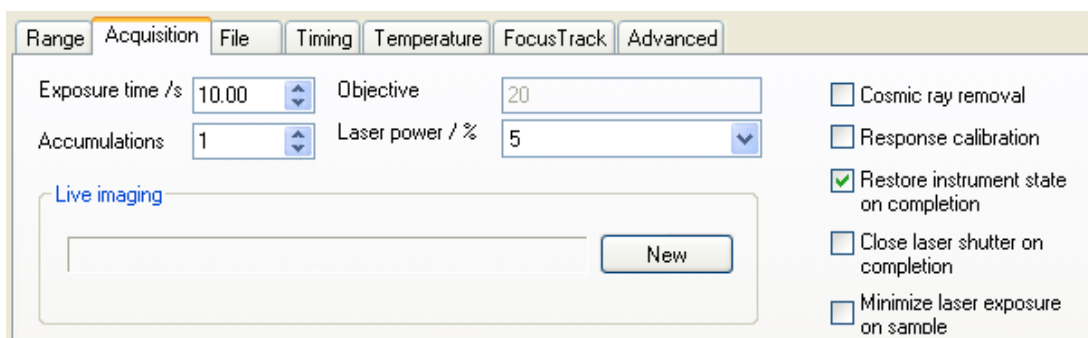


Figure 4-8: The spectral acquisition setups, including the information about the laser power, exposure time and accumulations

The spectrum result shown in Figure 4-9 presents the spectrum of the PET, which are indentified by different peaks.

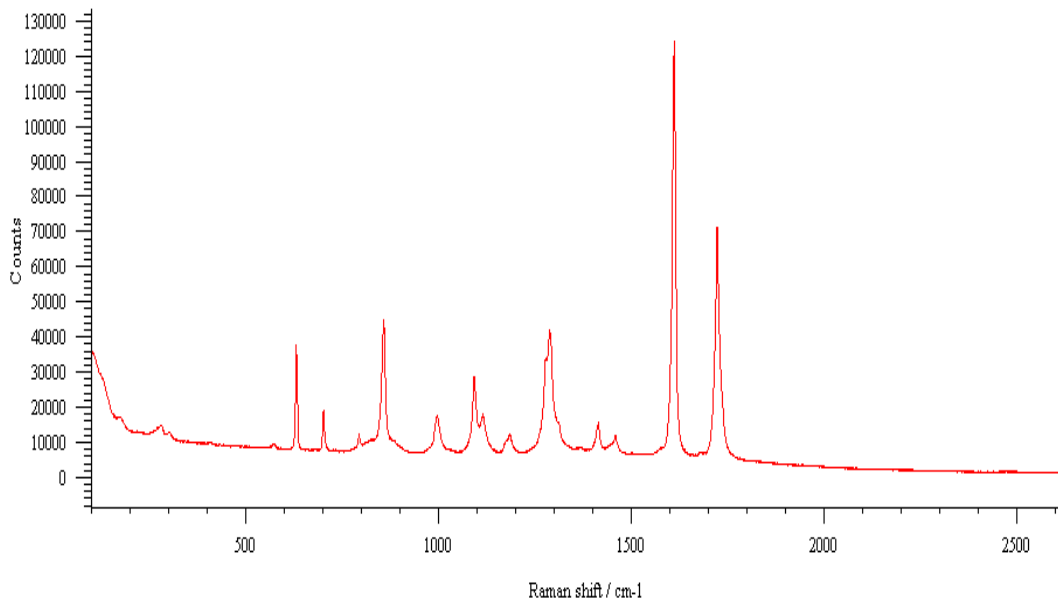


Figure 4-9: Spectrum results of the PET substrate under the Raman Microscope  
Renishaw 2000

### Step 3: Identifying SWNT networks

In this step, the PET substrate with CNT networks was examined under the same scanning setups as described in step 2.

The spectrum result of the pure CNT film is shown in Figure 4-10. In this figure, there are three new peaks appear at  $0-500\text{cm}^{-1}$  shift and  $1500-1800\text{ cm}^{-1}$  shift, as shown in the red circles. The characterization of SWNTs identified by Keszler *et al.* (2004) under Raman spectroscopy also shows the peaks appearing at the same shift range. Therefore these new peaks shown in red circles mean the existence of SWNTs in the pure CNT film. The amplitude of counts here demonstrates the density of SWNTs on

the PET substrate in each scanning spot.

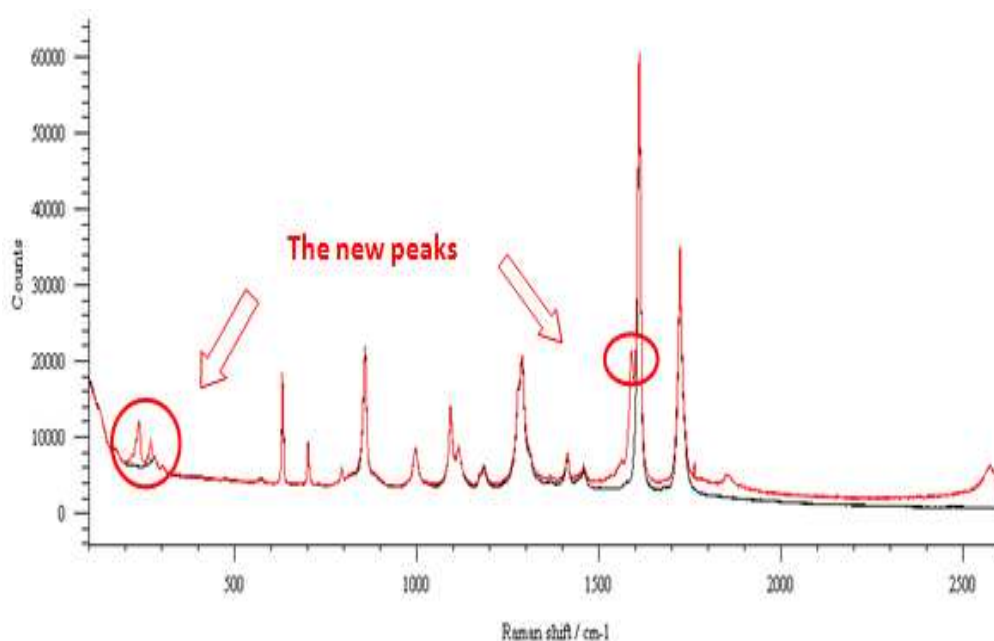


Figure 4-10: Spectrum of SWNT deposited on PET substrate (in red) and Spectrum of the PET substrate (in black), the difference between the two spectrums marked in red circles presenting the existence of SWNTs

#### Step 4: Measuring the uniformity of SWNT networks

Within the coating area, 40 spots were picked and scanned. The results in Figure 4-11 show that there is variation in amplitude of count at  $1589\text{ cm}^{-1}$  shift, which exhibits the variance in density of SWNTs at different scanning spots. This variation affects the uniformity of the multilayered SWNT networks.

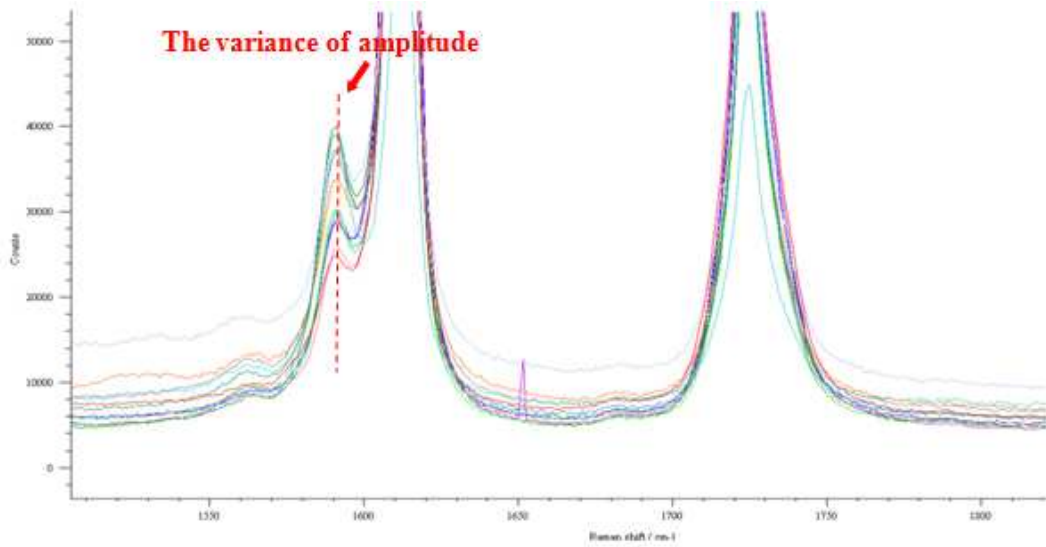


Figure 4-11: Amplitudes of Count Peaks in different scanning spots at  $1589\text{cm}^{-1}$  shift, the variance of amplitude representing the difference of density of SWNTs at each scanning spot

#### Step 5: Data analysis

The amplitudes of peaks at  $1589\text{ cm}^{-1}$  shift were collected in 40 different scanning spots shown in Table 4-1 and 4-2. The coefficient of dispersion is calculated based on these data. The coefficient of dispersion here is used as the measurement of coating uniformity, defined as the ratio of the standard variance  $\sigma^2$  to the mean  $\mu$ . Measurements by Hagrasy *et al.* (2006) showed, in the uniform coating; the range of the coefficient of dispersion was from 0.075 to 0.126 based on their samples.

Table 4-1: The value of amplitude at  $1590\text{ cm}^{-1}$  shift in the pure CNT film (10 layers of CNT network at  $0.8\text{mg/ml}$ )

15029	18845.6	15875.7	19895.8	15052.5	22657.4	17729.1	18755.4	17452.1	18936.2
14880.6	17975.7	18856.8	18424	18233	17620.2	16151.3	20918.2	17209.3	18318
18278.8	19076.1	12124.3	13406.1	17032.3	18965.02	14985.5	16073.8	19061.3	16696.8
17641.96	17443.7	15111.9	14189.8	16087.2	18712	15128.6	15960.2	17777.1	16429.7
Standard Deviation:		2063.484							
Mean:		17224.95							

Table 4-2: The value of amplitude at  $1590\text{ cm}^{-1}$  shift in the pure CNT film (20 layers of CNT network at  $0.8\text{mg/ml}$ )

48304	45039.7	53056.7	52741	56745	50758	55760.3	44215.9	60274.7	45765.5
54255.2	44934	54655	44446	48593	52385	54392.6	44931.5	37477.7	40087.5
45957.6	47634.6	51201.1	43907.7	43313.9	51426	52607	60500.8	46106.8	51978.2
42344.4	48626.6	49960.8	41183	53039	50858.7	60166.1	50536	47438	46359.7
Standard Deviation:		5506.709							
Mean:		49349.11							

In the pure SWNT film with 10 and 20 layered SWNT networks, the coefficient of dispersion is 0.12 and 0.11. Both values are within the range of the coefficient of dispersion proposed by Hagrasy *et al.* (2006); thus the multilayered SWNT networks are uniform.

## 4.6 Conclusion

The fabrication of the multilayered pure CNT film was proposed and presented in this chapter. Four steps are needed to deposit each layer of CNT networks on the substrate. The coating quality of multilayered pure CNT films is measured with the help of the Raman spectroscopy. The multilayered CNT networks fabricated with the proposed approach are within an acceptable uniformity in comparison with the standards presented by Hagrasy *et al.* (2006).

## **Chapter 5**

### **Optimizing Piezoresistive Sensitivity of the SWNT film**

#### **5.1 Introduction**

Optimizing piezoresistive sensitivity of multilayer CNT composite film was studied by Lynch *et al.* (2007). In their experiment, they demonstrated that CNT based sensor strain can be tailored to a wide variety of piezoresistive properties including sensitivity, linearity and conductivity. These properties are related to the fabrication parameters. In this thesis, three independent fabrication parameters, namely (1) SWNT concentration (2) Film thickness (the number of layers of CNT networks) and (3) Sonication hours, are varied to correlate their influences on the piezoresistive sensitivity of pure SWNT films. In addition, the best multilayered CNT film for strain sensor will be determined from an optimal combination of these parameters.

#### **5.2 Control experiment I**

The concentration of SWNT with 2 hour sonication in 1% SDS solution was varied.

Specifically, three different SWNT concentrations were investigated, namely:



0.5mg/ml, 0.8mg/ml and 1.0mg/ml. Selection of the concentrations of the SWNT and surfactants were based on the work by Vigolo *et al.* (2000). They showed that such combination of concentrations can provide an adequate dispersion of SWNT with surfactants in solutions.

Generally speaking, the solution with a high SWNT concentration produces a high density SWNT network on the substrate after the coating process; thus more junctions are created in the SWNT network. The changes in the number of junctions will affect piezoresistive sensitivities in SWNT networks. This theory that was first presented by Stadermann *et al.* (2004) allows us to hypothesize that additional junctions created would contribute to the increase in piezoresistive response under in-plane stretching.

### **5.3 Control experiment II**

The layers of SWNT deposited on the PET substrate were varied. Correspondingly, this control experiment on the varying layers of SWNT also mainly affects the density of the CNT networks. In the control experiment, six different layers of SWNT networks were investigated: namely, 5, 10, 15, 20, 25 and 30 layers.

Both control experiment I and II affected the density of SWNT networks. Two control experiments were combined to investigate piezoresistive response of CNT films caused by the density of SWNT networks. A total of 45 samples of SWNT films were

fabricated for the two experiments. The fabrication of the multilayered pure SWNT film followed the same process and setups proposed in Chapter 5. The experiment of piezoresistive response in the sample films followed the same test method proposed in Chapter 4. Figure 5-1 shows the experimental result of piezoresistive response in a pure SWNT film under in-plane stretching.

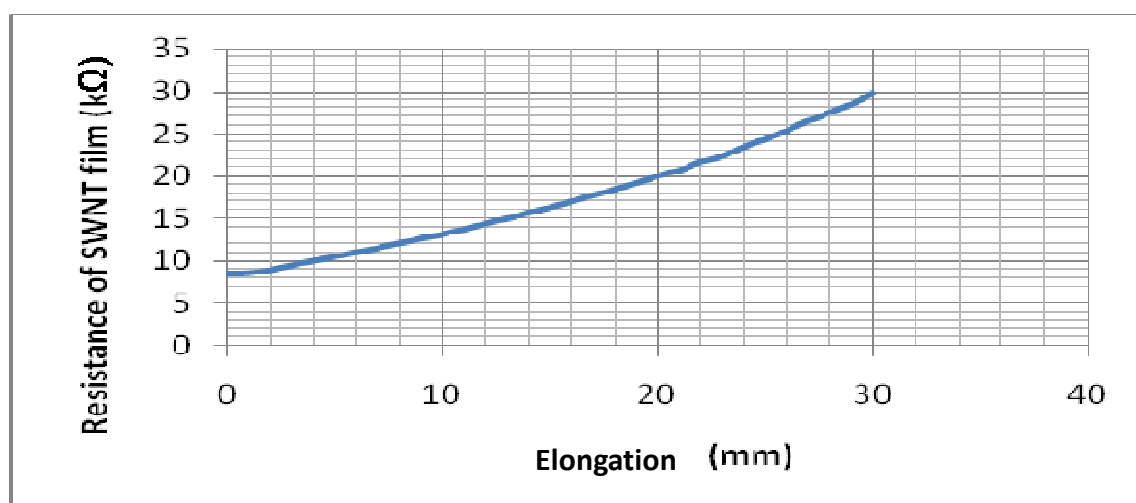


Figure 5-1: The relation of resistance versus elongation in a SWNT film with 10 layers of SWNT networks at CNT concentration 1 *mg/ml*

#### 5.4 Control experiment III

Hours of sonication in SWNT/SDS solution were varied. The SWNT/SDS solution was sonicated for various lengths of time, from 1 hour to 21 hours, using the same probe sonicator. A sample of the SWNT-SDS solution was removed from the sonicator. After every 2 hours, the suspension was carefully decanted to a coating container and deposited on the PET substrate to form 10 layers of SWNT networks.

The concentration of SWNT in this experiment was controlled at  $0.8\text{mg/ml}$ . The fabrication and experiment method in control experiment III was the same as control experiments I and II, as described before.

In the three control experiments, the calculation of piezoresistive sensitivity and linearity in different samples was based on the same elongation range. Figure 5-2 shows a linear relation between strain and resistance in one of the samples. This linear relation can be represented by a line with slope of 0.6259 with the linearity of 99.57% and gauge factor of 2.211.

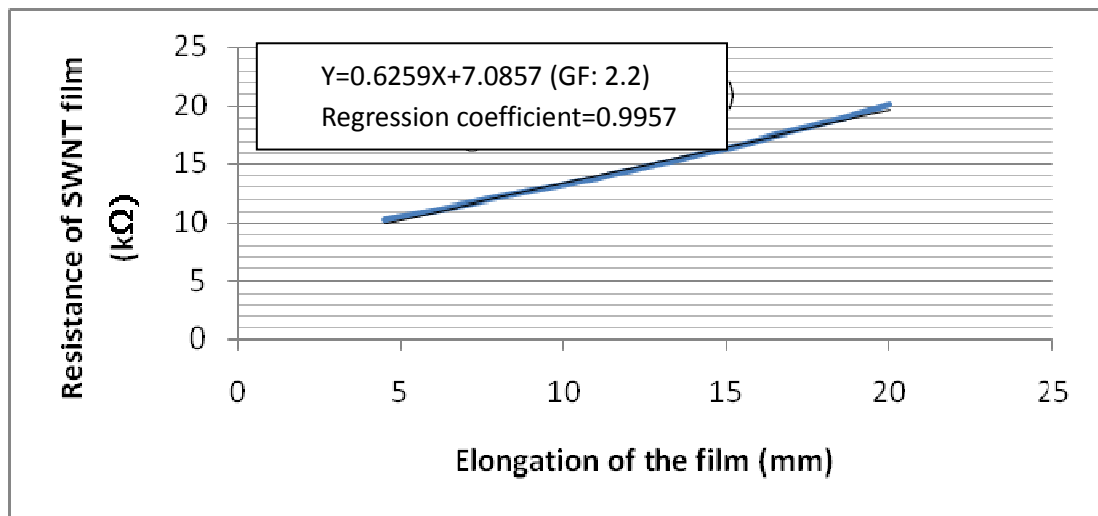


Figure 5-2: Calculated linear function and linear regression of the SWNT film with 10 layers of SWNT networks at CNT concentration  $1\text{mg/ml}$

## 5.5 Results and Discussion

### Control experiment I and II

In control experiments I and II, the density of SWNTs influences conductivity and piezoresistive response in the pure SWNT film. The measurements show that the resistance of the 10 layered SWNT film with  $0.5\text{mg/ml}$ ,  $0.8\text{mg/ml}$  and  $1\text{mg/ml}$  is on the order of  $10^3\sim 10^4\text{k}\Omega$ ,  $10\sim 10^2\text{k}\Omega$  and  $0\sim 10\text{k}\Omega$  per square respectively. This result is in agreement with the fact that the CNT networks with high density have high conductivity, which was previously presented by Hu *et al.* (2004). In their studies, they developed a relation between the conductivity and the density of SWNT networks, shown in Equation (5-1) and (5-2), respectively.

$$\sigma \propto (N - N_c)^\alpha \quad (5-1)$$

$$l\sqrt{\pi N_c} = 4.236 \quad (5-2)$$

where  $\sigma$  refers to the conductivity per square of the pure SWNT networks,  $N$  is the CNT bundles(CB) density, and  $N_c$  is the critical density corresponding to the percolation threshold,  $\alpha$  is 1.33 for a film in two dimensions, and  $l$  is the length of CB. Under the same sonication time, the length of CNT bundles is considered to be the same in all samples. Based on equation (5-1), the high conductivity of the pure SWNT networks can only be caused by the high density of CS in SWNT networks, when the lengths of CNT bundles are the same.

In the CNT networks with high density, more junctions exist and contribute to

piezoresistive response. Previous research from Lynch *et al.* (2007) showed that junctions between CNTs directly influence the piezoresistivity of CNT networks during in-plane stretching. Figure 5-3 shows the gauge factor of pure SWNT film with different concentrations of SWNT solutions and with different layers of SWNT networks. The detailed experimental results are shown in Table 5-1.

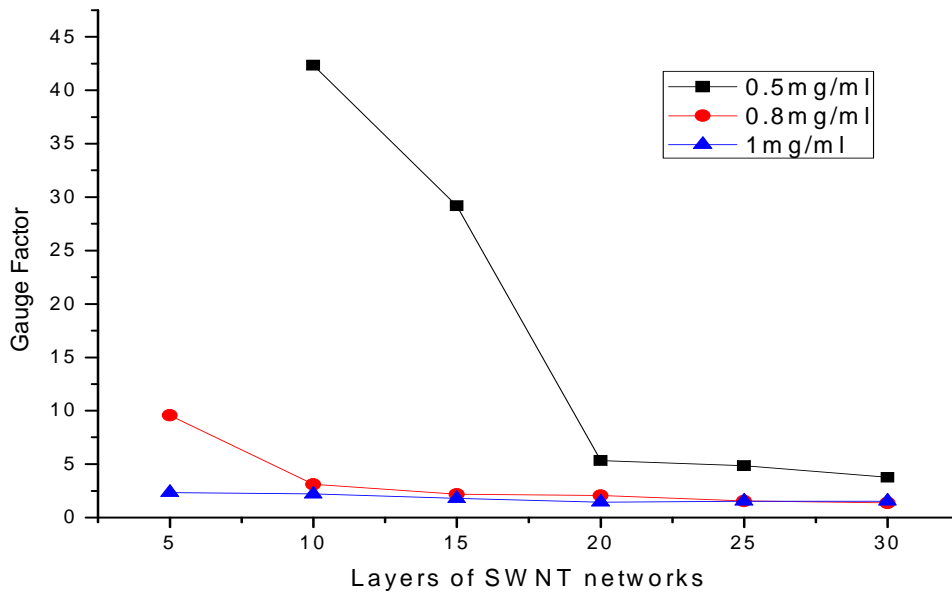


Figure 5-3: Gauge factor versus numbers of layers of SWNT networks at different concentration of SWNT solution

Table 5-1: Gauge factors at different numbers of layers of SWNT networks with different concentration of SWNT solution

Gague factor			
SWNT layers/concentraions	0.5mg/ml	0.8mg/ml	1mg/ml
5Layers	N/A	11.26	2.34
10Layers	42.34	2.59	1.99
15Layers	26.82	1.99	1.79
20Layers	5.36	1.77	1.435
25Layers	4.836	1.56	1.53
30Layers	3.77	1.375	1.54

In the SWNT networks with the same concentration of SWNT solution, the result shows that piezoresistive sensitivity of pure SWNT films decreases as the number of layers increases. In the films with the same layers of SWNT networks, the SWNT networks with a lower concentration have higher piezoresistive sensitivity. The two results are in agreement with each other; that is the SWNT networks with high density will produce more junctions to contribute to piezoresistive response; however piezoresistive sensitivity (gauge factor) of such SWNT networks decreases.

The above results have shown that the SWNT networks with high density will have better conductivity and lower piezoresistive sensitivity.

The piezoresistive linearity represents the changes in piezoresistive sensitivity in the materials which is also an important parameter for strain detection. In the pure SWNT film, the piezoresistive sensitivity is supposed not to change while CNT networks

experience different strains. However, piezoresistive response in the SWNT networks with low density present high non-linearity to the strains shown in Figure 5-4. The high non-linearity in the SWNT networks can be considered as the result of the instability of the low density SWNT networks. In the SWNT networks, the low density of SWNTs provides weak VDW interactions, which was proposed by Cao *et al.* (2005). In their studies, they discussed that the VDW interaction is positively proportional to the number of SWNTs. In CNT networks, the VDW interaction directly influences their mechanical properties. The stronger the VDW interaction provides extra mechanical strength in CNT networks; thus the CNT networks with low density tend to be unstable as they are in straining.

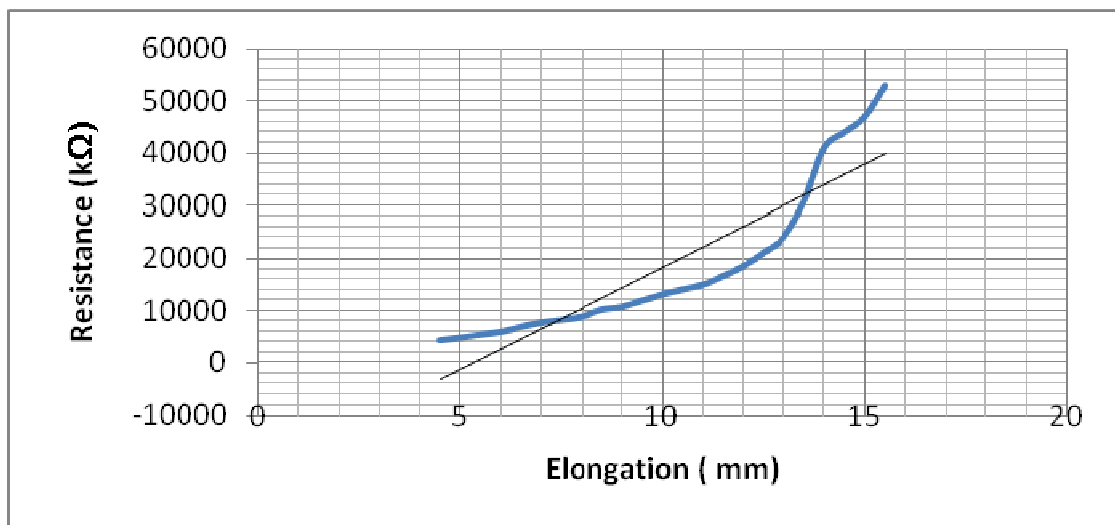


Figure 5-4: Relation between resistance and elongation in the pure SWNT film with 10 layers of SWNT networks at the CNT concentration 0.5 mg/ml

Figure 5-4 and 5-5 provide a comparison of piezoresistive linearity between the film

with high and low density of CNT networks. In Figure 5-6 , the linearity of the piezoresistive response is improved as the densities of CNT networks increase. These results are in agreement with the proposed conclusion in the last paragraph. The more detailed results are shown in Table 5-2.

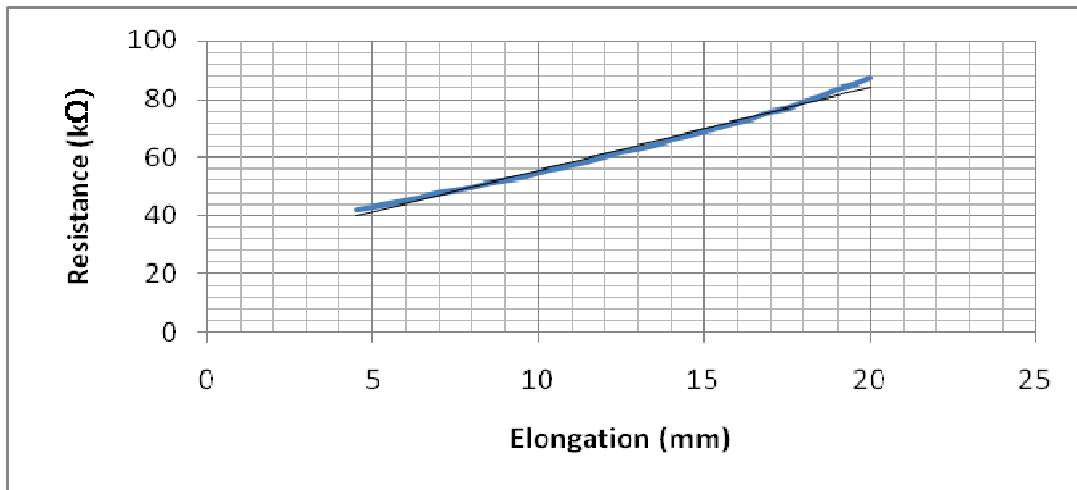


Figure 5-5: The relation between resistance and elongation in the pure SWNT film with 10 layers of SWNT networks at the CNT concentration  $1\text{mg/ml}$



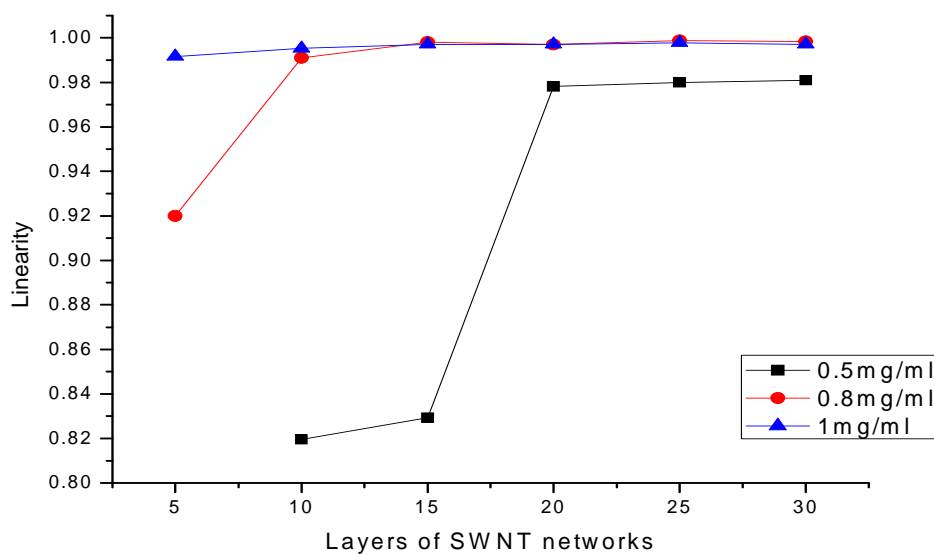


Figure 5-6: Piezoresistive linearity versus numbers of layers of SWNT networks at different concentration of SWNT solution

Table 5-2: Linearity at different numbers of layers of SWNT networks with different concentration of SWNT solution

Regression Coefficient			
SWNT layers/concentraions	0.5mg/ml	0.8mg/ml	1mg/ml
5Layers	N/A	0.92	0.9917
10Layers	0.8196	0.9911	0.9953
15Layers	0.8293	0.9981	0.9971
20Layers	0.9782	0.997	0.9971
25Layers	0.98	0.9988	0.9979
30Layers	0.981	0.9983	0.9971

### Control experiment III

The sonication time can affect the distribution of SWNT networks, which causes piezoresistive response to change. Hecht *et al.* (2006) presented that the length of the tubes decreases exponentially with sonication time from  $4\mu\text{m}$  initially to  $0.4\mu\text{m}$ , after about 21 hours of sonication, and that the diameter of the bundles decreases dramatically, initially from  $5\text{nm}$  to  $3\text{nm}$  in the first 5 min of sonication, and then remains constant between  $2\text{nm}$  and  $3\text{nm}$  after that. In addition, the number of junctions between SWNTs increases in the SWNT networks, when more SWNT bundles are cut and separated during a longer sonication time. Therefore, an experiment with different sonication times is applied here to investigate the influence of the length of SWNT and number of junctions on piezoresistive response in the SWNT networks.

At each sonication time, the resistance of three samples was measured. In Figure 5-7, the measurement shows that the resistance of the pure SWNT film with different sonication times. The conductivities of these films are within the same order of  $10^2$  resistances; thus the sonication time has less influence on the resistance of these films than the density of CNT networks.

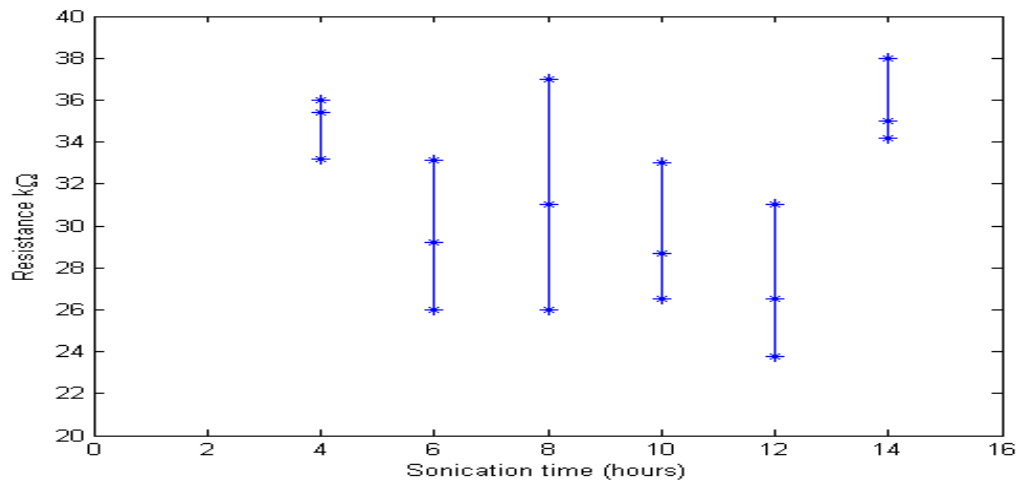


Figure 5-7: Resistance of the pure SWNT film at different sonication time (three samples measured at each sonication time)

However, more junctions are created contributing to piezoresistive response in the SWNT networks, as a longer sonication time may break down more SWNT bundles and cuts SWNTs. Figure 5-8 shows that piezoresistive sensitivity of SWNT networks decreases with the increase in sonication time. This result is consistent with the conclusion of control experiments I and II that the CNT networks with more junctions have a lower piezoresistive sensitivity. The detailed results are shown in Table 5-3.

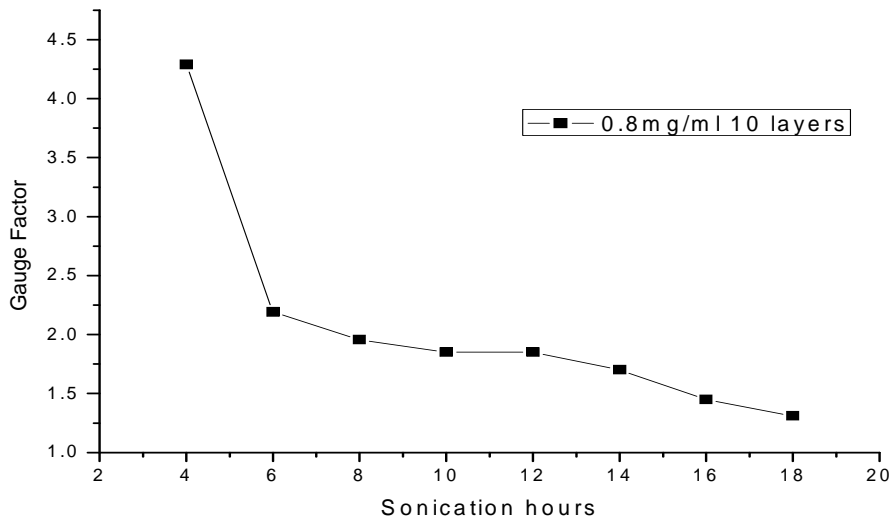


Figure 5-8: Gauges factor versus different sonication time in the pure SWNT film with 10 layers of SWNT networks at the CNT concentration  $0.8\text{mg/ml}$

Table 5-3: Gauge Factor and linearity of SWNT films ( $0.8\text{mg/ml}$  SWNT) at different sonication hours

Sonication time	4hours	6hours	8hours	10hours
Gage Factor	4.288	2.19	1.956	1.85
Regression Coefficient	0.975	0.9959	0.9961	0.9982
Sonication time	12hours	14hours	16hours	18hours
Gage Factor	1.85	1.7	1.45	1.31
Regression Coefficient	0.9966	0.996	0.9995	0.99865

In addition, the experimental result also show that the linearity of piezoresistive response in the SWNT networks does not change dramatically at different sonication times, as shown in Figure 5-9; thus sonication times have less influence on the stability of SWNT networks than the density of CNT networks.

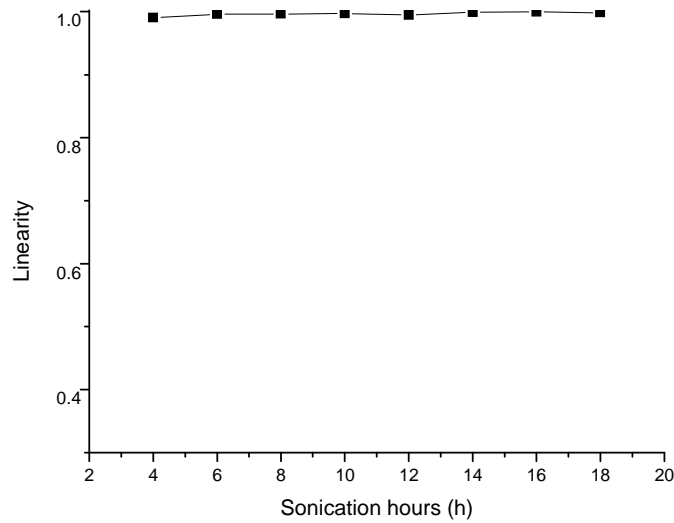


Figure 5-9: Linearity versus different sonication hours in the pure SWNT film with 10 layers of SWNT networks at the CNT concentration  $0.8\text{mg/ml}$

The stability of SWNT networks with different sonication times can be investigated under a controlled tensile test. Based on the studies by Hecht *et al.* (2006) and Cao *et al.* (2004), it can be predicted that a longer sonication time causes more SWNT bundles to cut and separate; thus the total VDW interactions in SWNT networks decrease. This decrease of the VDW interaction in SWNT networks can be detected by changes in the mechanical properties of the pure SWNT film.

The PET substrate without SWNT networks was first tested in the tensile test device Instron 1122. After that, the PET substrates with 20 layers of SWNT networks at different sonication hours were loaded in the tensile test device. A total of 16 samples were made for this test at the crosshead speed  $5\text{mm/min}$ .

In Figure 5-10, it shows that the pure SWNT film with a short sonication time presents extra strength in mechanical properties, where the elongation and the rupture load increase. This result is consistent with the predictions in the studies by Hecht *et al.* (2006) and Cao *et al.* (2004).

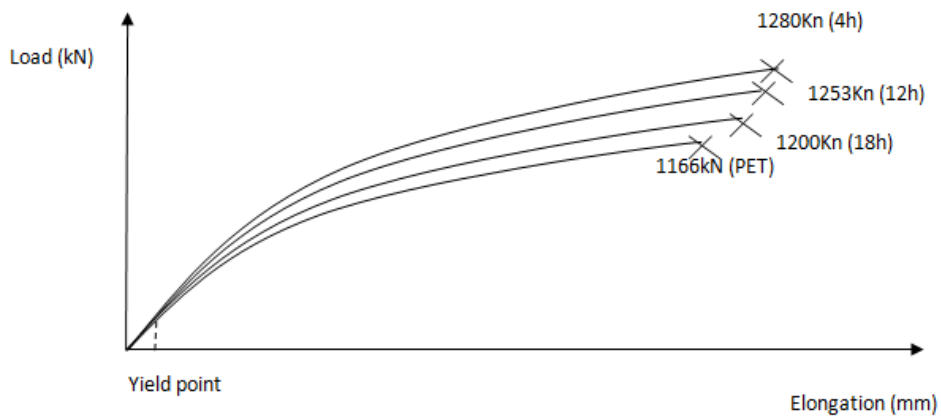


Figure 5-10: Relation between load and elongation in the PET substrate and the PET substrate with different layers of SWNT networks

## 5.5 Conclusion

The three control experiments were designed to investigate that density and distribution of SWNT networks would have influence on piezoresistive response. In control experiments I and II, the results show that the SWNT networks with high density have low piezoresistive sensitivity; however, they provide extra mechanical strength in CNT networks, which contributes to the high linearity in piezoresistive response.

In control experiment III, a longer sonication time produces more junctions, which contributes to piezoresistive response in SWNT networks; however, such SWNT networks show low piezoresistive sensitivity. In addition, the tensile tests show that the SWNT networks with longer sonication times have low VDW interactions, which cause a decrease in the mechanical properties of the pure SWNT film.

In terms of piezoresistive sensitivity and linearity, the 10 layered SWNT networks at concentration  $0.8\text{mg/ml}$  have the optimal piezoresistive response for strain detection under 2 hours of sonication time. The gauge factor of such SWNT networks is 2.59 with non-linearity of 0.89%.

## **Chapter 6**

# **Roles of Surfactants in CNT Networks for Strain Detection**

### **6.1 Introduction**

In the fabrication of CNT films, surfactants have to be used in order to suspend and disperse the CNTs in an aqueous solution. Moore *et al.* (2003) presented many surfactants that can disperse CNT in water. There are two mechanisms which govern the dispersion of surfactants: ionic bonding and polymer wrapping.

In the group of surfactants based on polymer wrapping, the results show that in general, higher molecular-weight polymers tend to form higher quality CNT solutions (Rastogi *et al.*, 2008). For instance, in the work of Lynch *et al.* (2007), they used high molecular-weight polymers PSS (1,000,000  $M_w$ ) as surfactant to develop CNT solutions. In Kang's work, they chose high molecular-weight PMMA (2,000,000  $M_w$ ) as surfactant (Kang *et al.*, 2006)



In the group of surfactants based on the ionic bonding, a wide variety of surfactants have been investigated, such as sodium dodecyl benzenesulfonate (SDBS), dodecyltrimethylammonium bromide (DTAB), hexadecyltrimethylammonium bromide (CTAB) and sodium dodecyl sulfate (SDS). In the fabrication of the pure CNT film, SDS was used to disperse the CNT in an aqueous solution according to the specification of one layer pure CNT film commercially available and our own experience as presented in Chapter 4.

The influence of surfactants on piezoresistive response in CNT networks will be studied in this chapter for two purposes. First, the study may generate new knowledge for further optimizing the design of the CNT film strain sensor. Second, the study provides a post-evidence support to the primary hypothesis behind this thesis study. It is noted that CNT is meant for SWNT throughout this chapter.

## **6.2 The SWNT/PSS and SWNT/SDS composite networks**

As a comparison, SDS was used as an ionic surfactant and PSS (1,000,000  $M_w$ ) was used as the polymer wrapping surfactant to disperse CNTs in solutions with 2 hours of sonication. The concentration of CNT solution was  $0.8\text{mg/ml}$  and the concentration of SDS and PSS each was  $1\%wt$ .

The CNT/SDS and CNT/PSS solutions were further deposited on the PET substrate

by spray coating described in Chapter 4. After air drying, the CNT/PSS and CNT/SDS composite networks were laid on the PET substrate. The fabrication of the multilayered CNT composite networks here follows the same procedure as the fabrication of the multilayered pure CNT film, as described in Chapter 4.

The experiment of the piezoresistive response in the CNT composited networks follows the same setups as discussed in Chapter 3. The 30x30mm CNT composite film was loaded under the tensile test device Instron 1122 at crosshead speed 0.5mm/min.

### **6.3 Results and discussion**

The film with CNT/PSS composite networks showed a resistance over the order of  $10^5 k\Omega$  with 30 layers of the film. Such higher resistance cannot be detected by a regular multimeter. For a 40 layer film, the film showed 56  $M\Omega$  in resistance and, gauge factor is 1.1, as calculated. For the film with more than 40 layers, the experimental results presented by Lynch *et al.* (2007) show that the gauge factor of 50 and 100 layers of CNT/PSS composite networks is about 1.54 and 1.2 respectively.

In the CNT/PSS composite networks, the PSS with long polymer chains tend to surround CNTs and thus block and change the conductive path in the CNT networks; as a result the conductivity in such CNT composite networks decrease and the overall

piezoresistive sensitivity is lower than pure CNT films.

However, the CNT/PSS composite networks showed good linearity and stability in piezoresistive response, as shown in Figure 6-1. The high molecular weight polymer PSS left in the CNT networks may be considered one of the reasons for such good linearity and stability. In the CNT/PSS composite networks, the PSS polymeric matrix provides a strong VDW bonding with CNTs to make the CNT networks stay stable during in-plane loading.

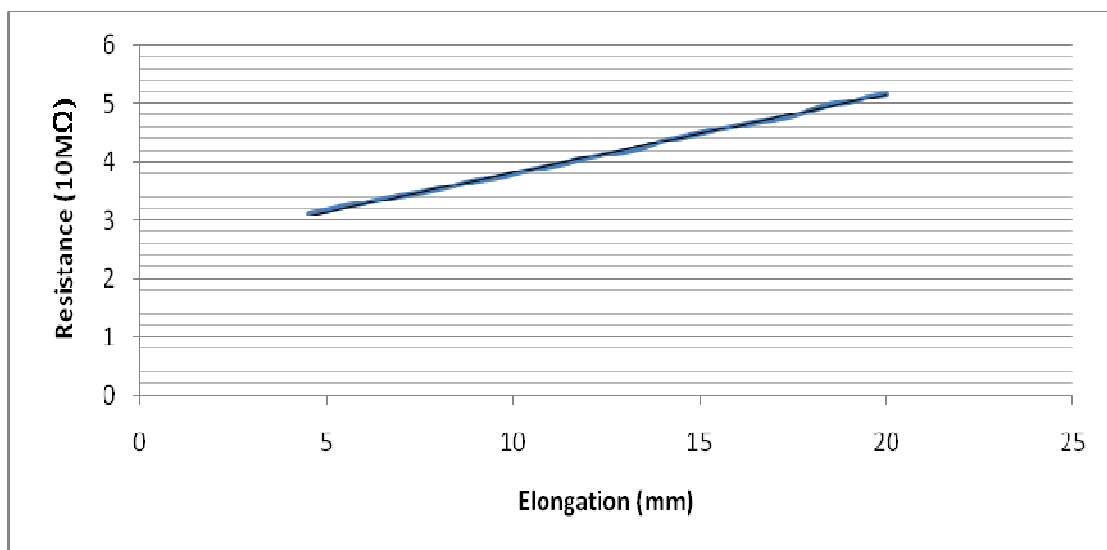


Figure 6-1: The relation between resistance and elongation in the film with 40 layers of the SWNT/PSS networks

The gauge factors of the films with different layers of CNT/SDS composite networks are shown in Figure 6-2. At the same concentration of CNT and surfactant SDS, piezoresistive sensitivity decreases as the increase of the layer of CNT networks,

which is consistent with the result discussed in Chapter 5 for the pure CNT network. In addition, the sensitivity of CNT/SDS composite networks is not significantly different from the sensitivity of the pure CNT networks. Piezoresistive sensitivity in CNT composite networks does not seem to be influenced as much by the surfactant SDS compared with the PSS. The different stabilization mechanisms between SDS and PSS are the main reason for this result.

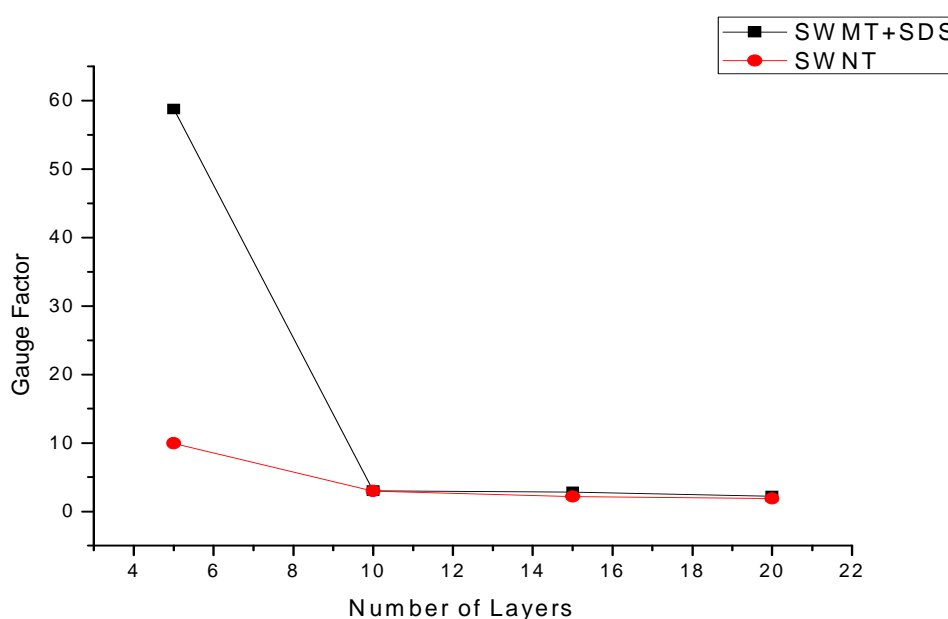


Figure 6-2: Gauge factor in the SWNT/SDS film and the pure SWNT film at different layers of SWNT networks

The SDS as ionic surfactants, unlike polymer wrapping, is absorbed to nanotube surfaces, because SDS has long alkyl chains (Islam *et al.*, 2002). They proposed a mechanism about such behavior. It is energetically favorable for the long chains to lie along the length of the nanotubes rather than to bend around the circumference of the

nanotubes, as shown in Figure 6-3. Therefore, the SDS does not block and change the conductive path in the CNT networks. As a result, the CNT/SDS networks have higher piezoresistive sensitivity than CNT/PSS networks.

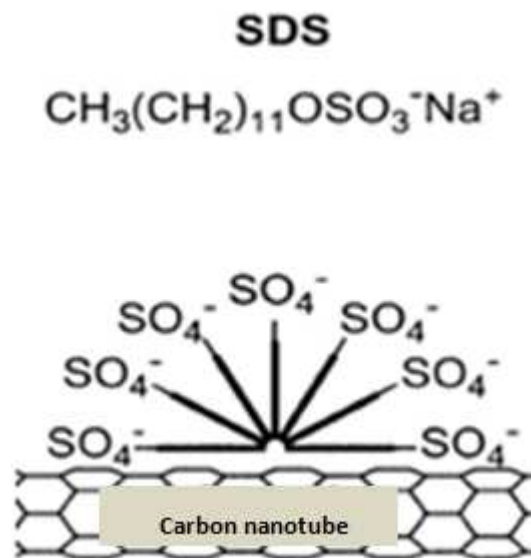


Figure 6-3: Schematic representation of SDS adsorb onto the nanotube surface. Tube stabilization depends on the surfactant molecules that lie on the tube surface parallel to the cylindrical axis (Islam *et al.*, 2003)

Nevertheless, Figure 6-4 and Figure 6-5 show that the CNT/SDS films have poor linearity in piezoresistive response, compared with both pure CNT films and CNT/PSS film. The SDS as the surfactant may be the reason for this poor linearity.

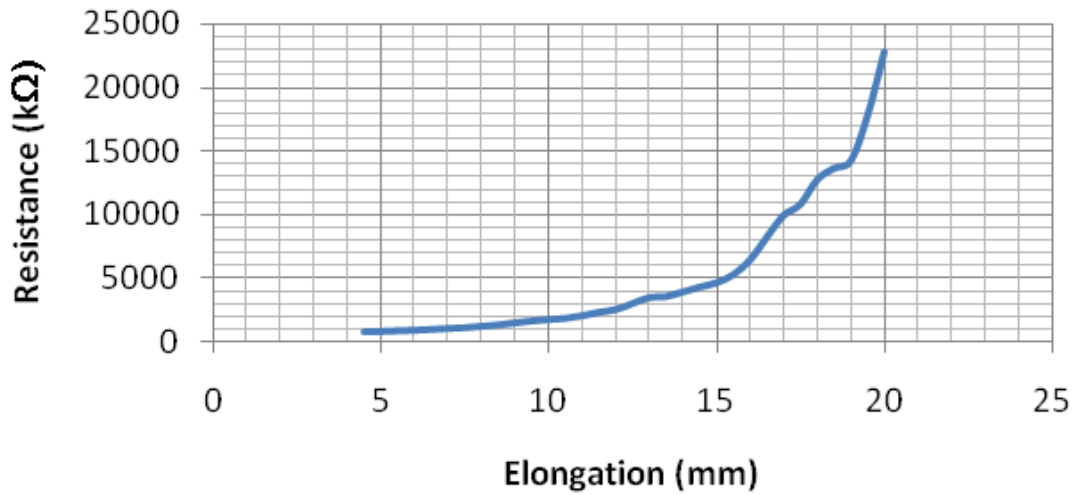


Figure 6-4: Relation between elongation and resistance of the film with 5 layers of SWNT/SDS composite networks

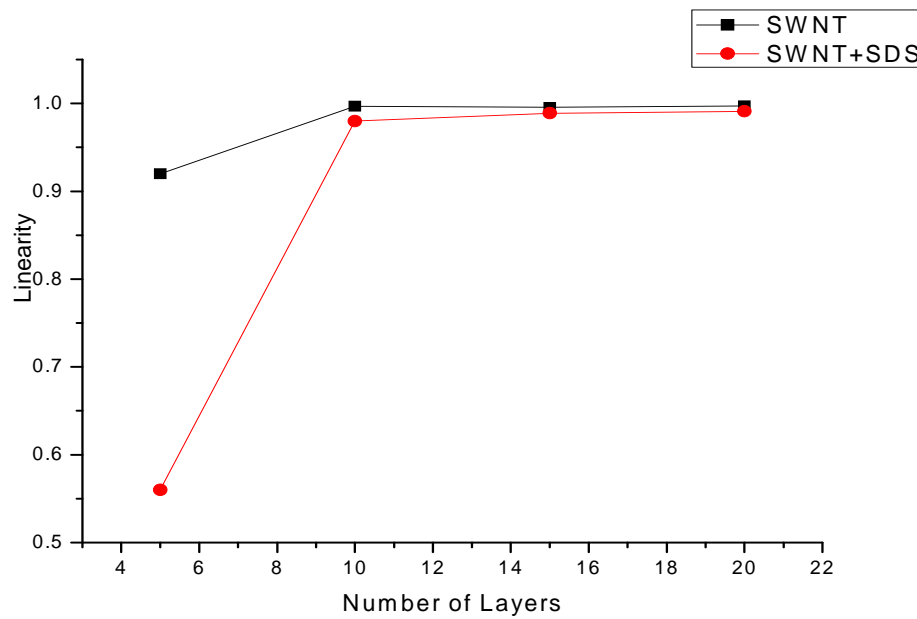


Figure 6-5: Linearity (Regression coefficient) of piezoresistive response in the SWNT/SDS film and the pure SWNT film at different layers of SWNT networks

In the CNT/SDS composite networks, the SDS would merely separate CNTs by increasing the distance between CNTs. Unlike the PSS, the SDS (288.38 M<sub>w</sub>) is not a high molecular weight polymer (which can provide a strong matrix bonding with CNTs). Thus, the VDW interaction in CNT/SDS networks is not as strong as that in the pure CNT networks and nor that in the CNT/PSS composite networks. The lower VDW interaction may be another reason for the poor linearity of piezoresistive response in the CNT/SDS networks.

#### **6.4 Conclusion**

Piezoresistive response in the CNT composite networks follows the same piezoresistive response theory (junction based), as applied to the pure CNT networks. However, the surfactant left in the CNT networks seems to strongly affect the piezoresistive response, depending on their stabilization mechanisms.

The PSS based polymer as surfactant blocks and changes the conductive path in the CNT composite networks; as a result, the conductivity of such CNT composite films decreases and piezoresistive sensitivity tends to decrease, more influenced by the PSS surfactant. The SDS, as the ionic surfactants, may attach onto the surface of the CNTs rather than surround the CNTs; as a result, the piezoresistive sensitivity in these CNT networks is less influenced by the SDS surfactant.

Nevertheless, PSS as polymer matrix seem to provide a stronger VDW bonding with CNTs than SDS surfactant. The experimental results show that the CNT/PSS composite networks present better linearity, compared with CNT/SDS composite networks.



# **Chapter 7**

## **Repeatability of Piezoresistive Response of Pure SWNT Films**

### **7.1 Introduction**

In strain sensors, the repeatability of piezoresistive response is another important parameter to measure the quality of the sensors. For instance, the repeatability of CNT composite films (SWNT/PSS-PVA) has been reported by Lynch *et al.* (2008) and shows a strong and stable piezoresistive response in a low cycle strain. Their experiment also shows some decay in the resistance of these films. They discussed that the decay is attributed to the applied DC current source which causes a rise in film temperature over time. In this chapter, pure CNT films were tested in a low cycle strain to investigate the repeatability of piezoresistive response of these films.

### **7.2 Low cycle compression experiment**

Pure CNT films were cut into rectangles ( $1\text{cm} \times 5\text{cm}$ ) and affixed to the PVC block using glue (Prism 401 Loctite), as shown in Figure 7-1. Electrical contact was

established by drying a silver paste (MG chemical) over the twisted-strand wire to form two probes on the SWNT film. To measure the resistance of these films, pure CNT films were connected to an amplification circuit. The output of this circuit was sampled at 1 Hz by the DAQ system, which will be discussed later in Chapter 8.

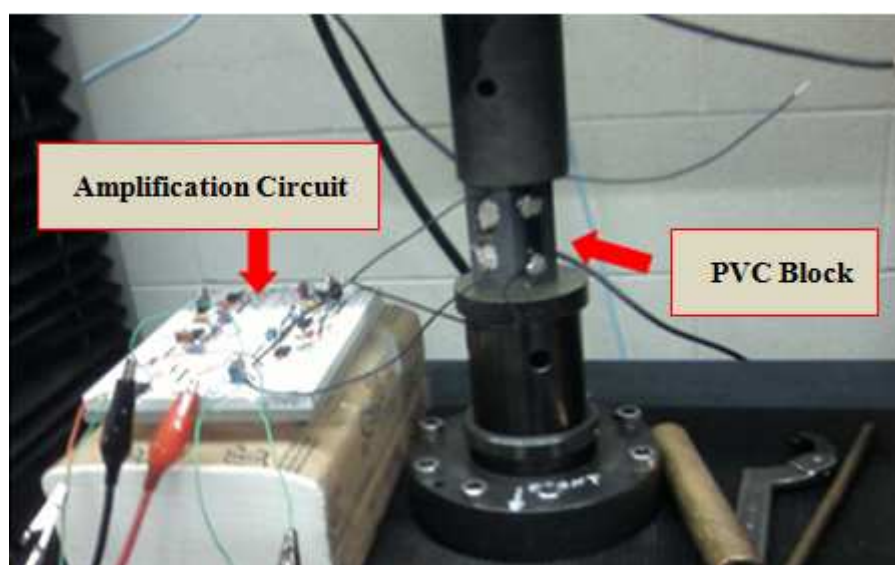


Figure 7-1: A pure CNT film affixed on a PVC block and connected to an amplification circuit for the compression test, (the PVC block loaded in the tester Instron 5500 with crosshead speed  $0.5\text{min/mm}$ )

In the compression experiment, three cycles of compression loads were controlled to generate a 5000 microstrain on the PVC block, as shown in Figure 7-2. The films with 10 layers of CNT networks (at concentration of CNT  $0.8\text{mg/ml}$ ) experienced the compression strain from the PVC block and were supposed to exhibit piezoresistive response.

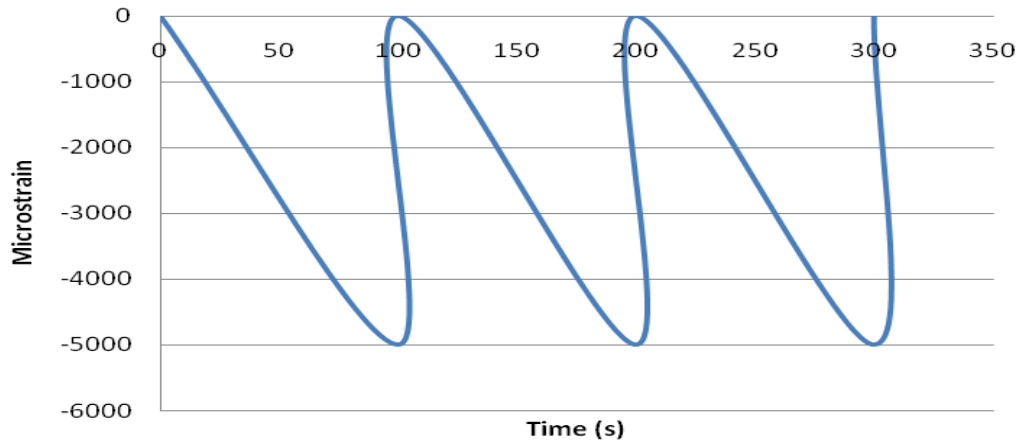


Figure 7-2: Three cycle compression load applied on the PVC block to generate 5000 microstrain on the pure CNT film

### 7.3 Low cycle tensile experiment

Pure CNT films were loaded in a three cycle tensile load. The tensile load was controlled to generate 3500 microstrain on the pure CNT film, as shown in Figure 7-3. The measurement of their piezoresistive response followed the same procedure in the low cycle compression experiment as discussed in Section 7.2.

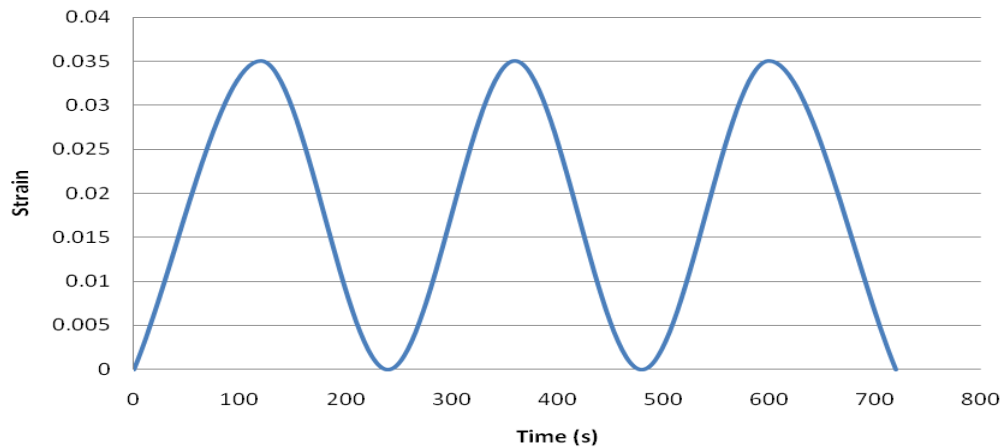


Figure 7-3: Three cycle tensile load applied on the pure SWNT film to generate 3500 microstrain on the film

#### 7.4 Discussion

In the low cycle compression experiment, the pure CNT films exhibited a strong and stable piezoresistive response, which is consistent with the applied load pattern, as shown in Figure 7-4. After unloading the compression, the resistance of the films returned to the beginning resistance. Based on the experimental results shown in Figure 7-4, the repeatability of piezoresistive response is around 0.1% (calculated by  $(13.76 \text{ k}\Omega - 13.66 \text{ k}\Omega) / 13.66 \text{ k}\Omega$ ) in these pure CNT films. In addition, the films did not show any decay in resistance, which was the case in the CNT/PSS-PVA film, found by Lynch *et al.* (2008). The gauge factor of the 10 CNT networks is about 3, as calculated with the information put in Appendix I.

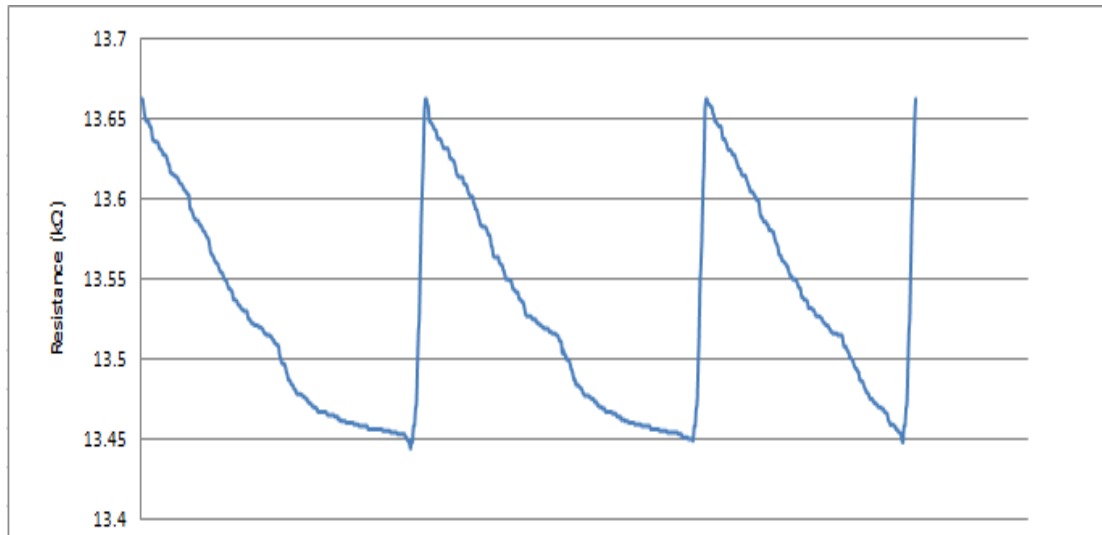


Figure 7-4: Piezoresistive response of the 10 layered pure CNT film with the concentration of  $0.8\text{mg/ml}$  under the three cycle compression load

In the low cycle tensile experiment, the films with different layers of pure CNT networks also exhibited a strong and stable piezoresistive response, which is consistent with the load pattern. The gauge factor of the film with 10 layer pure CNT networks is around 2.1. One important phenomenon has been identified, which is the increase in resistance in three cycles of tensile loads, as shown in Figure 7-5. Such increase in resistance does not happen at the low cycle compression experiment.

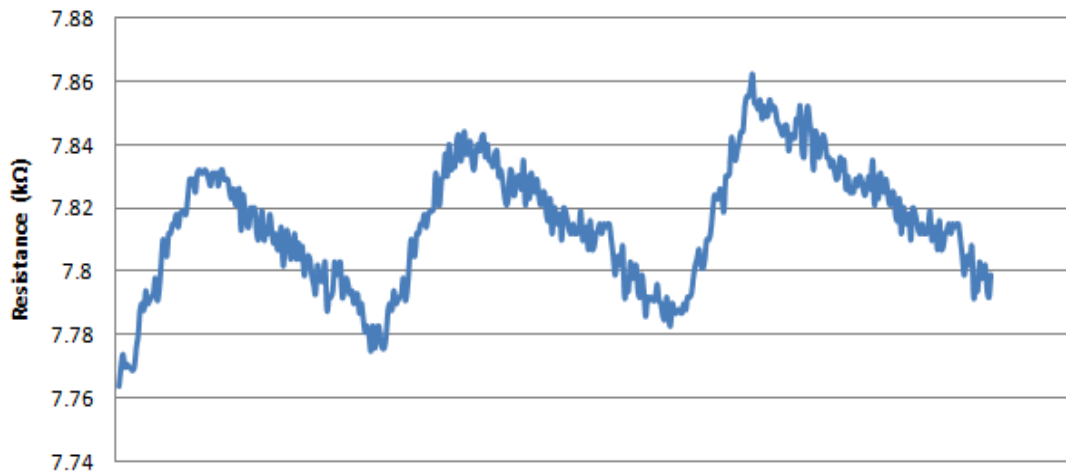


Figure 7-5: Piezoresistive response of the 10 layered pure CNT film with the concentration of  $0.8\text{mg/ml}$  under the three cycle tensile load

By analysis of the tensile load recorded in the tester Instron 1122, the increase in resistance appears to be caused by plastic deformation of the films; in particular the load returns to zero before the elongation returns to the original length. Therefore, the increase in resistance is attributed to the CNT networks that experience the distortion of the PET substrate during the low cycle tensile stretching. Such increase in resistance can be avoided with more accurate control of the tensile strain.

## 7.5 Conclusion

The pure CNT film exhibits piezoresistive response in the low cycle strain. The repeatability of piezoresistive response of pure CNT films is around 0.1% in the low cycle compression period. In the low cycle tensile period, there will be some increase

in resistance of CNT networks, likely caused by the irreversible elongation of the PET substrate. It seems that the CNT networks in themselves have high repeatability under a cyclic loading. In addition, the resistance decay that was found in CNT composite films does not happen in pure CNT films.

# **Chapter 8**

## **Electrical System for the Pure SWNT Film Sensor**

### **8.1 Introduction**

In the experiment of piezoresistive response of the pure CNT film, the film is connected to an electrical system to obtain the response signal. In section 8.2, the amplification circuit is discussed. In section 8.3, the data acquisition (DAQ) system is discussed.

### **8.2 Amplification circuit**

When the pure CNT film experiences the strain, changes in resistance of the film are detected and amplified by the circuit as shown Figure 8-1. This circuit contains four main parts: Wheatstone bridges, Precision Voltage transducer REF02, and two amplifiers AMP04 and OP90. The function of each part will be discussed in the following.



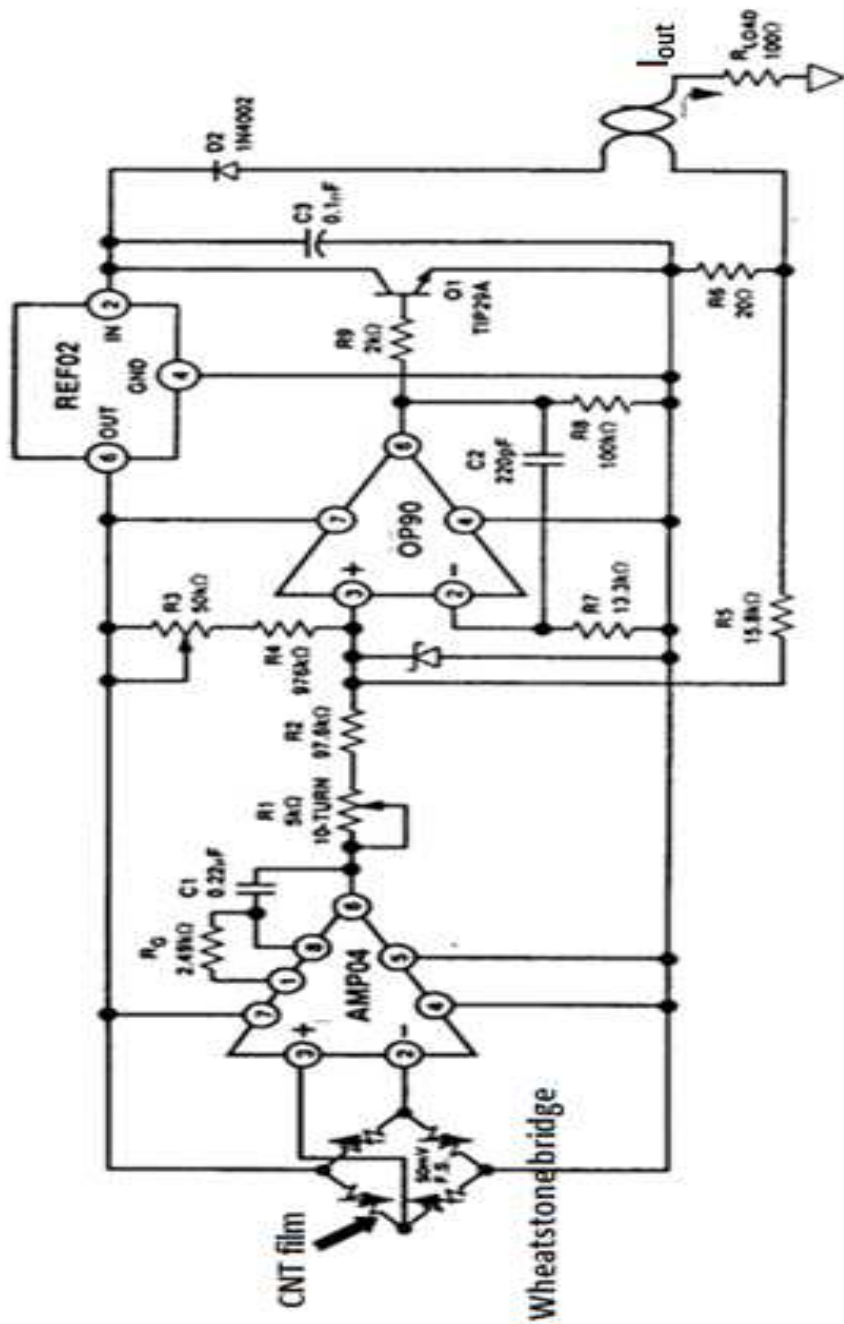


Figure 8-1: Amplification circuit: Precision 6.28-20 mA Loop Transmitter with Noninteractive Trim, (National Instrument (NI) Inc)

## Wheatstone bridges

A full Wheatstone bridge was used to measure changes in resistance of the pure SWNT film by balancing two legs of the bridge circuit, one leg of which includes the resistance of the SWNT film.

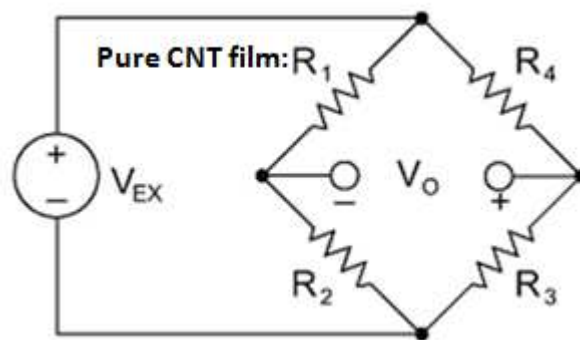


Figure 8-2: Wheatstone bridge, including two balance resistors ( $R_2$  and  $R_3$ ), one compensate resistor ( $R_4$ ) and one pure CNT film ( $R_1$ )

The advantage of these bridges is that changes in resistance of the SWNT film caused by the temperature can be compensated by other resistors in the bridges, where these resistors have the same temperature coefficient of the resistance of the SWNT film.

The experiment in this study was carried out in the laboratory condition (constant temperature); thus  $R_4$  here is a regular adjustable resistor to balance to voltage output, where  $V_0$  is adjusted to be zero at the beginning of the experiment. When the

resistance of the pure CNT film changed, the two bridges became unbalanced and  $V_0$  changed. The  $V_0$  thus represents the changes in resistance of sensors and is further amplified. The relation between the output voltage and the resistance of pure CNT film can be expressed by Equation (8-1).

$$V_O = \left[ \frac{R_3}{R_3 + R_4} - \frac{R_2}{R_1 + R_2} \right] \cdot V_{EX} \quad (8-1)$$

where  $V_{ex}$  is the work voltage, 5V in this case is provided by voltage transducer REF02.  $R_2$  and  $R_3$  will be chosen based on the resistance of the sensing material.

The linear amplification circuit contains two amplification components AMP04 and OP09, which will be discussed respectively. The power supply is regulated by the REF02, which provides a stable 5 V output with  $\pm 6\%$  range and with the minimal effect on temperature stability.

#### Amplifier AMP04

AMP04 is a linear voltage amplifier with the nonlinearity of 0.005% and an adjustable gain from 1 to 1000. The output voltage from the half Wheatstone bridge will transmit to the amplifier AMP04. The gain of AMP04 can be programmed by selecting the external resistor  $R_G$ .

$$Gain = 100 \text{ k}\Omega / R_G \quad (8-2)$$

where  $R_G$  here is 2.49 k $\Omega$ . The gain of AMP04 is 40.16. In Figure 8-1,  $C_I$  is a 0.22 $\mu F$  capacitor which is used as a 10 $H_z$  low pass filter to filter noises.

## Operational Amplifier OP09

In Figure 8-1, the input voltage of OP09 is the sum of the voltage drop from the output of AMP04 through  $R_1$  and  $R_2$ , the voltage drop from  $R_3$  and  $R_4$ , and the feedback voltages from  $R_{sense}$ . From the input voltage, the amplifier OP09 regulates the output current based on Equation (8-3):

$$I_{OUT} = \frac{1}{R_6} \left( \frac{R_5 V_{IN}}{R_2 R_1} + \frac{5V R_5}{R_3 R_4} \right) \quad (8-3)$$

With no bridge signal, 4 mA null is simply set up by  $R_3$  and  $R_4$  that inject an offset that forces a 62 mV drop across  $R_5$ . Adjustment of  $R_2$  will provide an offset trim and adjustment of  $R_1$  will provide a gain trim. The current  $I_{out}$  causes a voltage drop on  $R_{load}$  which is the final output of the circuit and transmitted to the monitoring computer.

The amplification circuit in the experiment was built upon the circuit shown in Figure 8-1. The adjustment of such circuit is needed. Based on the results of adjustment shown in Figure 8-3, it should be noted that there is no perfect correlation between real and theoretical results. The details of the adjustment can be found in Appendix II.

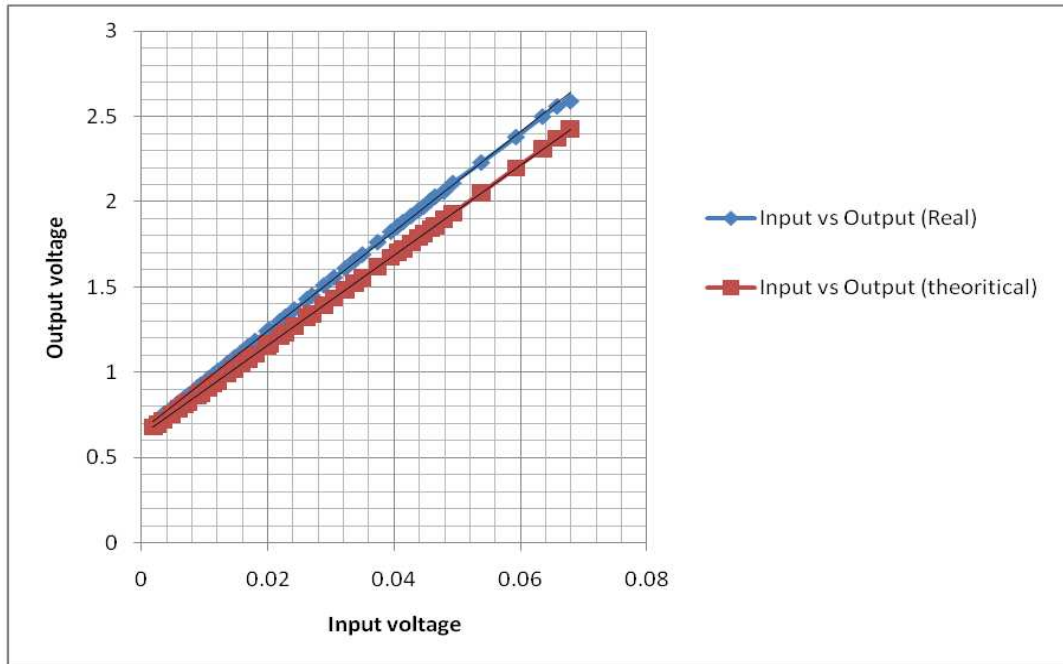


Figure 8-3: Relation between input ( $V_0$ ) and output ( $R_s I_{out}$ ) in the linear amplification circuit (Red line: the theoretical results calculated by Equation (8-1) to (8-3); blue line: the experimental results from the adjustment)

### 8.3 Data acquisition (DAQ) system

The output of the linear amplification circuit will be transmitted to a monitoring computer through an A/D transducer and a DAQ card, as shown in Figure 8-4.

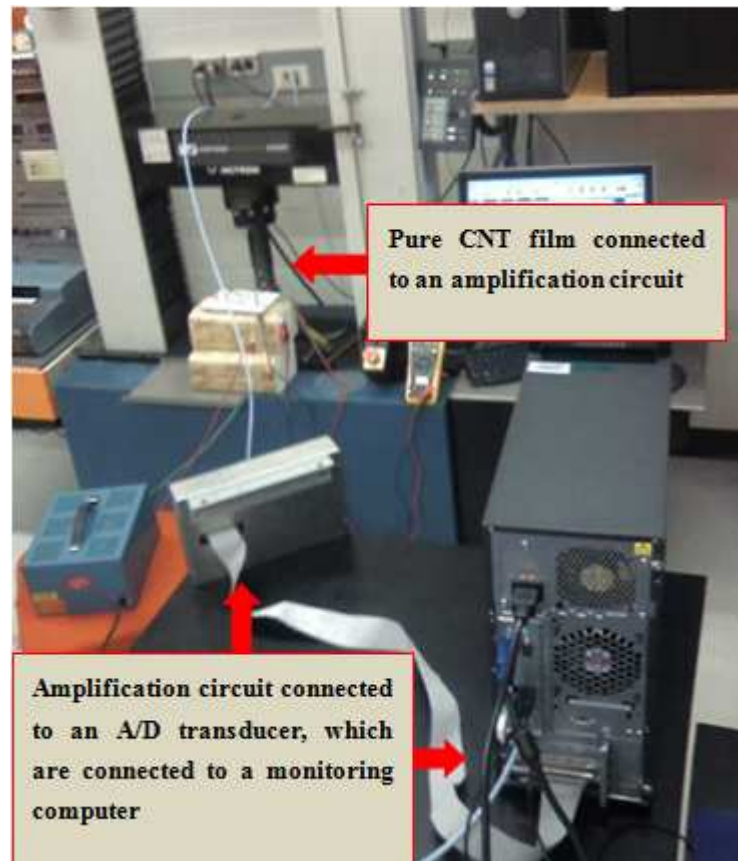


Figure 8-4: Electrical system of the pure CNT film sensor, containing the amplification circuit, a D/A transducer and the monitoring computer

### Amplification

The data collection is completed through the DAQ card NI-PCI-M10164-4. The data is processed in the software LABVIEW2009 and saved as the Excel. file, as shown

Figure 8-5.

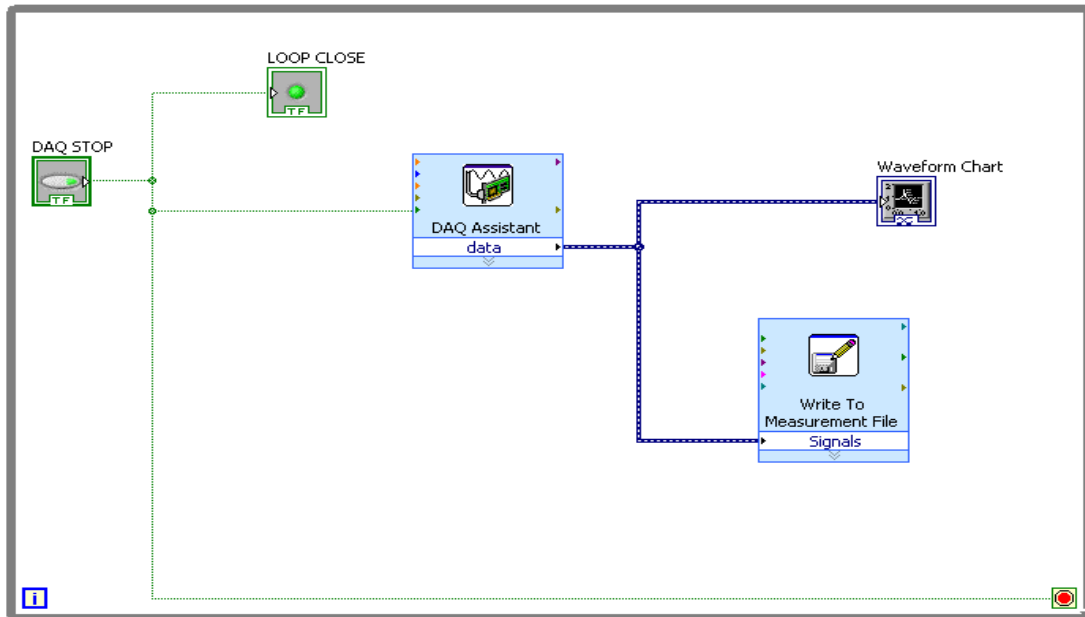


Figure 8-5: The function panel programmed in the LABVIEW 2009, (The DAQ assistant: the signal collection in the card NI-PCI-M10164-4, the experimental results saved and shown in the “Write to measurement file” and in the “Waveform Chart”, respectively)

The adjustment of the electrical system was tested under the load pattern applied on the pure CNT film, as shown in Figure 8-6.

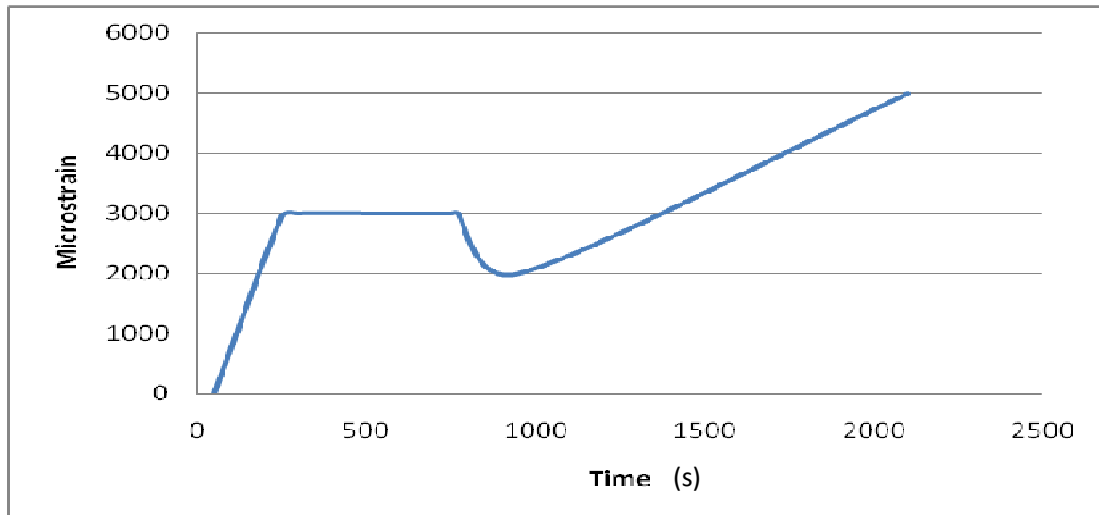


Figure 8-6: Tensile load applied on the pure CNT film to test the electrical system

The film with 10 layers of CNT networks is experienced the load pattern, and exhibited piezoresistive response, which was detected by the electrical system. The result is shown in Figure 8-7, which is a shortcut obtained from the “Waveform Chart” in Figure 8-5. The appearances of sharp peaks represent the noise in the electrical system.



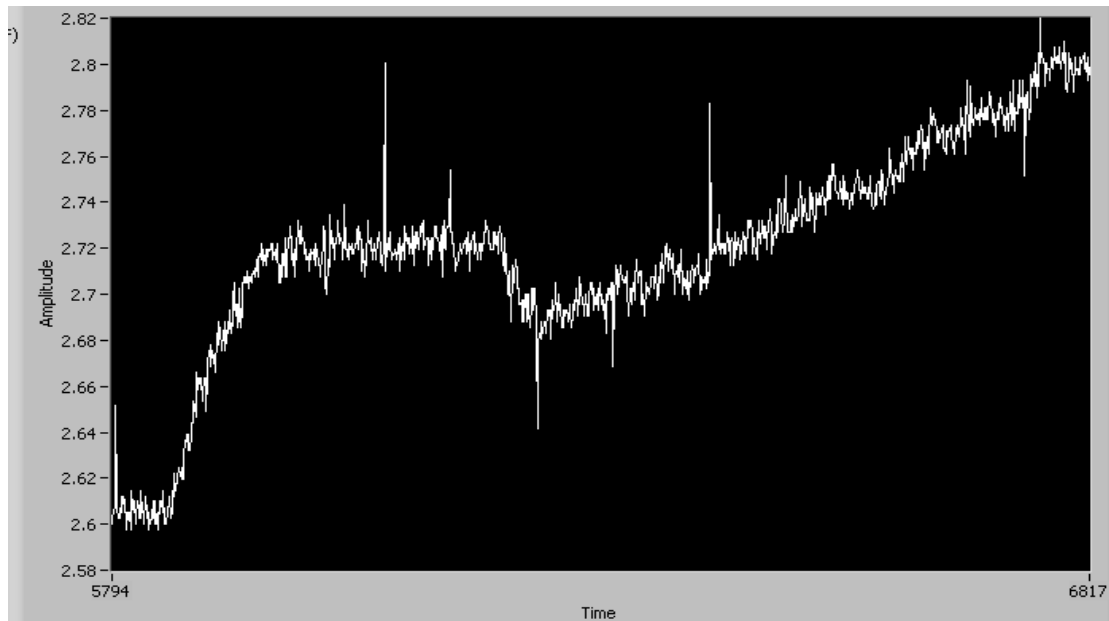


Figure 8-7: Piezoresistive response in the pure CNT film processed in the Labview 2009 by the electrical system (Pure CNT film: 10 layers of CNT networks at concentration of  $0.8\text{mg/ml}$ )

#### 8.4 Summary

The electrical system of the pure CNT film sensor contains the signal amplification and a signal collection. The input signal in this system was first amplified through two amplification components. After the amplification, the signal was collected and transmitted to a monitoring computer by the DAQ system. The signal processing was programmed in the Labview 2009 and tested under the applied load pattern. The information is stored as the MS excel file.

## **Chapter 9**

### **Conclusion and Recommendation**

#### **9.1 Overview of the thesis**

A new type of strain sensors, the pure CNT film sensor, was proposed in this study. Piezoresistive response of this strain sensor was experimentally studied. The mechanism for such piezoresistive response was analyzed; in particular piezoresistive response is caused by the change of conductive paths in the CNT networks, when the CNT film experiences strains.

The fabrication technique for the pure film with multilayered CNT networks was proposed in this study, which was inspired by the fabrication of one layer pure CNT film and the LBL method. The uniformity of such multilayered CNT networks was measured with the aid of the Raman spectroscopy technique.

Piezoresistive responses were optimized in the multilayered CNT networks by varying their distribution and density. The results have shown that a high density of CNT networks can provide an additional mechanical strength to improve the linearity

in piezoresistive response; however, high density decreases the overall piezoresistive sensitivity in CNT networks due to potentially increased agglomeration of junctions; clearly, a trade-off exists between mechanical properties and piezoresistive properties.

Based on the experimental results, the optimal piezoresistive response for strain sensors is found with the film that has 10 layers and  $0.8\text{mg/ml}$  concentration. Such film can achieve the gauge factor of 2.59, non-linearity of 0.89%, and repeatability of 0.1%.

In addition, the influence of surfactants on piezoresistive response in CNT networks was studied. The experimental results have shown that surfactants, depending on their stabilization mechanisms, have different influences on piezoresistive response in CNT networks.

## **9.2 Conclusion**

Pure CNT films show many advantages as a new type of strain sensors compared with other related sensors. These advantages, such as their high sensitivity, superior mechanical properties, and long detection range, are discussed in the following.

### 9.2.1 Comparison with CNT composite films

The “Buckypaper” fabrication and LBL methods both allow CNT networks to inter-mix with polymer surfactants to form CNT composite networks. In CNT composite networks, the junctions between CNTs and the junctions between CNTs and polymer surfactants are formed by van der Waals force. The polymer surfactants left in CNT networks provide a stronger matrix bonding with CNTs due to their high molecular weight. Such improvement in bonding provides extra mechanical strength in CNT composite networks.

However, the overall mechanical properties of these CNT composite films are still insubstantial. For instance, Kang *et al.* (2004) used PAMMA to improve the mechanical properties of “Buckypaper”. Their experiment shows that PAMMA provided a strong van der Waals interaction in CNT composite networks. However, elastic deformation of such “Buckypaper” can only apply up to 2000 microstrain.

In pure CNT films, CNT networks are deposited on polymer substrates. The bonding within CNT networks and the bonding between CNTs and the substrate both belong to physical connections. The polymer substrate, such as the PET polymer substrate used in this study, has a high molecular weight; thus the bonding between CNT and the polymer substrate are strong enough to allow CNTs to be located on the substrate.

Studies so far have shown that a polymer substrate is the key factor for the mechanical strength in pure CNT films but not in CNT networks. For instance, the experiments have shown that pure CNT films based on PET substrates have elastic deformation up to 10000 microstrain, which is around the yield point of PET polymers. Therefore the mechanical properties of pure CNT films are similar to the properties of PET material. The overall mechanical strength of pure CNT films is thus higher than that of CNT composite film. In addition, this study has also demonstrated that pure CNT films can be used in different mechanical conditions by changing them to an equivalent polymer substrate.

In strain detection, the CNT composite film and pure CNT film are based on the same piezoresistive response theory, namely, the junction based piezoresistive response theory. However, the surfactants used in CNT composite film affect piezoresistive response in CNT networks, which, generally speaking, will cause negative effects on the overall sensing performances. The studies have shown that pure CNT films show higher sensitivity in piezoresistive response compared with CNT composite films shown in Figure 9-1.

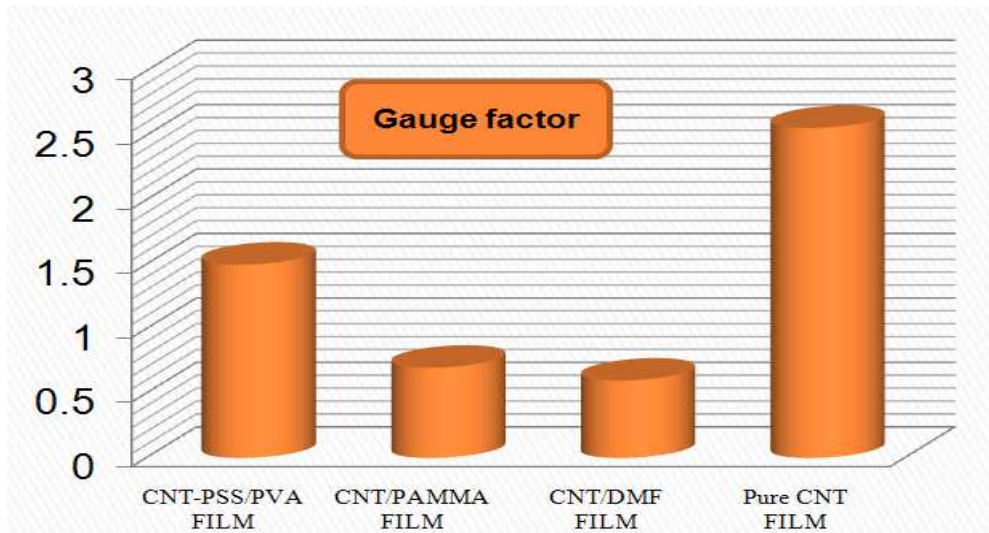


Figure 9-1: Gauge factor of CNT composite films and the pure CNT. The pure CNT film with 10 layers of CNT networks at the CNT concentration of  $0.8\text{mg/ml}$

In addition, the fabrication of pure CNT films uses a spray coating to deposit CNT networks on a substrate. This method is easier to be achieved compared with the vacuumed filtered coating and the Layer-By-Layer coating required by “Buckypaper” and LBL fabrication.

### 9.2.2 Comparison with traditional metal foil gauges

Piezoresistive responses in metal foil gauges are based on the band gap theory, which is similar with the band gap theory of CNTs in piezoresistive response. When strain is applied on the metal gauge, changes in band gap cause changes in conductivity in the metal materials.

In metal foil gauges, the band gap is involved with atomic structure, which is strongly related to their mechanical properties. The main drawback of such behavior is that the same amount of strain applied on the metal material will cause different amounts of changes in the band gap before and after elastic deformation. As a result, most of metal foil gauges show changes in sensitivity when strain exceeds the yield point. The average gauge factor in the traditional metal foil gauges is around 2.

In pure CNT films, piezoresistive response is based on the changes in the junctions between CNTs; thus the piezoresistive response only happens in CNT networks rather than in CNTs. Therefore, the sensitivity of CNT networks will not change as long as no deformation happens in CNTs to change their band gap. The experimental results have shown that piezoresistive sensitivity in pure CNT films does not change up till the breaking point of the polymer substrate, which allows the CNT film to be applied for detecting a large deformation range. The overall gauge factor in pure CNT films is also higher than that of most metal foil gauges, as shown in Figure 9-2

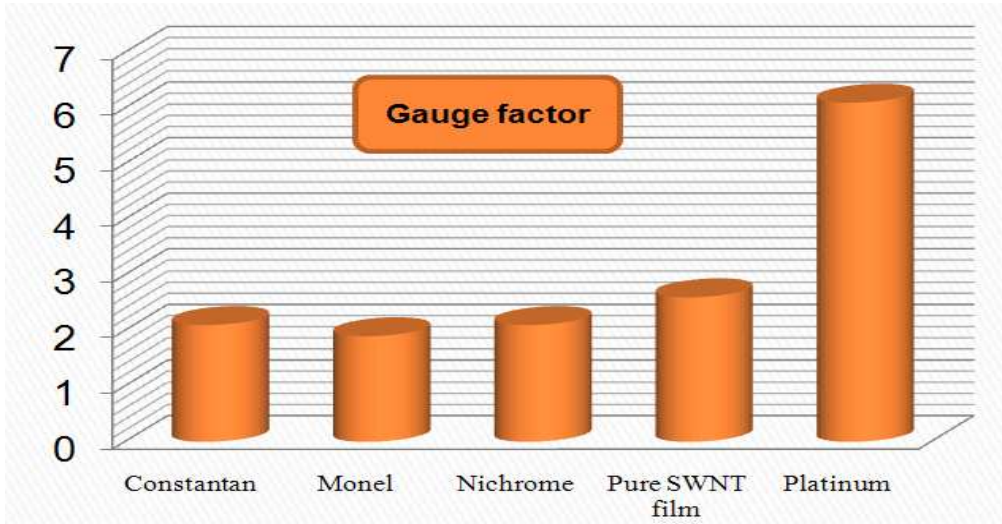


Figure 9-2: Gauge factor of different metal foil gauges and the pure SWNT film. The pure SWNT film with 10 layers of CNT networks at the CNT concentration of  $0.8mg/ml$

In addition, most metal gauges are made from the rare and expensive metals, which have a higher cost in fabrication. In the fabrication of pure CNT films, the experiment has shown that 1000\$ of CNTs can fabricate at least 1500 pieces of strain sensors and each sensor contains 10 layers of CNT networks with  $0.8mg/ml$  density. Therefore, the cost of pure CNT films is much lower than the cost of most metal gauges.

### 9.3 Contribution

The first contribution of this study is the proposal of a new type of strain sensor for structural health monitoring. This new strain sensor contains a polymer substrate and CNT networks, called pure CNT film. The new sensors exhibit strong and stable



piezoresistive response. More importantly, these films show higher sensitivity compared with metal foil gauges and CNT composite films.

The second contribution of the study is the investigation of piezoresistive response in CNT networks. The experimental results have shown that piezoresistive response in pure CNT networks is solidly related to their distribution and density. The relationship is a tradeoff between piezoresistive and mechanical properties of CNT networks.

In addition, the influence of surfactants on piezoresistive response in CNT networks is studied. The surfactants which exhibit different stabilization mechanisms to disperse CNT in solution have different influences on the piezoresistive response in CNT networks. Generally speaking, the surfactants left in CNT networks will cause defective affects on the overall sensing issues, which also exist in the CNT composite films proposed seen by previous researchers.

#### **9.4 Future work**

Pure CNT films as strain sensors show the promising electrical sensing and mechanical properties; however some improvements for such new strain sensors are needed for their more effective application in the future.

In pure CNT films, CNT networks deposited on substrates are unstable due to a weak

physical bonding with substrates. For instance, a touch or shake of these films may cause damage in CNT networks, where the distribution of CNT networks changes. A future work has been proposed to improve such weak bonding by adding a polymer solvent to the CNT solution. During the coating, the solvent will bring CNT networks deeper into the polymer substrate by etching it rather than depositing it on the surface of the substrate.

The fabrication of multilayered pure CNT films proposed in this study shows acceptable coating uniformity; however, the processes in this fabrication are not very well controlled, and as results, the CNT films fabricated under the same procedures show different parameters in their resistance and thickness. A future work will focus on improving the robustness of this fabrication in effort to yield a constant product output.

Based on the current studies, an improved piezoresistive response in CNT networks is promising and applicable. From the experimental results, low density CNT networks exhibit high sensitivity; however such loose CNT networks show low conductivity and inferior linearity in the piezoresistive response, which is caused by the weak VDW bonding. Such drawbacks are the main open issues of these CNT networks being used as strain sensors. A future experiment has been proposed to increase these bonds by replacing some of the SWNTs by MWNTs in CNT networks. The MWNT contains more carbon atoms which will increase the VDW bonding between CNTs

and the overall conductivity in CNT networks.

Piezoresistive response in CNT networks is the combination of studies in the magnetic and mechanical fields. The CNT network experienced deformation and exhibited magnetic changes in conductive paths. So far, the tradeoff between electrical sensing and mechanical strength has been proposed in this study. A future work will focus on building a mathematical model to develop the relationship between their magnetic and mechanical properties.

Pure CNT films, as strain sensors, so far are only studied under lab conditions. In practical situations, the application of such pure CNT films would involve many other factors which should be further examined, such as sensor installation, temperature influence, and electrical connection.

## References

Cao, D.P.; Wang, W.H.; (2007) “*Interaction between two single-walled carbon nanotubes revisited: Structural stability of nanotube bundles*” *Chemical Engineering Science*, Vol.62, pp.6879 – 6884.

Dharap, P.; Li, Z.; Nagarajaiah, S.; Barrera, E.V.; (2004) “*Carbon Nanotube film sensors*” *Nanotechnology*, Vol.15, pp.379-400.

Dharap, P.; Li, Z.L.; Nagarajaiah, S.; Barrera, E.V.; (2004) “*Flexural strain sensing using carbon nanotube film Sensor*” *Sensor Review*, Vol.24, pp.271–273.

Dresselhaus, D.; Spanke, F.U.; Hillebrecht, E.; (1996) “*Antiferromagnetic coupling of Mn adsorbates to Fe (100)*” *Phys. Rev. B*, Vol.56, Issue 9.

Hagrasy, S.E.; Chang, S.Y.; Desai, D.; Kiang, S.; (2006) “*Raman spectroscopy for the determination of coating uniformity of tablets: assessment of product quality and coating pan mixing efficiency during scale-up*” *Journal of Pharmaceutical Innovation*, Vol.5, pp 36-40.

Hecht, D.; Hu, L.B.; Grünera, G.; (2006) “*Conductivity scaling with bundle length and diameter in single walled carbon nanotube networks*” Applied physics letter, Vol.89, pp.133112- 133115.

Hecht, D.S.; Thomas, D.; Hu, L.B.; Ladous, C.; Lam, T.; Park, Y.; Irvin, G.; Drzaic, P.; (2007) “*Carbon-nanotube film on plastic as transparent electrode for resistive touch screens*” available online: [http://www.unidym.com/files/CNT\\_Film\\_on\\_Plastic.pdf](http://www.unidym.com/files/CNT_Film_on_Plastic.pdf).

Hu, L.; Hecht, D.S.; (2004) “*Percolation in Transparent and Conducting Carbon Nanotube Networks*” Nano. Lett, Vol.4, No.12, pp.2513-2517.

Hu, C.H.; Liu, C.H.; Peng, L.Z.; (2008) “*Resistance-pressure sensitivity and a mechanism study of multiwall carbon nanotube networks/poly (dimethylsiloxane) composites*” Applied. Phys. Lett, Vol.93, pp.033108-033112.

Iijima, S.; Ajayan, S.; Ichihashi, P.M.; (1991) “*Growth model for carbon nanotubes*” Phys. Rev. Lett, Vol.69, pp.3100–3103.

Islam, M.F.; Rojas, E.; Bergey, D.M.; Johnson, A.T.; Yodh, A.G.; (2003) “*High Weight Fraction Surfactant Solubilization of Single-Wall Carbon Nanotubes in Water*” Nano. Lett, Vol.3, No.2, pp269-273.

Jeong, S.H.; Lee, O.J.; Lee, K.H.; (2002) “*Preparation of Aligned Carbon Nanotubes with Prescribed Dimensions: Template Synthesis and Sonication Cutting Approach*” Chem. Mater, Vol.14, pp.1859-1862.

Kaempgen, M.; Artukovic, E.; Hecht, D.S.; Roth, S.; (2005) “*Transparent and Flexible Carbon Nanotube Transistors*” Nano letters, Vol.5, No.4, pp.757-760.

Kane, C.L.; Mele, E.J.; Lee, R.S.; Fischer, J.E.; Petit, P.; Dai, H.; (1998) “*Temperature-dependent resistivity of single-wall carbon nanotubes*” Europhys. Lett, Vol.41, pp.683-688.

Kang, I.; Heung, Y.Y.; Kim, J.H.; Lee, J.W.; Gollapudi, R.; Subramaniam, S.; Narasimhadevara, S.; Hurd, D.; Kirikera, R.; (2006) “*Introduction to carbon nanotube and nanofiber smart materials*” Elsevier Composites, Part B, Vol.37, pp.382–394.

Kang, I.; Schulz, M.J.; Kim, H.J.; Shanov, V.; Shi, D.L.; (2006) “*A carbon nanotube strain sensor for structural health monitoring*” Smart Mater, Vol.15, pp.737–748.

Keszler, M.; Nemes, L.; Ahmad, S.R.; Fang, X.; (2004) “*Characterization of carbon nanotube materials by Raman spectroscopy and microscopy- a case study of multiwalled and singlewalled samples*” Journal of Optoelectronics and Advanced

Materials, Vol.6, No.4.

Kim, P.; Shi, L.; Majumdar, A.; McEuen, P.L.; (2001) “*Thermal Transport Measurements of Individual Multiwalled Nanotubes*” Phys. Rev. Lett, Vol.87, pp.215502-215507.

Kong, J.; Franklin, N.R.; Zhou, C.; Chapline, M.G.; Peng, S.; Cho, K.; Dai, H.; (2000) “*Nanotube molecular wires as chemical sensors*” Science, Vol.287, pp.622-627.

Laguno; Fischer, J.E.; Hone, J.; Johnson, A.T.; (2004) “*Observation of Thermopower Oscillations in the Coulomb Blockade Regime in a Semiconducting Carbon Nanotube*” Nano. Lett, Vol.4, pp.45-49.

Lee, K.W.; Lee, S.S.; Lee, K.C.; (2010) “*Carbon nanotube film piezoresistors embedded in polymer membranes*” Applied Phys. Lett, Vol.96, pp.13511-13515.

Liu, J.; Dai, H.; (2002) “*Design, fabrication, and testing of piezoresistive pressure sensors using carbon nanotubes*” available online: <http://www.nnf.cornell.edu/2002reu/Liu.pdf>.

Loh, J.K; Lynch, P.J.; Kotov, A.N.; (2005) “*Conformable Single-Walled Carbon Nanotube Thin Film Strain Sensors for Structural Monitoring*” Proceedings of the 5th

International Workshop on Structural Health Monitoring, Stanford, CA, USA,

Lourie, O.; Wagner, H.D.; (1998) "*Evaluation of Young's modulus of carbon nanotubes by micro-Raman spectroscopy*" Mater. Res, Vol.13 pp.2418-2423.

Lu, K.B.; Yu, J.R.; Grossiord, N.; Koning, C.E.; Loos, J.; (2007) "*Conductive Carbon Nanotube Polymer Nanocomposites Prepared by Latex Technology*" Microsc Microanal, Vol.13, pp.442-443.

Lynch, J.P.; Loh, K.J.; Shim, B.S.; Kotov, N.A.; (2007) "*Tailoring Piezoresistive Sensitivity of Multilayer Carbon Nanotube Composite Strain Sensors*" Journal of Intelligent Material Systems and Structures, Vol.19, pp.747-749.

Lynch, J.P.; Kenneth, J.; Nicholas, A.; (2008) "*Inductively Coupled Nanocomposite Wireless Strain and pH sensor*" Smart Structure and system, Techno Press, Vol.4, pp.531-548.

Mizel; Benedict, L.X.; Cohen, M.L.; Louie, S.G.; Zettl, A.; Budraa, N.K.; Beyermann, W.P.; (1999) "*Analysis of the low-temperature specific heat of multiwalled carbon nanotubes and carbon nanotube ropes*" Phys. Rev. B, Vol.60, pp.3264-3267.

Minot, E.D.; Park, J.Y.; Brink, M.; McEwen, P.L.; (2002) "*Tuning Carbon Nanotube*



*Band Gaps with Strain*” Phys. Rev. Lett, Vol.90, No.15.

Moore, V.C.; Strano, M.S.; Haroz, E.H.; Hauge, R.H.; Smalley, R.E.; (2003)

*“Individually Suspended Single-Walled Carbon Nanotubes in Various Surfactants”*

Nano. Lett, Vol.3, No.3, pp.1379-1382.

Paloniemi, H., Lukkarinen, M.; Aaritalo, T.; Areva, S.; Leiro, J.; Heinonen, M.;

Haapakka, K.; and Luddari, J.; (2006) *“Layer-by-Layer Electrostatic Self-Assembly of*

*Single-Wall Carbon Nanotube Polyelectrolytes”* Langmuir, Vol.22, pp74–83.

Peng, S.; O’Keeffe, J.; Wei, C.Y.; Cho, K.; (2002) *“Carbon Nanotube Chemical and*

*Mechanical Sensors”* Conference Paper for the 3rd International Workshop on

Structural Health Monitoring.

Rastogi, R.; Kaushal, R.; Tripathi, S.K.; Sharma, A.L.; Kaur, I.; (2008) *“Comparative*

*study of carbon nanotube dispersion using surfactants”* Carbon, Vol.328,

pp.421–428.

Shim, B.S.; Kotov, A.N.; (2005) *“Single-Walled Carbon Nanotube Combing during*

*Layer-by-Layer Assembly: From Random Adsorption to Aligned Composites”*

Langmuir letters, Vol.21, No.21, pp.9381-9385.

Sinha, N.; Ma, J.Z.; John, T.W.; (2006) “*Carbon Nanotube-Based Sensors*” Journal of Nanoscience and Nanotechnology, Vol.6, pp.573–590.

Someya, T.; Small, J.; Kim, P.; Nuckolls, C.; Yardley, J.T.; (2003) “*Alcohol Vapor Sensors Based on Single-Walled Carbon Nanotube Field Effect Transistors*” Nano. Lett, Vol.3, pp.877-880.

Stadermann, M.; Papadakis, S.J.; Falvo, M.R.; Fu, Q.; Liu, J.; Fridman, Y.; Boland, J. J.; Superfine, R.; Washburn, S.; (2005) “*Exponential decay of local conductance in single-wall carbon nanotubes*” Phys. Rev. B, Vol.72, pp.245406-245410.

Sun, C.H.; Yin, L.C.; Li, F.; Lu, G.Q.; Cheng, H.M.; (2005) “*Van der Waals interactions between two parallel infinitely long single-walled nanotubes*” Chemical Phys.Lett, Vol.403, pp.343–346.

Tan, H.; Jiang, L.Y.; Huang, Y.; Liu, B.; Hwang, K.C.; (2007) “*The effect of van der Waals-based interface cohesive law on carbonnanotube-reinforced composite materials*” Composite Science and Technology, Vol.67, pp.2941-2946.

Tersoff, J.; Ruoff, R.S.; (1994) “*Structural Properties of a Carbon-Nanotube Crystal*” Phys. Rev. Lett, Vol.73, Issue.5.

Tomblor, T.M.; Zhou, C.W.; Alexseyev, L.; Kong, J.; (2000) “*Reversible electromechanical characteristics of carbon nanotubes under local-probe manipulation*” *Nature*, Vol.405, pp.769-772.

Vigolo, B.; Pénicaud, A.; Coulon, C.; Sauder, C.; (2000) “*Macroscopic Fibers and Ribbons of Oriented Carbon Nanotubes*” *Science*, Vol.290, No.5495, pp.1331-1334.

Wong, T.S.; Li, W.J.; (2003) “*Dielectrophoretic Batch Fabrication of Bundled Carbon Nanotube Thermal Sensors*” *Nanotechnology*, Vol.3, No.3.

Xing, Y.; Zhao, Z.Y.; Xiao, M.F.; (2007) “*Measurement and simulation of carbon nanotube’s piezoresistive property by a micro/nano combined structure*” *Applied Phy*, Vol.45, pp.282-286.

Xu, H.; Zhang, S.X.; Anlage, S.M.; (2008) “*Frequency- and electric-field-dependent conductivity of single-walled carbon nanotube networks of varying density*” *Phys. Rev. B*, Vol.77, pp.075418-075422.

Yang, X.; Zhou, Z.Y.; Wu, Y.; Xiao, M.F.; (2007) “*Measurement and simulation of carbon nanotube’s piezoresistance property by a micro/nano combine structure*” *Indian Journal of Pure & Applied Physics*. Vol.45, pp.282-286.

Yong, L.; Lu, W.W.; Jun, L.K.; Guo, H.C.; (2003) “*Piezoresistive effect in carbon nanotube films*” Chinese. Science. Bulletin, Vol.48, No.2 pp.125-127.

Yu, J.R.; Grossiord, N.; Koning, C.E.; Loos, J.; (2007) “*Controlling the dispersion of multi-wall carbon nanotubes in aqueous surfactant solution*” Carbon, Vol.45, pp.618–623.

Zhang, M.; Gorski, W.; (2005) “*Electrochemical sensing based on redox mediation at carbon nanotubes*” Anal. Chem, Vol.77, pp.3960-3965.

Zhao, Y.P.; Wei, B.Q.; Ajayan, P.M.; Ramanath, G.; Lu, T.M.; (2001)  
“*Frequency-dependent electrical transport in carbon nanotubes*” Phys. Rev. B,  
Vol.64, pp.201402-201406.

## Appendix I

### Appendix I:

This appendix contains the data processed in the adjustment of the amplification circuit. The input signal generates two outputs. One of the outputs is the real amplification result. The other one is the theoretical amplification results, which provide a comparison with the former output.

Vinput (v)	Calculated AMP04(Vout) (V)	Real AMP04(Vout) (V)	Calculated OP09(Iout)(A)	Calculated VRLoad(V)	Real VRLoad (V)
0	0	0.0026	0.0062	0.62	0.65
0.0019	0.07630514	0.0762	0.006792075	0.679207487	0.699
0.0026	0.10441756	0.102	0.006978892	0.697889193	0.72
0.0034	0.13654604	0.139	0.007192397	0.719239714	0.749
0.0048	0.19277088	0.192	0.007566031	0.756603125	0.788
0.0059	0.23694754	0.237	0.007859601	0.785960091	0.822
0.0068	0.27309208	0.273	0.008099794	0.809979427	0.848
0.0074	0.29718844	0.296	0.008259923	0.825992318	0.865
0.0089	0.35742934	0.357	0.008660245	0.866024545	0.911
0.0094	0.37750964	0.378	0.008793686	0.87936862	0.926
0.0106	0.42570236	0.428	0.009113944	0.911394401	0.963
0.0114	0.45783084	0.457	0.009327449	0.932744922	0.984
0.0121	0.48594326	0.487	0.009514266	0.951426628	1.007
0.0136	0.54618416	0.548	0.009914589	0.991458855	1.052
0.0147	0.59036082	0.592	0.010208158	1.020815821	1.085
0.0159	0.63855354	0.639	0.010528416	1.052841602	1.12
0.0169	0.67871414	0.681	0.010795298	1.079529753	1.151
0.018	0.7228908	0.724	0.011088867	1.108886719	1.183
0.0199	0.79919594	0.8	0.011595942	1.159594206	1.24
0.0203	0.81526018	0.816	0.011702695	1.170269467	1.251
0.0219	0.87951714	0.88	0.012129705	1.212970509	1.298
0.0228	0.91566168	0.918	0.012369898	1.236989845	1.326
0.0242	0.97188652	0.974	0.012743533	1.274353256	1.368
0.0262	1.05220772	1.055	0.013277296	1.327729558	1.428

0.027	1.0843362	1.086	0.013490801	1.349080079	1.45
0.0289	1.16064134	1.165	0.013997876	1.399787566	1.51
0.0305	1.2248983	1.227	0.014424886	1.442488608	1.556
0.0323	1.29718738	1.299	0.014905273	1.49052728	1.609
0.0338	1.35742828	1.365	0.015305595	1.530559506	1.657
0.035	1.405621	1.408	0.015625853	1.562585288	1.69
0.0374	1.50200644	1.508	0.016266369	1.62663685	1.763
0.0395	1.5863437	1.589	0.01682682	1.682681968	1.824
0.0406	1.63052036	1.634	0.017120389	1.712038934	1.857
0.0414	1.66264884	1.666	0.017333895	1.733389455	1.881
0.0427	1.71485762	1.719	0.017680841	1.768084051	1.917
0.0439	1.76305034	1.767	0.018001098	1.800109832	1.951
0.0447	1.79517882	1.798	0.018214604	1.821460353	1.972
0.0458	1.83935548	1.845	0.018508173	1.850817319	2.01
0.0465	1.8674679	1.872	0.01869499	1.869499025	2.03
0.0479	1.92369274	1.928	0.019068624	1.906862437	2.06
0.0493	1.97991758	1.989	0.019442258	1.944225848	2.11
0.0538	2.16064028	2.17	0.020643225	2.064322528	2.23
0.0593	2.38152358	2.39	0.022111074	2.211107359	2.38
0.0635	2.5501981	2.56	0.023231976	2.323197593	2.5
0.0658	2.64256748	2.65	0.023845803	2.384580341	2.56
0.0679	2.72690474	2.68	0.024406255	2.440625458	2.59

R1+R2=118.88K $\Omega$

R3+R4=994.26K $\Omega$

Vref=2.8mV

Iref=6.285mA

## Appendix II

Appendix II:

This appendix contains two sheets, which includes the data processed in the two experiments of piezoresistive repeatability in CNT networks. Based on the records in the monitoring computer, resistance in the pure CNT films is generated by the theoretical calculation of the amplification circuit.

Data recorded in Labview 2009(V)	$V_0$ (V)	$-V_0$ (V)	$R_1$ ( $k\Omega$ )
0.975691396	0.013003423	-0.013003423	13.663
0.975691396	0.013003423	-0.013003423	13.663
0.987614887	0.013449996	-0.013449996	13.658
0.999543419	0.013896757	-0.013896757	13.653
1.00670296	0.014164905	-0.014164905	13.65
1.009089877	0.014254303	-0.014254303	13.649
1.009089877	0.014254303	-0.014254303	13.649
1.009089877	0.014254303	-0.014254303	13.649
1.01625184	0.014522541	-0.014522541	13.646
1.01625184	0.014522541	-0.014522541	13.646
1.021027491	0.014701404	-0.014701404	13.644
1.035359294	0.015238176	-0.015238176	13.638
1.037748636	0.015327664	-0.015327664	13.637
1.037748636	0.015327664	-0.015327664	13.637
1.040138179	0.01541716	-0.01541716	13.636
1.040138179	0.01541716	-0.01541716	13.636
1.040138179	0.01541716	-0.01541716	13.636
1.042527925	0.015506664	-0.015506664	13.635
1.049698375	0.01577522	-0.01577522	13.632
1.049698375	0.01577522	-0.01577522	13.632
1.05208893	0.015864754	-0.015864754	13.631
1.054479687	0.015954295	-0.015954295	13.63
1.059261808	0.016133401	-0.016133401	13.628

1.059261808	0.016133401	-0.016133401	13.628
1.059261808	0.016133401	-0.016133401	13.628
1.061653172	0.016222965	-0.016222965	13.627
1.066436508	0.016402116	-0.016402116	13.625
1.07361303	0.0166709	-0.0166709	13.622
1.07361303	0.0166709	-0.0166709	13.622
1.085577952	0.017119024	-0.017119024	13.617
1.085577952	0.017119024	-0.017119024	13.617
1.087971545	0.017208672	-0.017208672	13.616
1.087971545	0.017208672	-0.017208672	13.616
1.09036534	0.017298327	-0.017298327	13.615
1.09036534	0.017298327	-0.017298327	13.615
1.092759338	0.01738799	-0.01738799	13.614
1.092759338	0.01738799	-0.01738799	13.614
1.095153538	0.017477661	-0.017477661	13.613
1.099942548	0.017657024	-0.017657024	13.611
1.102337357	0.017746717	-0.017746717	13.61
1.102337357	0.017746717	-0.017746717	13.61
1.104732369	0.017836418	-0.017836418	13.609
1.107127584	0.017926127	-0.017926127	13.608
1.111918622	0.018105566	-0.018105566	13.606
1.111918622	0.018105566	-0.018105566	13.606
1.114314446	0.018195298	-0.018195298	13.605
1.116710473	0.018285036	-0.018285036	13.604
1.119106703	0.018374783	-0.018374783	13.603
1.119106703	0.018374783	-0.018374783	13.603
1.138283853	0.019093028	-0.019093028	13.595
1.140681911	0.019182843	-0.019182843	13.594
1.143080172	0.019272666	-0.019272666	13.593
1.147877305	0.019452334	-0.019452334	13.591
1.152675251	0.019632032	-0.019632032	13.589
1.155074529	0.019721892	-0.019721892	13.588
1.157474011	0.019811761	-0.019811761	13.587
1.157474011	0.019811761	-0.019811761	13.587
1.157474011	0.019811761	-0.019811761	13.587
1.159873696	0.019901637	-0.019901637	13.586
1.164673677	0.020081411	-0.020081411	13.584
1.164673677	0.020081411	-0.020081411	13.584
1.167073973	0.02017131	-0.02017131	13.583
1.171875175	0.02035113	-0.02035113	13.581
1.174276081	0.020441052	-0.020441052	13.58
1.174276081	0.020441052	-0.020441052	13.58
1.179078505	0.020620918	-0.020620918	13.578



1.181480023	0.020710862	-0.020710862	13.577
1.183881744	0.020800814	-0.020800814	13.576
1.186283669	0.020890774	-0.020890774	13.575
1.195893407	0.021250689	-0.021250689	13.571
1.205506407	0.021610727	-0.021610727	13.567
1.207910167	0.021700755	-0.021700755	13.566
1.210314131	0.021790791	-0.021790791	13.565
1.212718299	0.021880835	-0.021880835	13.564
1.217527247	0.022060946	-0.022060946	13.562
1.219932028	0.022151012	-0.022151012	13.561
1.222337012	0.022241087	-0.022241087	13.56
1.222337012	0.022241087	-0.022241087	13.56
1.227147593	0.022421258	-0.022421258	13.558
1.231958991	0.02260146	-0.02260146	13.556
1.234364997	0.022691573	-0.022691573	13.555
1.236771207	0.022781693	-0.022781693	13.554
1.236771207	0.022781693	-0.022781693	13.554
1.241584239	0.022961957	-0.022961957	13.552
1.246398089	0.023142251	-0.023142251	13.55
1.246398089	0.023142251	-0.023142251	13.55
1.248805321	0.023232409	-0.023232409	13.549
1.253620398	0.023412749	-0.023412749	13.547
1.258436292	0.02359312	-0.02359312	13.545
1.260844546	0.023683316	-0.023683316	13.544
1.260844546	0.023683316	-0.023683316	13.544
1.263253005	0.023773521	-0.023773521	13.543
1.265661669	0.023863733	-0.023863733	13.542
1.275298369	0.024224658	-0.024224658	13.538
1.277708055	0.024314908	-0.024314908	13.537
1.277708055	0.024314908	-0.024314908	13.537
1.277708055	0.024314908	-0.024314908	13.537
1.280117947	0.024405167	-0.024405167	13.536
1.284938345	0.024585706	-0.024585706	13.534
1.284938345	0.024585706	-0.024585706	13.534
1.287348851	0.024675987	-0.024675987	13.533
1.289759561	0.024766276	-0.024766276	13.532
1.292170477	0.024856572	-0.024856572	13.531
1.292170477	0.024856572	-0.024856572	13.531
1.294581598	0.024946876	-0.024946876	13.53
1.294581598	0.024946876	-0.024946876	13.53
1.294581598	0.024946876	-0.024946876	13.53
1.294581598	0.024946876	-0.024946876	13.53
1.304228131	0.02530817	-0.02530817	13.526

1.306640276	0.025398512	-0.025398512	13.525
1.306640276	0.025398512	-0.025398512	13.525
1.311465183	0.02557922	-0.02557922	13.523
1.311465183	0.02557922	-0.02557922	13.523
1.313877944	0.025669586	-0.025669586	13.522
1.313877944	0.025669586	-0.025669586	13.522
1.31629091	0.025759959	-0.025759959	13.521
1.31629091	0.025759959	-0.025759959	13.521
1.31629091	0.025759959	-0.025759959	13.521
1.31629091	0.025759959	-0.025759959	13.521
1.318704082	0.02585034	-0.02585034	13.52
1.318704082	0.02585034	-0.02585034	13.52
1.318704082	0.02585034	-0.02585034	13.52
1.321117458	0.025940729	-0.025940729	13.519
1.321117458	0.025940729	-0.025940729	13.519
1.325944827	0.026121529	-0.026121529	13.517
1.32835882	0.026211941	-0.026211941	13.516
1.32835882	0.026211941	-0.026211941	13.516
1.330773017	0.02630236	-0.02630236	13.515
1.330773017	0.02630236	-0.02630236	13.515
1.330773017	0.02630236	-0.02630236	13.515
1.330773017	0.02630236	-0.02630236	13.515
1.33318742	0.026392787	-0.026392787	13.514
1.33318742	0.026392787	-0.026392787	13.514
1.338016842	0.026573665	-0.026573665	13.512
1.338016842	0.026573665	-0.026573665	13.512
1.342847086	0.026754573	-0.026754573	13.51
1.342847086	0.026754573	-0.026754573	13.51
1.345262516	0.026845038	-0.026845038	13.509
1.345262516	0.026845038	-0.026845038	13.509
1.347678152	0.026935511	-0.026935511	13.508
1.359759414	0.027387993	-0.027387993	13.503
1.364593358	0.02756904	-0.02756904	13.501
1.371845817	0.027840667	-0.027840667	13.498
1.374263715	0.027931225	-0.027931225	13.497
1.374263715	0.027931225	-0.027931225	13.497
1.374263715	0.027931225	-0.027931225	13.497
1.379100128	0.028112364	-0.028112364	13.495
1.386356292	0.028384131	-0.028384131	13.492
1.391194764	0.028565347	-0.028565347	13.49
1.398454017	0.028837229	-0.028837229	13.487
1.398454017	0.028837229	-0.028837229	13.487
1.40087418	0.028927872	-0.028927872	13.486

1.405715125	0.029109181	-0.029109181	13.484
1.405715125	0.029109181	-0.029109181	13.484
1.408135907	0.029199847	-0.029199847	13.483
1.412978089	0.029381202	-0.029381202	13.481
1.412978089	0.029381202	-0.029381202	13.481
1.417821095	0.029562588	-0.029562588	13.479
1.420242908	0.029653292	-0.029653292	13.478
1.420242908	0.029653292	-0.029653292	13.478
1.420242908	0.029653292	-0.029653292	13.478
1.420242908	0.029653292	-0.029653292	13.478
1.420242908	0.029653292	-0.029653292	13.478
1.422664927	0.029744005	-0.029744005	13.477
1.422664927	0.029744005	-0.029744005	13.477
1.425087153	0.029834725	-0.029834725	13.476
1.425087153	0.029834725	-0.029834725	13.476
1.427509585	0.029925453	-0.029925453	13.475
1.427509585	0.029925453	-0.029925453	13.475
1.432355068	0.030106931	-0.030106931	13.473
1.432355068	0.030106931	-0.030106931	13.473
1.434778119	0.030197682	-0.030197682	13.472
1.434778119	0.030197682	-0.030197682	13.472
1.437201376	0.030288441	-0.030288441	13.471
1.43962484	0.030379207	-0.030379207	13.47
1.43962484	0.030379207	-0.030379207	13.47
1.43962484	0.030379207	-0.030379207	13.47
1.442048511	0.030469982	-0.030469982	13.469
1.442048511	0.030469982	-0.030469982	13.469
1.446896472	0.030651553	-0.030651553	13.467
1.446896472	0.030651553	-0.030651553	13.467
1.446896472	0.030651553	-0.030651553	13.467
1.446896472	0.030651553	-0.030651553	13.467
1.446896472	0.030651553	-0.030651553	13.467
1.446896472	0.030651553	-0.030651553	13.467
1.446896472	0.030651553	-0.030651553	13.467
1.446896472	0.030651553	-0.030651553	13.467
1.446896472	0.030651553	-0.030651553	13.467
1.446896472	0.030651553	-0.030651553	13.467
1.449320762	0.030742351	-0.030742351	13.466
1.451745259	0.030833156	-0.030833156	13.465
1.451745259	0.030833156	-0.030833156	13.465
1.451745259	0.030833156	-0.030833156	13.465
1.451745259	0.030833156	-0.030833156	13.465
1.451745259	0.030833156	-0.030833156	13.465
1.451745259	0.030833156	-0.030833156	13.465

1.451745259	0.030833156	-0.030833156	13.465
1.454169962	0.030923969	-0.030923969	13.464
1.454169962	0.030923969	-0.030923969	13.464
1.454169962	0.030923969	-0.030923969	13.464
1.454169962	0.030923969	-0.030923969	13.464
1.45901999	0.031105618	-0.031105618	13.462
1.45901999	0.031105618	-0.031105618	13.462
1.45901999	0.031105618	-0.031105618	13.462
1.461445313	0.031196454	-0.031196454	13.461
1.461445313	0.031196454	-0.031196454	13.461
1.461445313	0.031196454	-0.031196454	13.461
1.461445313	0.031196454	-0.031196454	13.461
1.461445313	0.031196454	-0.031196454	13.461
1.463870844	0.031287298	-0.031287298	13.46
1.463870844	0.031287298	-0.031287298	13.46
1.463870844	0.031287298	-0.031287298	13.46
1.463870844	0.031287298	-0.031287298	13.46
1.463870844	0.031287298	-0.031287298	13.46
1.463870844	0.031287298	-0.031287298	13.46
1.463870844	0.031287298	-0.031287298	13.46
1.463870844	0.031287298	-0.031287298	13.46
1.466296581	0.031378149	-0.031378149	13.459
1.466296581	0.031378149	-0.031378149	13.459
1.466296581	0.031378149	-0.031378149	13.459
1.466296581	0.031378149	-0.031378149	13.459
1.466296581	0.031378149	-0.031378149	13.459
1.468722525	0.031469008	-0.031469008	13.458
1.468722525	0.031469008	-0.031469008	13.458
1.468722525	0.031469008	-0.031469008	13.458
1.468722525	0.031469008	-0.031469008	13.458
1.468722525	0.031469008	-0.031469008	13.458
1.468722525	0.031469008	-0.031469008	13.458
1.468722525	0.031469008	-0.031469008	13.458
1.468722525	0.031469008	-0.031469008	13.458
1.468722525	0.031469008	-0.031469008	13.458
1.473575034	0.03165075	-0.03165075	13.456
1.473575034	0.03165075	-0.03165075	13.456
1.473575034	0.03165075	-0.03165075	13.456
1.473575034	0.03165075	-0.03165075	13.456
1.473575034	0.03165075	-0.03165075	13.456
1.473575034	0.03165075	-0.03165075	13.456
1.473575034	0.03165075	-0.03165075	13.456
1.473575034	0.03165075	-0.03165075	13.456
1.473575034	0.03165075	-0.03165075	13.456

1.473575034	0.03165075	-0.03165075	13.456
1.473575034	0.03165075	-0.03165075	13.456
1.473575034	0.03165075	-0.03165075	13.456
1.473575034	0.03165075	-0.03165075	13.456
1.473575034	0.03165075	-0.03165075	13.456
1.473575034	0.03165075	-0.03165075	13.456
1.473575034	0.03165075	-0.03165075	13.456
1.476001599	0.031741633	-0.031741633	13.455
1.476001599	0.031741633	-0.031741633	13.455
1.476001599	0.031741633	-0.031741633	13.455
1.476001599	0.031741633	-0.031741633	13.455
1.476001599	0.031741633	-0.031741633	13.455
1.476001599	0.031741633	-0.031741633	13.455
1.476001599	0.031741633	-0.031741633	13.455
1.476001599	0.031741633	-0.031741633	13.455
1.476001599	0.031741633	-0.031741633	13.455
1.476001599	0.031741633	-0.031741633	13.455
1.47842837	0.031832523	-0.031832523	13.454
1.47842837	0.031832523	-0.031832523	13.454
1.47842837	0.031832523	-0.031832523	13.454
1.47842837	0.031832523	-0.031832523	13.454
1.47842837	0.031832523	-0.031832523	13.454
1.47842837	0.031832523	-0.031832523	13.454
1.47842837	0.031832523	-0.031832523	13.454
1.47842837	0.031832523	-0.031832523	13.454
1.480855349	0.031923421	-0.031923421	13.453
1.480855349	0.031923421	-0.031923421	13.453
1.480855349	0.031923421	-0.031923421	13.453
1.480855349	0.031923421	-0.031923421	13.453
1.480855349	0.031923421	-0.031923421	13.453
1.480855349	0.031923421	-0.031923421	13.453
1.480855349	0.031923421	-0.031923421	13.453
1.480855349	0.031923421	-0.031923421	13.453
1.480855349	0.031923421	-0.031923421	13.453
1.485709927	0.032105241	-0.032105241	13.451
1.485709927	0.032105241	-0.032105241	13.451
1.490565333	0.032287091	-0.032287091	13.449
1.490565333	0.032287091	-0.032287091	13.449
1.495421568	0.032468973	-0.032468973	13.447
1.502707473	0.032741853	-0.032741853	13.444
1.490565333	0.032287091	-0.032287091	13.449
1.492993347	0.032378028	-0.032378028	13.448
1.468722525	0.031469008	-0.031469008	13.458
1.468722525	0.031469008	-0.031469008	13.458
1.442048511	0.030469982	-0.030469982	13.469
1.434778119	0.030197682	-0.030197682	13.472
1.381518643	0.028202945	-0.028202945	13.494

1.32835882	0.026211941	-0.026211941	13.516
1.299404454	0.025127508	-0.025127508	13.528
1.222337012	0.022241087	-0.022241087	13.56
1.155074529	0.019721892	-0.019721892	13.588
1.109523002	0.018015843	-0.018015843	13.607
1.064044739	0.016312537	-0.016312537	13.626
1.001929731	0.013986132	-0.013986132	13.652
0.975691396	0.013003423	-0.013003423	13.663
0.975691396	0.013003423	-0.013003423	13.663
0.982844886	0.013271344	-0.013271344	13.66
0.987614887	0.013449996	-0.013449996	13.658
1.009089877	0.014254303	-0.014254303	13.649
1.009089877	0.014254303	-0.014254303	13.649
1.011476996	0.014343708	-0.014343708	13.648
1.013864317	0.01443312	-0.01443312	13.647
1.01625184	0.014522541	-0.014522541	13.646
1.021027491	0.014701404	-0.014701404	13.644
1.021027491	0.014701404	-0.014701404	13.644
1.02341562	0.014790847	-0.014790847	13.643
1.032970155	0.015148695	-0.015148695	13.639
1.035359294	0.015238176	-0.015238176	13.638
1.035359294	0.015238176	-0.015238176	13.638
1.035359294	0.015238176	-0.015238176	13.638
1.037748636	0.015327664	-0.015327664	13.637
1.042527925	0.015506664	-0.015506664	13.635
1.047308023	0.015685694	-0.015685694	13.633
1.049698375	0.01577522	-0.01577522	13.632
1.049698375	0.01577522	-0.01577522	13.632
1.049698375	0.01577522	-0.01577522	13.632
1.049698375	0.01577522	-0.01577522	13.632
1.049698375	0.01577522	-0.01577522	13.632
1.054479687	0.015954295	-0.015954295	13.63
1.064044739	0.016312537	-0.016312537	13.626
1.064044739	0.016312537	-0.016312537	13.626
1.066436508	0.016402116	-0.016402116	13.625
1.066436508	0.016402116	-0.016402116	13.625
1.06882848	0.016491703	-0.016491703	13.624
1.07361303	0.0166709	-0.0166709	13.622
1.080791376	0.016939752	-0.016939752	13.619
1.087971545	0.017208672	-0.017208672	13.616
1.09036534	0.017298327	-0.017298327	13.615
1.092759338	0.01738799	-0.01738799	13.614
1.092759338	0.01738799	-0.01738799	13.614

1.092759338	0.01738799	-0.01738799	13.614
1.092759338	0.01738799	-0.01738799	13.614
1.092759338	0.01738799	-0.01738799	13.614
1.102337357	0.017746717	-0.017746717	13.61
1.102337357	0.017746717	-0.017746717	13.61
1.104732369	0.017836418	-0.017836418	13.609
1.104732369	0.017836418	-0.017836418	13.609
1.111918622	0.018105566	-0.018105566	13.606
1.116710473	0.018285036	-0.018285036	13.604
1.119106703	0.018374783	-0.018374783	13.603
1.121503135	0.018464537	-0.018464537	13.602
1.121503135	0.018464537	-0.018464537	13.602
1.121503135	0.018464537	-0.018464537	13.602
1.131090898	0.018823629	-0.018823629	13.598
1.133488346	0.018913421	-0.018913421	13.597
1.140681911	0.019182843	-0.019182843	13.594
1.140681911	0.019182843	-0.019182843	13.594
1.145478637	0.019362496	-0.019362496	13.592
1.152675251	0.019632032	-0.019632032	13.589
1.157474011	0.019811761	-0.019811761	13.587
1.164673677	0.020081411	-0.020081411	13.584
1.164673677	0.020081411	-0.020081411	13.584
1.167073973	0.02017131	-0.02017131	13.583
1.167073973	0.02017131	-0.02017131	13.583
1.167073973	0.02017131	-0.02017131	13.583
1.167073973	0.02017131	-0.02017131	13.583
1.169474472	0.020261216	-0.020261216	13.582
1.174276081	0.020441052	-0.020441052	13.58
1.179078505	0.020620918	-0.020620918	13.578
1.179078505	0.020620918	-0.020620918	13.578
1.183881744	0.020800814	-0.020800814	13.576
1.195893407	0.021250689	-0.021250689	13.571
1.198296351	0.021340687	-0.021340687	13.57
1.210314131	0.021790791	-0.021790791	13.565
1.212718299	0.021880835	-0.021880835	13.564
1.212718299	0.021880835	-0.021880835	13.564
1.212718299	0.021880835	-0.021880835	13.564
1.212718299	0.021880835	-0.021880835	13.564
1.212718299	0.021880835	-0.021880835	13.564
1.219932028	0.022151012	-0.022151012	13.561
1.222337012	0.022241087	-0.022241087	13.56
1.2247422	0.022331169	-0.022331169	13.559
1.2247422	0.022331169	-0.022331169	13.559

1.231958991	0.02260146	-0.02260146	13.556
1.234364997	0.022691573	-0.022691573	13.555
1.241584239	0.022961957	-0.022961957	13.552
1.246398089	0.023142251	-0.023142251	13.55
1.246398089	0.023142251	-0.023142251	13.55
1.246398089	0.023142251	-0.023142251	13.55
1.246398089	0.023142251	-0.023142251	13.55
1.248805321	0.023232409	-0.023232409	13.549
1.248805321	0.023232409	-0.023232409	13.549
1.253620398	0.023412749	-0.023412749	13.547
1.260844546	0.023683316	-0.023683316	13.544
1.260844546	0.023683316	-0.023683316	13.544
1.263253005	0.023773521	-0.023773521	13.543
1.265661669	0.023863733	-0.023863733	13.542
1.265661669	0.023863733	-0.023863733	13.542
1.265661669	0.023863733	-0.023863733	13.542
1.275298369	0.024224658	-0.024224658	13.538
1.275298369	0.024224658	-0.024224658	13.538
1.277708055	0.024314908	-0.024314908	13.537
1.280117947	0.024405167	-0.024405167	13.536
1.280117947	0.024405167	-0.024405167	13.536
1.284938345	0.024585706	-0.024585706	13.534
1.292170477	0.024856572	-0.024856572	13.531
1.299404454	0.025127508	-0.025127508	13.528
1.30181619	0.025217835	-0.025217835	13.527
1.30181619	0.025217835	-0.025217835	13.527
1.30181619	0.025217835	-0.025217835	13.527
1.30181619	0.025217835	-0.025217835	13.527
1.30181619	0.025217835	-0.025217835	13.527
1.304228131	0.02530817	-0.02530817	13.526
1.306640276	0.025398512	-0.025398512	13.525
1.306640276	0.025398512	-0.025398512	13.525
1.306640276	0.025398512	-0.025398512	13.525
1.306640276	0.025398512	-0.025398512	13.525
1.311465183	0.02557922	-0.02557922	13.523
1.311465183	0.02557922	-0.02557922	13.523
1.313877944	0.025669586	-0.025669586	13.522
1.313877944	0.025669586	-0.025669586	13.522
1.31629091	0.025759959	-0.025759959	13.521
1.31629091	0.025759959	-0.025759959	13.521
1.318704082	0.02585034	-0.02585034	13.52
1.318704082	0.02585034	-0.02585034	13.52
1.321117458	0.025940729	-0.025940729	13.519



1.321117458	0.025940729	-0.025940729	13.519
1.321117458	0.025940729	-0.025940729	13.519
1.321117458	0.025940729	-0.025940729	13.519
1.321117458	0.025940729	-0.025940729	13.519
1.325944827	0.026121529	-0.026121529	13.517
1.325944827	0.026121529	-0.026121529	13.517
1.325944827	0.026121529	-0.026121529	13.517
1.32835882	0.026211941	-0.026211941	13.516
1.32835882	0.026211941	-0.026211941	13.516
1.32835882	0.026211941	-0.026211941	13.516
1.32835882	0.026211941	-0.026211941	13.516
1.330773017	0.02630236	-0.02630236	13.515
1.330773017	0.02630236	-0.02630236	13.515
1.33318742	0.026392787	-0.026392787	13.514
1.338016842	0.026573665	-0.026573665	13.512
1.340431862	0.026664115	-0.026664115	13.511
1.340431862	0.026664115	-0.026664115	13.511
1.35734275	0.027297481	-0.027297481	13.504
1.35251004	0.027116481	-0.027116481	13.506
1.359759414	0.027387993	-0.027387993	13.503
1.359759414	0.027387993	-0.027387993	13.503
1.367010638	0.027659574	-0.027659574	13.5
1.367010638	0.027659574	-0.027659574	13.5
1.367010638	0.027659574	-0.027659574	13.5
1.369428125	0.027750117	-0.027750117	13.499
1.374263715	0.027931225	-0.027931225	13.497
1.381518643	0.028202945	-0.028202945	13.494
1.383937364	0.028293534	-0.028293534	13.493
1.391194764	0.028565347	-0.028565347	13.49
1.398454017	0.028837229	-0.028837229	13.487
1.398454017	0.028837229	-0.028837229	13.487
1.405715125	0.029109181	-0.029109181	13.484
1.405715125	0.029109181	-0.029109181	13.484
1.405715125	0.029109181	-0.029109181	13.484
1.408135907	0.029199847	-0.029199847	13.483
1.410556895	0.02929052	-0.02929052	13.482
1.410556895	0.02929052	-0.02929052	13.482
1.412978089	0.029381202	-0.029381202	13.481
1.417821095	0.029562588	-0.029562588	13.479
1.420242908	0.029653292	-0.029653292	13.478
1.422664927	0.029744005	-0.029744005	13.477
1.422664927	0.029744005	-0.029744005	13.477
1.422664927	0.029744005	-0.029744005	13.477

1.422664927	0.029744005	-0.029744005	13.477
1.422664927	0.029744005	-0.029744005	13.477
1.425087153	0.029834725	-0.029834725	13.476
1.425087153	0.029834725	-0.029834725	13.476
1.427509585	0.029925453	-0.029925453	13.475
1.427509585	0.029925453	-0.029925453	13.475
1.427509585	0.029925453	-0.029925453	13.475
1.432355068	0.030106931	-0.030106931	13.473
1.432355068	0.030106931	-0.030106931	13.473
1.432355068	0.030106931	-0.030106931	13.473
1.437201376	0.030288441	-0.030288441	13.471
1.437201376	0.030288441	-0.030288441	13.471
1.43962484	0.030379207	-0.030379207	13.47
1.43962484	0.030379207	-0.030379207	13.47
1.43962484	0.030379207	-0.030379207	13.47
1.442048511	0.030469982	-0.030469982	13.469
1.442048511	0.030469982	-0.030469982	13.469
1.442048511	0.030469982	-0.030469982	13.469
1.446896472	0.030651553	-0.030651553	13.467
1.446896472	0.030651553	-0.030651553	13.467
1.446896472	0.030651553	-0.030651553	13.467
1.446896472	0.030651553	-0.030651553	13.467
1.446896472	0.030651553	-0.030651553	13.467
1.446896472	0.030651553	-0.030651553	13.467
1.446896472	0.030651553	-0.030651553	13.467
1.449320762	0.030742351	-0.030742351	13.466
1.449320762	0.030742351	-0.030742351	13.466
1.449320762	0.030742351	-0.030742351	13.466
1.449320762	0.030742351	-0.030742351	13.466
1.451745259	0.030833156	-0.030833156	13.465
1.454169962	0.030923969	-0.030923969	13.464
1.454169962	0.030923969	-0.030923969	13.464
1.454169962	0.030923969	-0.030923969	13.464
1.454169962	0.030923969	-0.030923969	13.464
1.45901999	0.031105618	-0.031105618	13.462
1.45901999	0.031105618	-0.031105618	13.462
1.45901999	0.031105618	-0.031105618	13.462
1.45901999	0.031105618	-0.031105618	13.462
1.461445313	0.031196454	-0.031196454	13.461
1.461445313	0.031196454	-0.031196454	13.461
1.461445313	0.031196454	-0.031196454	13.461
1.461445313	0.031196454	-0.031196454	13.461
1.463870844	0.031287298	-0.031287298	13.46



1.47842837	0.031832523	-0.031832523	13.454
1.47842837	0.031832523	-0.031832523	13.454
1.47842837	0.031832523	-0.031832523	13.454
1.47842837	0.031832523	-0.031832523	13.454
1.47842837	0.031832523	-0.031832523	13.454
1.47842837	0.031832523	-0.031832523	13.454
1.480855349	0.031923421	-0.031923421	13.453
1.480855349	0.031923421	-0.031923421	13.453
1.480855349	0.031923421	-0.031923421	13.453
1.480855349	0.031923421	-0.031923421	13.453
1.485709927	0.032105241	-0.032105241	13.451
1.485709927	0.032105241	-0.032105241	13.451
1.485709927	0.032105241	-0.032105241	13.451
1.485709927	0.032105241	-0.032105241	13.451
1.485709927	0.032105241	-0.032105241	13.451
1.485709927	0.032105241	-0.032105241	13.451
1.485709927	0.032105241	-0.032105241	13.451
1.488137527	0.032196162	-0.032196162	13.45
1.488137527	0.032196162	-0.032196162	13.45
1.488137527	0.032196162	-0.032196162	13.45
1.488137527	0.032196162	-0.032196162	13.45
1.488137527	0.032196162	-0.032196162	13.45
1.490565333	0.032287091	-0.032287091	13.449
1.468722525	0.031469008	-0.031469008	13.458
1.468722525	0.031469008	-0.031469008	13.458
1.442048511	0.030469982	-0.030469982	13.469
1.434778119	0.030197682	-0.030197682	13.472
1.381518643	0.028202945	-0.028202945	13.494
1.32835882	0.026211941	-0.026211941	13.516
1.251212757	0.023322575	-0.023322575	13.548
1.222337012	0.022241087	-0.022241087	13.56
1.176677192	0.020530981	-0.020530981	13.579
1.109523002	0.018015843	-0.018015843	13.607
1.071220654	0.016581298	-0.016581298	13.623
0.994771401	0.01371803	-0.01371803	13.655
0.975691396	0.013003423	-0.013003423	13.663
0.975691396	0.013003423	-0.013003423	13.663
0.982844886	0.013271344	-0.013271344	13.66
0.982844886	0.013271344	-0.013271344	13.66
0.985229786	0.013360666	-0.013360666	13.659
0.987614887	0.013449996	-0.013449996	13.658
0.987614887	0.013449996	-0.013449996	13.658
0.99715731	0.01380739	-0.01380739	13.654
0.999543419	0.013896757	-0.013896757	13.653

1.009089877	0.014254303	-0.014254303	13.649
1.009089877	0.014254303	-0.014254303	13.649
1.011476996	0.014343708	-0.014343708	13.648
1.013864317	0.01443312	-0.01443312	13.647
1.01625184	0.014522541	-0.014522541	13.646
1.01625184	0.014522541	-0.014522541	13.646
1.01625184	0.014522541	-0.014522541	13.646
1.02341562	0.014790847	-0.014790847	13.643
1.035359294	0.015238176	-0.015238176	13.638
1.035359294	0.015238176	-0.015238176	13.638
1.035359294	0.015238176	-0.015238176	13.638
1.040138179	0.01541716	-0.01541716	13.636
1.042527925	0.015506664	-0.015506664	13.635
1.049698375	0.01577522	-0.01577522	13.632
1.05208893	0.015864754	-0.015864754	13.631
1.05208893	0.015864754	-0.015864754	13.631
1.05208893	0.015864754	-0.015864754	13.631
1.054479687	0.015954295	-0.015954295	13.63
1.059261808	0.016133401	-0.016133401	13.628
1.059261808	0.016133401	-0.016133401	13.628
1.059261808	0.016133401	-0.016133401	13.628
1.064044739	0.016312537	-0.016312537	13.626
1.06882848	0.016491703	-0.016491703	13.624
1.07361303	0.0166709	-0.0166709	13.622
1.078398391	0.016850127	-0.016850127	13.62
1.080791376	0.016939752	-0.016939752	13.619
1.080791376	0.016939752	-0.016939752	13.619
1.087971545	0.017208672	-0.017208672	13.616
1.09036534	0.017298327	-0.017298327	13.615
1.09036534	0.017298327	-0.017298327	13.615
1.09036534	0.017298327	-0.017298327	13.615
1.09036534	0.017298327	-0.017298327	13.615
1.095153538	0.017477661	-0.017477661	13.613
1.099942548	0.017657024	-0.017657024	13.611
1.104732369	0.017836418	-0.017836418	13.609
1.107127584	0.017926127	-0.017926127	13.608
1.114314446	0.018195298	-0.018195298	13.605
1.114314446	0.018195298	-0.018195298	13.605
1.114314446	0.018195298	-0.018195298	13.605
1.116710473	0.018285036	-0.018285036	13.604
1.119106703	0.018374783	-0.018374783	13.603
1.121503135	0.018464537	-0.018464537	13.602
1.12629661	0.018644068	-0.018644068	13.6

1.12629661	0.018644068	-0.018644068	13.6
1.12629661	0.018644068	-0.018644068	13.6
1.133488346	0.018913421	-0.018913421	13.597
1.147877305	0.019452334	-0.019452334	13.591
1.152675251	0.019632032	-0.019632032	13.589
1.152675251	0.019632032	-0.019632032	13.589
1.157474011	0.019811761	-0.019811761	13.587
1.159873696	0.019901637	-0.019901637	13.586
1.159873696	0.019901637	-0.019901637	13.586
1.159873696	0.019901637	-0.019901637	13.586
1.164673677	0.020081411	-0.020081411	13.584
1.164673677	0.020081411	-0.020081411	13.584
1.171875175	0.02035113	-0.02035113	13.581
1.171875175	0.02035113	-0.02035113	13.581
1.171875175	0.02035113	-0.02035113	13.581
1.174276081	0.020441052	-0.020441052	13.58
1.174276081	0.020441052	-0.020441052	13.58
1.179078505	0.020620918	-0.020620918	13.578
1.186283669	0.020890774	-0.020890774	13.575
1.19108813	0.021070716	-0.021070716	13.573
1.193490667	0.021160699	-0.021160699	13.572
1.198296351	0.021340687	-0.021340687	13.57
1.207910167	0.021700755	-0.021700755	13.566
1.210314131	0.021790791	-0.021790791	13.565
1.210314131	0.021790791	-0.021790791	13.565
1.217527247	0.022060946	-0.022060946	13.562
1.217527247	0.022060946	-0.022060946	13.562
1.219932028	0.022151012	-0.022151012	13.561
1.222337012	0.022241087	-0.022241087	13.56
1.222337012	0.022241087	-0.022241087	13.56
1.227147593	0.022421258	-0.022421258	13.558
1.227147593	0.022421258	-0.022421258	13.558
1.234364997	0.022691573	-0.022691573	13.555
1.239177621	0.022871821	-0.022871821	13.553
1.241584239	0.022961957	-0.022961957	13.552
1.241584239	0.022961957	-0.022961957	13.552
1.246398089	0.023142251	-0.023142251	13.55
1.246398089	0.023142251	-0.023142251	13.55
1.246398089	0.023142251	-0.023142251	13.55
1.246398089	0.023142251	-0.023142251	13.55
1.248805321	0.023232409	-0.023232409	13.549
1.253620398	0.023412749	-0.023412749	13.547
1.258436292	0.02359312	-0.02359312	13.545

1.258436292	0.02359312	-0.02359312	13.545
1.260844546	0.023683316	-0.023683316	13.544
1.272888887	0.024134415	-0.024134415	13.539
1.272888887	0.024134415	-0.024134415	13.539
1.275298369	0.024224658	-0.024224658	13.538
1.277708055	0.024314908	-0.024314908	13.537
1.277708055	0.024314908	-0.024314908	13.537
1.277708055	0.024314908	-0.024314908	13.537
1.280117947	0.024405167	-0.024405167	13.536
1.289759561	0.024766276	-0.024766276	13.532
1.289759561	0.024766276	-0.024766276	13.532
1.289759561	0.024766276	-0.024766276	13.532
1.289759561	0.024766276	-0.024766276	13.532
1.292170477	0.024856572	-0.024856572	13.531
1.292170477	0.024856572	-0.024856572	13.531
1.294581598	0.024946876	-0.024946876	13.53
1.299404454	0.025127508	-0.025127508	13.528
1.30181619	0.025217835	-0.025217835	13.527
1.30181619	0.025217835	-0.025217835	13.527
1.30181619	0.025217835	-0.025217835	13.527
1.30181619	0.025217835	-0.025217835	13.527
1.304228131	0.02530817	-0.02530817	13.526
1.304228131	0.02530817	-0.02530817	13.526
1.306640276	0.025398512	-0.025398512	13.525
1.311465183	0.02557922	-0.02557922	13.523
1.311465183	0.02557922	-0.02557922	13.523
1.313877944	0.025669586	-0.025669586	13.522
1.31629091	0.025759959	-0.025759959	13.521
1.31629091	0.025759959	-0.025759959	13.521
1.31629091	0.025759959	-0.025759959	13.521
1.321117458	0.025940729	-0.025940729	13.519
1.321117458	0.025940729	-0.025940729	13.519
1.325944827	0.026121529	-0.026121529	13.517
1.325944827	0.026121529	-0.026121529	13.517
1.32835882	0.026211941	-0.026211941	13.516
1.32835882	0.026211941	-0.026211941	13.516
1.32835882	0.026211941	-0.026211941	13.516
1.32835882	0.026211941	-0.026211941	13.516
1.32835882	0.026211941	-0.026211941	13.516
1.330773017	0.02630236	-0.02630236	13.515
1.330773017	0.02630236	-0.02630236	13.515
1.330773017	0.02630236	-0.02630236	13.515
1.330773017	0.02630236	-0.02630236	13.515

1.330773017	0.02630236	-0.02630236	13.515
1.338016842	0.026573665	-0.026573665	13.512
1.347678152	0.026935511	-0.026935511	13.508
1.347678152	0.026935511	-0.026935511	13.508
1.347678152	0.026935511	-0.026935511	13.508
1.35251004	0.027116481	-0.027116481	13.506
1.354926292	0.027206977	-0.027206977	13.505
1.35734275	0.027297481	-0.027297481	13.504
1.364593358	0.02756904	-0.02756904	13.501
1.364593358	0.02756904	-0.02756904	13.501
1.367010638	0.027659574	-0.027659574	13.5
1.369428125	0.027750117	-0.027750117	13.499
1.374263715	0.027931225	-0.027931225	13.497
1.379100128	0.028112364	-0.028112364	13.495
1.381518643	0.028202945	-0.028202945	13.494
1.381518643	0.028202945	-0.028202945	13.494
1.386356292	0.028384131	-0.028384131	13.492
1.386356292	0.028384131	-0.028384131	13.492
1.398454017	0.028837229	-0.028837229	13.487
1.398454017	0.028837229	-0.028837229	13.487
1.40087418	0.028927872	-0.028927872	13.486
1.40087418	0.028927872	-0.028927872	13.486
1.405715125	0.029109181	-0.029109181	13.484
1.410556895	0.02929052	-0.02929052	13.482
1.412978089	0.029381202	-0.029381202	13.481
1.417821095	0.029562588	-0.029562588	13.479
1.417821095	0.029562588	-0.029562588	13.479
1.420242908	0.029653292	-0.029653292	13.478
1.425087153	0.029834725	-0.029834725	13.476
1.427509585	0.029925453	-0.029925453	13.475
1.427509585	0.029925453	-0.029925453	13.475
1.427509585	0.029925453	-0.029925453	13.475
1.432355068	0.030106931	-0.030106931	13.473
1.432355068	0.030106931	-0.030106931	13.473
1.434778119	0.030197682	-0.030197682	13.472
1.434778119	0.030197682	-0.030197682	13.472
1.437201376	0.030288441	-0.030288441	13.471
1.43962484	0.030379207	-0.030379207	13.47
1.43962484	0.030379207	-0.030379207	13.47
1.43962484	0.030379207	-0.030379207	13.47
1.442048511	0.030469982	-0.030469982	13.469
1.442048511	0.030469982	-0.030469982	13.469
1.442048511	0.030469982	-0.030469982	13.469



1.446896472	0.030651553	-0.030651553	13.467
1.446896472	0.030651553	-0.030651553	13.467
1.449320762	0.030742351	-0.030742351	13.466
1.449320762	0.030742351	-0.030742351	13.466
1.45901999	0.031105618	-0.031105618	13.462
1.461445313	0.031196454	-0.031196454	13.461
1.466296581	0.031378149	-0.031378149	13.459
1.466296581	0.031378149	-0.031378149	13.459
1.466296581	0.031378149	-0.031378149	13.459
1.466296581	0.031378149	-0.031378149	13.459
1.468722525	0.031469008	-0.031469008	13.458
1.468722525	0.031469008	-0.031469008	13.458
1.473575034	0.03165075	-0.03165075	13.456
1.473575034	0.03165075	-0.03165075	13.456
1.476001599	0.031741633	-0.031741633	13.455
1.47842837	0.031832523	-0.031832523	13.454
1.47842837	0.031832523	-0.031832523	13.454
1.480855349	0.031923421	-0.031923421	13.453
1.490565333	0.032287091	-0.032287091	13.449
1.492993347	0.032378028	-0.032378028	13.448
1.468722525	0.031469008	-0.031469008	13.458
1.468722525	0.031469008	-0.031469008	13.458
1.442048511	0.030469982	-0.030469982	13.469
1.434778119	0.030197682	-0.030197682	13.472
1.381518643	0.028202945	-0.028202945	13.494
1.32835882	0.026211941	-0.026211941	13.516
1.299404454	0.025127508	-0.025127508	13.528
1.222337012	0.022241087	-0.022241087	13.56
1.155074529	0.019721892	-0.019721892	13.588
1.109523002	0.018015843	-0.018015843	13.607
1.064044739	0.016312537	-0.016312537	13.626
1.001929731	0.013986132	-0.013986132	13.652
0.975691396	0.013003423	-0.013003423	13.663

Amplification circuit:

$$R1+R2=118.88k\Omega \quad R6=20\Omega$$

$$R3+R4=994.26k\Omega \quad R5=15.8118.88k\Omega$$

$$I_{ref}=6.285mA$$

$$V_r/100= I_{out}$$

$$V_{in}=40.16V_o$$

Wheatstone bridges:

$$R_2=R_3=10k\Omega$$

$$R_4=13.8k\Omega$$

R1=Resistance of pure CNT films

$$V_{EX}=5V$$

$$V_O = \left[ \frac{R_3}{R_3 + R_4} - \frac{R_2}{R_1 + R_2} \right] \cdot V_{EX}$$

